Eesti Maaülikool
Estonian University of Life Sciences

ENCODING OF ENVIRONMENTAL HEAT BY THE SENSORY TRIAD OF INSECT ANTENNAL THERMO- AND HYGRORECEPTOR NEURONS

KÕRGETE VÄLISTEMPERATUURIDE SENSOORNE KODEERIMINE PUTUKATE ANTENNAALSETE TERMO- JA HÜGRONEURONITE TRIAADIS

KARIN NURME

A Thesis
submitted for the degree of Doctor of Philosophy
in Agriculture

Väitekiri
Filosoofiadoktori kraadi taotlemiseks põllumajanduse erialal

Tartu 2019

Eesti Maaülikooli doktoritööd

Doctoral Theses of the Estonian University of Life Sciences

Eesti Maaülikool
Estonian University of Life Sciences

ENCODING OF ENVIRONMENTAL HEAT BY THE SENSORY TRIAD OF INSECT ANTENNAL THERMO- AND HYGRORECEPTOR NEURONS

KÕRGETE VÄLISTEMPERATUURIDE SENSOORNE KODEERIMINE PUTUKATE ANTENNAALSETE TERMO- JA HÜGRONEURONITE TRIAADIS

KARIN NURME

A Thesis
submitted for the degree of Doctor of Philosophy
in Agriculture

Väitekiri
Filosoofiadoktori kraadi taotlemiseks põllumajanduse erialal

Tartu 2019

Institute of Agricultural and Environmental Sciences
Estonian University of Life Sciences

According to verdict No. 6-14/5-2, of April 17th 2019, the Doctoral Committee of Agricultural and Natural Sciences of the Estonian University of Life Sciences has accepted the thesis for the defence for the degree of Doctor of Philosophy in Agriculture.

Opponent: **Prof. Dr. Christoph Kleineidam**
University of Konstanz, Germany

Supervisors: **Dr. Enno Merivee**
Estonian University of Life Sciences, Estonia
Dr. Anne Must
Estonian University of Life Sciences, Estonia
Dr. Ivar Sibul
Estonian University of Life Sciences, Estonia

Reviewers: **Prof. Indrikis Krams**
University of Tartu, Estonia; University of Daugavpils, Latvia

Defence of this thesis:
Estonian University of Life Sciences, room D239, Fr. R. Kreutzwaldi 5, Tartu on June 19th 2019 at 14:15.

The English language was edited by Mr. Matthew Redfearn and the Estonian by Mr. Arvi Erusk.

Publication of this thesis is supported by the Estonian University of Life Sciences

ISSN 2382-7076
ISBN 978-9949-629-81-7 (trükis)
ISBN 978-9949-629-82-4 (pdf)

CONTENTS

LIST OF ORIGINAL PUBLICATIONS

This thesis is a review of the following papers, which are referred to by Roman numerals in the text. The papers are reproduced by permission of the publishers.

I **Nurme, K.**, Merivee, E., Must, A., Sibul, I., Muzzi, M., Di Giulio, A., Williams, I., Tooming, E. 2015. Responses of the antennal bimodal hygroreceptor neurons to innocuous and noxious high temperatures in the carabid beetle, *Pterostichus oblongopunctatus.* Journal of Insect Physiology, 81, 1−13.

II Must, A., Merivee, E., **Nurme, K.**, Sibul, I., Muzzi, M., Di Giulio, A., Williams, I., Tooming, E. 2017. Encoding noxious heat by spike bursts of antennal bimodal hygroreceptor (dry) neurons in the carabid *Pterostichus oblongopunctatus.* Cell and Tissue Research, 368 (1), 29-46.

III **Nurme, K.**, Merivee, E., Must, A., Di Giulio, A., Muzzi, M., Williams, I., Mänd, M. 2018. Bursty spike trains of antennal thermo- and bimodal hygro-thermoreceptor neurons encode noxious heat in elaterid beetles. Journal of Thermal Biology, 72, 101-117.

Table 1. Authors' contribution to each article

Paper	Idea and study design	Laboratory work	Data analysis	Manuscript preparation
I	EM	EM, KN, AM, ADG, MM	EM, KN, AM	All
II	EM	EM, KN, AM, ADG, MM	EM, AM, KN	All
III	EM	EM, KN, AM, ADG, MM	EM, KN, AM	All

ADG – Andrea Di Giulio; AM – Anne Must; EM – Enno Merivee; ET – Ene Tooming; **KN – Karin Nurme**; MM – Maurizio Muzzi; All – all authors of the papers.

ABBREVIATIONS

AH – absolute humidity
CHN – thermoreceptor neuron, reclassified as cold-hot neuron
CTmax – critical thermal maximum
CV of ISI - the coefficient of variance of ISIs in a spike train
DHN – dry air neuron, reclassified as dry-hot neuron
DSS – dome shaped sensilla
FIB/SEM – Focused ion beam / scanning electron microscope
ISI – inter spike intervals
LA – locomotor activity
MHN – moist air neuron, reclassified as moist-hot neuron
ODS – outer dendritic segments
OELA – onset of elevated locomotor activity
RH – relative humidity
MFR – mean firing rate
TP – total paralysis

1. INTRODUCTION

Temperature plays a major role in all levels of biological organization. Rises in temperature speed up biochemical reactions (Hochachka and Somero, 2002) and metabolic processes (Schulte, 2015) leading to physiological and behavioural changes of individual organisms (Denlinger and Yocum, 1998; Chown and Terblanche, 2006; Abram et al., 2017) and ecosystem processes (Brown et al., 2004; Yvon-Durocher et al., 2012). Dependence of life processes on ambient thermal conditions is the most predictable on small ectothermic animals such as insects, which, unlike endotherms, are typically not able to maintain their body temperature constant via thermal homeostasis. Warm-blooded homeostatic animals largely use internally generated metabolic heat for their thermoregulation. Insects mostly thermo-regulate behaviourally. Recent increase in research activity has been largely motivated by a necessity to explain how individual organisms and ecosystems respond to ongoing global warming when high- temperature trends and daily extremes could become more commonplace (Must et al., 2010; Huey et al., 2012; Morak et al., 2013; Stocker et al., 2013; Gilbert et al., 2014; Sunday et al., 2014; Abram et al., 2017; DeLong et al., 2017; Li et al., 2018). Thus, it is crucial to understand the basic mechanisms and ways of how ectothermic animals cope with high temperatures.

Temperature is a critical environmental factor driving the abundance and geographical distribution of ectothermic organisms (Price et al., 2011; Molles, 2012). In order to effectively control the occurrence and density of beneficial and pest insects in agricultural lands via their behaviour to boost crop yields, fundamental knowledge on sensory mechanisms of habitat and microhabitat selection, searching behaviour and thermoregulation of these animals is needed. For small poikilotherms, microclimatic conditions may be quite disadvantageous, if not lethal, in the shortage of instant and adequate information about their ambient temperature and humidity (Denlinger and Yocum, 1998; Chown and Terblanche, 2006; Abram et al., 2017). Data about heat reception in insects, including agriculturally important carabids and elaterids, is still insufficient (Dhaka et al., 2006).

In this study, for the first time in carabids and elaterids, inner fine structure and innervation peculiarities of the antennal thermo- and

hygroreceptive sensilla were analysed. Responses of the sensory neurons to temperature were quantified and analysed over a broad range of temperatures from moderate to lethal levels in both carabids and elaterids. In this study, for the first time in carabids and elaterids, inner fine structure and innervation peculiarities of the antennal thermo- and hygroreceptive sensilla were analysed. For the first time in insects, responses of the thermo- and hygroreceptor neurons to temperature were quantified and analysed over a broad range of temperatures from moderate to lethal levels in both carabids and elaterids. Three essential turning points (onset of elevated locomotor activity, critical thermal maximum and threshold temperature for total paralysis) characterising response of the beetles to heating were determined from temperature-locomotor activity curves and analysed. Probable involvement of the thermal information coded by spike trains of the sensory neurons in behavioural thermoregulation of the beetles was demonstrated and discussed. Stimulating temperatures were representative of those that carabids and elaterids would encounter in their habitats.

2. REVIEW OF THE LITERATURE

2.1. Deleterious effects of environmental heat to insects

Ambient temperature strongly affects all physiological processes, behaviour and ecology of ectothermic animals. Due to their small body size, insects are particularly sensitive to high temperature injury since both solar radiation and convective heat transfer can quickly raise their body temperature up to lethal levels (Denlinger and Yocum, 1998; Chown and Terblanche, 2007). Heat stress above a narrow, species specific range of preferred temperatures causes a number of abnormalities at the cellular level (Hochachka and Somero, 2002; Chown and Terblanche, 2007). High temperatures also harmfully affect insect metabolism, endocrine and nervous systems, development, growth, respiration, fecundity and behaviour (Neven, 2000; Chown and Terblanche, 2007). The term critical thermal maximum (CTmax) introduced by Cowles and Bogert (1944) is a widely used method for quantifying a species specific upper thermal tolerance limit, and can be broadly defined as the thermal point at which locomotion becomes disorganized resulting in an animal's inability to escape from areas that will rapidly lead to its overheating and death (Becker and Genoway, 1979; Lutterschmidt and Hutchison, 1997; DeVries et al., 2016). In most insects, upper thermotolerance limit varies between 30 and 53 °C (Chown and Nicolson, 2004; Chown and Terblanche, 2007). Avoiding high temperatures is especially challenging for ground dwelling insects. In various carabids, total heat paralysis begins in a narrow range between 47 and 52 °C (Thiele, 1977), first indications of partial paralysis occur at 44 °C (Must et al., 2010). On sunny days, steep temperature gradients occur in their epigeal habitats especially in areas with vegetation. At middle latitudes, in summer, maximum soil surface temperatures in sunlit areas may reach above 50 °C while in shaded microclimatic conditions below the foliage temperatures remain up to 30–40 °C lower (Must et al., 2006a). However, noxiously high temperatures causing thermal injuries and death are function of both the heat level and duration of exposure (Cossins and Bowler, 1987; Denlinger and Yocum, 1998).

Ectothermic insects possess an array of physiological and behavioural mechanisms to circumvent or minimize potential thermal injury (Denlinger and Yocum, 1998; Chown and Terblanche, 2007; Bowler

and Terblanche, 2008). For example, epigeal insects such as carabids can maintain their body temperature in a relatively narrow range of their thermal preference through behavioural thermoregulation shuttling between sunlit areas and shade (Thiele, 1977; Lövei and Sunderland, 1996). Thus, instantaneous and adequate information of ambient temperature conditions is particularly important for epigeal insects, such as carabids (Coleoptera, Carabidae) and many elaterids (Coleoptera, Elateridae), the model insects of this study, for their optimal performance functions and survival.

2.2. Thermosensation in insects

2.2.1 General structure of insect thermo- and hygrosensitive sensilla

Temperature sensitive neurons may occur in a variety of specialised cuticular structures classified as sensilla coeloconica, basiconica, trichodea, styloconica, capitula, coelocapitula etc. located in small numbers on the antennal flagellum of insects (Altner and Loftus, 1985; Merivee et al., 2003; Ruchty et al., 2009; Nagel and Kleineidam, 2015; Schneider et al., 2018). In a sensillum, they are most commonly associated with hygroreceptor neurons but their combinations with chemoreceptor and mechanoreceptor neurons also exist (Altner and Loftus, 1985; Chapman, 1998). In the classical, most common type of insect thermo-hygroreceptive organs known as a coeloconic sensillum, a single thermoreceptor neuron combines with two hygroreceptor neurons, forming a sensory triad (Altner and Loftus, 1985; Chapman, 1998; Piersanti et al., 2011). Its cuticular part consists of a small peg with an inflexible socket at the bottom of a shallow pit, wholly exposed to ambient air. The peg has no wall pores except for the terminal moulting pore. In the classical coeloconic sensillum, unbranched outer dendritic segments (ODS) of the two sensory cells tightly fill the peg lumen extending up to the very tip of the peg. They most likely belong to the hygroreceptor neurons. The ODS of the third neuron is typically lamellated and it terminates just below the peg base. These morphological features seem to be characteristic to the cell with thermoreceptor activity. Below the peg, three auxiliary cells, the thecogen, trichogen and tormogen cell, respectively, concentrically surround the dendrites of the sensory triad. The sensory modality of the neurons cannot be firmly determined by purely morphological criteria, however (Altner

and Loftus, 1985; Steinbrecht, 1989; Chapman, 1998; Tichy and Kallina, 2010). Electrophysiological evidence is required to find out their exact functional significance.

In carabids, temperature and humidity sensitive neurons innervate a specific morphological type of antennal sensilla earlier inconsistently classified as campaniform and/or dome-shaped sensilla (DSS) in different species and studies (Merivee et al., 2003; Must et al., 2006a,b; Merivee et al., 2010). By external morphology, similar sensilla have been described on the antennae of various carabid (Merivee et al., 2000, 2001, 2002; Di Giulio et al., 2012) and elaterid beetles (Merivee et al., 1997, 1998, 1999; Zauli et al., 2016). In order to fix the mentioned terminological disorder, additional studies on the internal fine structure of these sensilla are required for conclusive determination of their morphological type in both of these insect groups

2.2.2 Encoding temperature by spike trains of the cold neuron

Even though thermoreception is essential in behavioural thermoregulation, it has been studied incompletely and poorly understood in arthropods. Very little data is available on coding sublethal and lethal high temperatures by peripheral sensory neurons crucial for survival in these small ectothermic animals. The classical sensory triad of thermo- and hygroreceptor neurons is widespread in various morphological types of antennal sensilla. By reaction type, the thermoreceptor neuron of the triad is a cold neuron. Its firing rate phasic-tonically increases with the rapid step-decrease in temperature and *vice versa*, spike production of the neuron decreases as the temperature grows higher (Altner and Loftus, 1985; Chapman, 1998; Merivee et al., 2003; Piersanti et al., 2011). The two hygroreceptor neurons antagonistically respond with a sharp change in their spike frequency when confronted by rapid changes in ambient air humidity (Altner and Loftus, 1985; Chapman, 1998; Merivee et al., 2010; Piersanti et al., 2011). They are the moist air and dry air neuron, respectively.

At moderate temperatures from 20 to 30 °C, the stationary mean firing rate (MFR) of the cold neuron is relatively high, 10–40 spikes s^{-1} as demonstrated in many insect groups (Lacher, 1964; Loftus, 1968; Tichy, 1979; Ameismeier and Loftus, 1988; Nagel and Kleineidam, 2015) including carabids (Merivee et al., 2003; Must et al., 2006a,b, 2010).

Plots of MFR of the cold neuron versus steady temperature exhibit a wider or narrower dynamic range at a certain range of temperatures, potentially enabling them unambiguously to measure environmental thermal conditions within that particular range. For example, in the carabid *Platynus assimilis*, in the range of 20 to 30 °C, stationary firing rate of the cold neuron decreases with temperature increase, but above that range up to 45 °C, the firing rate remains at about 20 spikes s^{-1} independent of temperature (Must et al., 2010). Even though, MFR of the cold neuron can discriminate moderate temperatures in some insects, it cannot encode sublethal and lethal heat.

The cold neuron changes its spike frequency when confronted by rapid changes in temperature, but in a number of cases, it does not measure ambient temperature correctly. First, immediately after a sudden warming, especially at a noxious heat above 35 °C, the neuron stops spike firing for a shorter or longer period of time depending on thermal stimulation conditions (Altner and Prillinger, 1980; Tichy and Loftus, 1987; Nishikawa et al., 1992; Merivee et al., 2003; Must et al., 2006a,b) making detection of several successive warmings impossible. In contrast to the cold neuron, warm neurons of some insects increase their spike frequency in response to temperature increase. They have been found in blood-sucking arthropods, cave beetles (Coleoptera), some tropical katydids (Orthoptera) and spiders (Davis and Sokolove, 1975; Altner and Prillinger, 1980; Loftus and Corbière-Tichané, 1981; Hess and Loftus, 1984; Ehn and Tichy, 1996; Gingl and Tichy, 2001; Schneider et al., 2018), but not in the vast majority of other studied insects including carabids and elaterids. Unfortunately, no data is available on the functioning of the warm air neurons at the sublethal and lethal range of high temperatures above 35 °C. Second, in a number insects, MFR of either the warm nor the cold neuron permits unequivocal discrimination between temperatures in a broad range from 20 to 35 (40) °C, because a certain spike frequency could be produced by more than one ambient temperature (Loftus, 1968; Davis and Sokolove, 1975; Must et al., 2006a,b). Third, the cold neuron fires a brief phasic, high frequency spike burst in response to a rapid cooling with peak frequencies reaching up to 650 Hz depending on both the initial temperature and the magnitude of temperature drop (Loftus, 1968; Waldow, 1970; Loftus and Corbière-Tichané, 1981; Merivee et al., 2003; Must et al., 2006a). Loftus (1968) found that several different combinations of initial temperature and magnitude of temperature step-decrease could achieve a particular peak

frequency of the phasic response. This ambiguity makes it unlikely that the phasic component of the cold neuron's response can serve as useful thermometer for insects.

In this context, the discovery that at high temperatures above 25–30 °C both the antennal cold and warm neuron in mosquitoes (Davis and Sokolove, 1975) and the antennal cold neuron in carabids (Must et al., 2010) switch from regular spiking to spike bursting is of interest. In the carabid beetle *Platynus assimilis*, the threshold temperature of the cold neuron for burst firing varies in the range of 25 to 47 °C (Must et al., 2010). For the first time in insects, Must et al. (2010) showed that a couple of parameters of the bursty spike trains such as the number and frequency of spikes in a burst are temperature dependent and potentially may encode noxious heat in a graded manner. Behavioural experiments conducted on a special thermal arena have been shown that threshold temperature for heat escape behaviour of the *P. assimilis*' beetles is approximately equal to 25 °C (Must et al., 2010). These results suggest that information on ambient thermal conditions coded by spike bursts of the cold neuron is involved in behavioural thermoregulation of the beetles. Since below 30 °C, bursting probability of the cold neuron is a lot less than 0.05 (E. Merivee, unpublished data), encoding high temperatures at the low end of noxious heat remains enigmatic.

Hygroreceptor neurons of the sensory triad might also be involved in insect thermosensation. In the American cockroach, *Periplaneta americana*, and the African migratory locust, *Locusta migratoria migratorioides*, MFR of the dry neuron responds to both ambient air temperature and humidity (Waldow, 1970; Loftus, 1976; Altner and Loftus, 1985). Due to the excessive ambiguity, the unit is commonly known as bimodal. The moist air neuron of the stick insect *Carausius morosus*, the European honey bee, *Apis mellifera*, and *L. migratoria migratorioides* is another bimodal well-known neuronal unit whose firing rate depends on both humidity and temperature (Lacher, 1964; Waldow, 1970; Altner and Loftus, 1985; Tichy, 1987). Biological relevance of this type of bimodality remains unknown however, because the same MFR values of the neurons cannot encode air humidity and temperature at the same time. By contrast, the moist neuron of *P. americana* is not sensitive to thermal stimuli (Yokohari and Tateda, 1976; Yokohari, 1978). So far, no data is available on temperature sensitivity of the hygroreceptor neurons in carabids and elaterids.

2.3. The model beetles of the study

The common Euro-Siberian carabid *Pterostichus oblongopunctatus* (Fabricius, 1787) is a predatory eurytopic forest inhabitant (Lindroth, 1986; Löbl and Smetana, 2003) but it also migrates into open agricultural lands in the presence of hedges (Lövei et al., 2002) or close to forest margins (Magura, 2002, Fusser et al., 2017). It is a spring breeding species. Young adults emerge in the autumn and preferably overwinter in felled, brown-rotted timber and are euryhygric to dry-prefering (Thiele, 1977; Lindroth, 1986). Thermal preference of the species lies between 10 and 25 °C (Thiele, 1977). *P. oblongopunctatus* is the only carabid species in which the cold neuron and two antagonistic hygroreceptor neurons have been electrophysiologically identified and investigated (Must et al., 2006a; Merivee et al., 2010). Thus, it is considered as a good representative of all carabids for further research on heat sensation aimed in this study.

The dark elaterid beetle, *Agriotes obscurus* (Linnaeus, 1758), belongs to the most destructive agricultural pests whose larvae live in the soil and damage a wide range of crops in Central and North Europe and Siberia (Dolin, 1978; Gurjeva, 1979). Its reproduction period lasts from May to August in the forest zone and from April to June in the steppe zone (Cherepanov, 1957; Gurjeva, 1979). Adults emerge in summer, remain in their pupal cradle and overwinter in the soil at a depth of 10–25 cm (Cherepanov, 1957; Gurjeva, 1979). *A. obscurus* serves as a good model of studies on insect thermoreception for several reasons. First, it allows comparing modality and functioning of the sensory neurons in morphologically identical antennal sensilla between two large insect groups, carabids and elaterids. Second, *A. obscurus* flies seldom and mostly walks on the ground. It prefers open agricultural grasslands and crop fields (Traugott et al., 2015), where its encounters with dangerously high temperature zones on the soil surface are an everyday threat. Thus, sensory neurons on its antennae, able to encode noxious heat, would be expected. So far, no electrophysiological work has been done on thermoreception of elaterids.

3. HYPOTHESES AND AIMS OF THE STUDY

The hypotheses of the study were:

- Considering external structural similarity, low numbers and similar distribution pattern of the thermo-hygroreceptive sensilla on the antennal flagellum of carabids and elaterids, suggesting their functional similarity, similar inner fine structure of these cuticular sensory organs is expected.

- Considering that externally, antennal thermo- and hygroreceptive sensilla of carabids and elaterids differ from all known morphological types of insect sensilla, their internal fine structure conclusively evidence's their belonging to a distinct morphological type of sensilla, not described in insects before.

- In a sensillum, depending on insect species, thermo- and hygroreceptor neurons may occur in different numbers and even in various combinations with neurons of other sensory modalities. Considering that in electrophysiological experiments, three spike shapes belonging to three different neurons have been discriminated in thermo- and hygroreceptive sensilla of carabids, morphologically, innervation of these sensilla by three neurons in both carabids and elaterids is expected.

- Electrophysiologically, classical sensory triad composed of a cold neuron and two antagonistic hygroreceptor neurons in antennal thermo- and hygroreceptive sensilla of elaterid beetles is expected.

- At high temperatures, the temperature sensitive (cold) neuron of elaterids switches from regular spiking to temperature dependent spike bursting enabling unambiguous encoding of noxious heat.

- Considering that spike trains of the two antagonistic hygroreceptor neurons in the sensory triad are able to unambiguously encode air humidity they, being unimodal, have no sensitivity to temperature, both in carabids and elaterids.

- Spike bursting of the antennal cold neuron is linked to behavioural thermoregulation of the beetles.

Based on the hypotheses the following tasks were formulated:

- To perform morphological analysis of the inner fine structure of the antennal DSS using a novel FIB/SEM combined technique in both *P. oblongopunctatus* and *A. obscurus*.

- In temperature and humidity stimulation experiments, to identify modality and reaction type of the neurons in antennal thermo- and hygroreceptive sensilla of *A. obscurus* using electrophysiology.

- To establish relationship between stationary MFR of the antennal hygroreceptor neurons and temperature (20 to 45 °C) in *A. obscurus* using electrophysiology.

- To establish bursting probability of the antennal cold neuron at different temperatures up to lethal high levels (20 to 45 °C) in *P. oblongopunctatus* using electrophysiology.

- To establish relationship between several important spike burst parameters (spike burst frequency, number of spikes per burst, coefficient of variation of interspike intervals of the bursty spike trains (CV of ISIs), bursting probability, mean interspike interval in a burst (ISI in a burst)) of the antennal cold neuron of *P. oblongopunctatus* and temperature up to lethal high levels (25 to 45 °C).

- To determine three main turning points (onset of elevated locomotor activity (OELA), CTmax and threshold temperature for total paralysis (TP)) extracted from the locomotor activity (LA)/ temperature curves of the beetles in a slow heating (20 to 45 °C) experiment.

4. MATERIAL AND METHODS

4.1. Test beetles

Adult *P. oblongopunctatus* and *A. obscurus* specimens were collected in Southern Estonia from brown-rotted down wood (**I**, **II**) or soil (**III**). The test insects were preserved in 20 cm × 30 cm × 10 cm plastic boxes filled with moistened-brown rotten wood crumbs (**I**, **II**) or moistened sand and moss (**III**) in a refrigerator at 5 °C (**I**, **II**) and 2–3 °C (**III**). Three to five days prior to the experiments the beetles were transferred to room temperature (20 °C) and placed individually in Petri dishes with moistened filter paper (**I**, **II**, **III**). The beetles were provided with clean tap water and fed with larvae of *Tenebrio molitor* (**I**, **II**) or not fed (**III**).

4.2. Focused ion beam/scanning electron microscope (FIB/SEM) combined technique

The FIB/SEM combined technique was used to investigate external and internal morphology of antennal DSS of ground beetles *P. oblongopunctatus* (**I**, **II**) and elaterids *A. obscurus* (**III**). The embedded apical antennomeres of the *P. oblongopunctatus* and *A. obscurus* were extracted from the epoxy resin, positioned on a stub with a conductive adhesive carbon disk and coated with a thin layer of gold in an Emitech K550 unit. The samples were examined by Dualbeam (FIB/SEM) Helios Nanolab (FEI, Eindhoven, The Netherlands) at L.I.M.E. (Roma Tre University, Rome, Italy). FIB column was used to cross-section the surface of the DSS and high-resolution micrographs were acquired by using the SEM column and backscattered electrons (Di Giulio et al., 2015).

4.3. Electrophysiology

4.3.1. Single sensillum recordings

The extracellular single sensillum recordings (**I**, **II**, **III**) were made from one apical DSS of each test beetle using tungsten electrodes. The grounded indifferent electrode was inserted into the antennal lumen at the base of flagellum. The recording electrode was forced into the

base of the DSS located at the tip of the terminal flagellomere using DC-3KS micromanipulator (Stoelting, USA) under visual control with the microscope Eclipse FN1 (Nikon, Japan) at a magnification of ×750–1000. All recordings were made in a Faraday Cage FAR01 (ThorLabs, UK). The electrical activity picked up by the recording electrode via a custom-made Preamplifier Board (Interspectrum, Estonia) was led to the input of the main amplifier ISO-DAM 8 A (World Precision Instruments, USA), monitored on an oscilloscope screen and relayed to a PC hard disc for data storage for further data management.

4.3.2. Stimulation and control of air humidity and temperature

Steady as well as rapid, stepped warming and hygro-stimuli were presented by way of one or two airstreams, depending on the experiment. Initially, the carbon filtered air was divided and led through two separate units, one with KOH pellets and other with air-moistening bubbler vessel. Required humidity levels of the airstreams were achieved by mixing the dried air (relative humidity (RH) 5%) and moistened air (95% RH) in appropriate ratio. Thereafter, the airstreams were warmed up by heating units to the required temperature level. Lastly, the airstreams at a velocity 2 m s^{-1} were directed through 8-mm outlet tubes to the terminal flagellomere of the insects in the distance of 10 mm. An electromagnetic air valve (Model 062 4E1; Humphrey Products, USA) EMV and a digital timer (Model 4030; Kaiser Fototechnik, Germany) were used to switch rapidly between the two airstreams. When the recordings from the sensilla were measured at different steady temperatures, the sensillum were allowed to be adapted to each stimulating steady temperature for 10 min before the recording was made.

A custom-made electronic airflow hygrometer (Interspectrum, Estonia) was used for measurements of the airstream's RH at 20 °C. Since the temperature and RH are inversely related i.e. if temperature increases, the RH decreases and vice versa, the necessary calculations were made for higher temperatures to achieve the required humidity. The airstreams temperature was measured with copper–constantan thermocouple circuit.

4.4. Behavioural experiments

For behavioural experiments (**III**) the test beetles *A. obscurus* were put singly on plastic arenas lined with polypropylene plant fleece and transferred into a Versatile Environmental Test Chamber MLR-35 1H (SANYO Electric, Japan) pre-set 20 °C and constant absolute humidity 9 g m^{-3}. The light conditions were chosen in accordance of the *A. obscurus* preference 2000 lx, measured with Digital Light Meter TES-1335 (TES Electrical Electronic Corp., Taipei, Taiwan). Locomotor activity of the beetles were video-recorded in linearly increasing temperature conditions from 20 to 45 °C (warming rate 1 °C min^{-1}) with a resolution of 1920 x 1080 pixels at 5 frames per second by USB Logitech HD Pro Webcam C920 (Logitech Inc., USA) and a computer software Debut Video Capture (NCH Software, USA).

4.5. Data management and statistical analysis

Spike trains recorded from different neurons innervating antennal DSS were analysed with Spike 2 software (Cambridge Electronic Design LTD, UK) in combination with visual inspection (detailed description presented in article **III**). Burstiness or regularity of the spike trains was determined with inter-spike interval histogram analysis with visual reviewing process (**I**, **II**, **III**).

Various spike train parameters were measured and analysed:

1) Mean firing rate, spikes s^{-1}, MFR (**I**, **II**, **III**)
2) Coefficient of variation of ISIs in a spike train, CV of ISI (**I**, **II**, **III**)
3) Percentage of bursty spikes (**I**, **II**)
4) Number of spikes per burst (**I**, **II**)
5) ISI in a burst (**I**, **II**)
6) Spike burst frequency, spike bursts s^{-1} (**I**, **II**)

One-way ANOVA and Fisher LSD (**I**) or Tukey (**III**) post hoc tests were used to assess the effect of steady temperature and rapid step warming of the neurons innervated antennal DSS responses and to calculate the significance of different means. The experiment results from rapid step cooling and rapid change RH experiments were analysed with paired t-test (**III**). The temperature effect on measured parameters of bursty spike trains were evaluated with Kruskal–Wallis test, to compare the

parameters at various temperatures the Wilcoxon signed rank test and Mann–Whitney U test were used (**II**).

Video-recordings from the behavioural experiments (**III**) were analysed with EthoVision XT Version 9 software (Noldus Information Technology, The Netherlands). Significant turning points in locomotor activity curves in changing temperature conditions were determined: threshold temperature for OELA, CTmax and TP.

All test results were considered statistically significant at $p < 0.05$ and all statistical analyses were done by using program STATISTICA 11 (StatSoft, USA) (**I**, **II**, **III**).

5. RESULTS

5.1. Morphology of DSS

5.1.1. Cuticular structure of antennal DSS in *P. oblongopunctatus* and *A. obscurus*

SEM-FIB analysis showed that the external appearance and distribution of the DSS were quite similar in both studied species (Figs. 3, **I**; 2 **II**; 3, 4, **III**). They occurred in low numbers on the ventral side of the flagellomeres and additionally, at the apical margin of the terminal flagellomere. Cuticular part of these sensilla consisted of a low, round dome 4–9.5 μm in diameter and a small conical peg with an aporous wall except for a terminal moulting pore. The domes towered several micrometres above the flagellar surface and were well exposed to surrounding air. The peg, round in cross-section and 3–5 μm in length, was tightly located in the cuticular peg socket. Only the tip of the peg slightly, up to one μm, protruded above the dome surface being directly exposed to ambient air. The peg socket, formed by invagination of the two outermost layers of the dome cuticle, positioned deep in the dome. Structural diagrams of the DSSs in *P. oblongopunctatus* (Figs. 5, **I**; 9, **II**) and *A. obscurus* (Fig. 4, **III**) revealed that by their morphological type, these sensilla were identical in the two species but they fundamentally differed from the classical thermo- and hygroreceptive (coeloconic) sensilla (Fig. 1, **II**). The main difference between the two morphological types of sensilla related to the type and extent of exposure of the cuticular peg to ambient air.

5.1.2. Internal fine structure and innervation of the DSSs

The inner fine structure and innervation of the DSSs differentiated only in details between *P. oblongopunctatus* and *A. obscurus*. In both, three sensory neurons innervated the sensilla. The ODS of two hygroreceptor neurons tightly filled the peg lumen and unbranching, reached up to the tip of the peg (Figs. 3C–J, **II**; 4A–F, **II**; 4B–F, **III**; 5A–H, **III**). In contrast to *A. obscurus*, in *P. oblongopunctatus*, the ODSs of the two neurons in some DSS had numerous, tiny apical branches (Figs. 2C, **II**; 3B, **II**). In *P. oblongopunctatus*, the branched ODS of the third (thermoreceptor)

neuron also entered deeply into the peg cavity whereby at the basal part of the peg, they were strongly lamellated (Figs. 4A,B, **I**; 3D–J, **II**; 4B–F, **II**). By contrast, in *A. obscurus*, the ODS of the thermoreceptor neuron ended below the peg base and no indications of dendritic branching and lamellation were observed (Figs. 4E,F, **III**; 5E–H, **III**). In both species, ODS of the thermoreceptor neuron was larger in diameter compared to that of the two hygroreceptor neurons (Figs. 4A,B, **I**; 3G,H,J, **II**; 4C–E, **II**; 5G–I, **III**). Below the peg base, perikarya and ODSs of the sensory triad were concentrically enveloped by a dendrite sheath and three auxiliary cells, the thecogen, trichogen and tormogen cell, respectively (Figs. 3F–J, **II**; 4E,F, **II**; 4C–F, **III**; 5E–J, **III**). Schematic diagrams of the DSSs' inner structure were reconstructed for both *P. oblongopunctatus* and *A. obscurus*, in the Fig. 9 (**II**) and Fig. 6 (**III**), respectively. In general terms, the cellular complexes were similar in both the DSSs and classical coeloconic sensilla (Fig. 1, **II**).

5.2. Electrophysiology

5.2.1. Electrophysiological identification of the DSS neurons in *A. obscurus*

Three types of spike shapes produced by the three sensory neurons of the DSSs were recorded during electrophysiological experiments – one with a large and two with a small amplitude (Fig. 1A–D, **III**). The large and small spikes were produced by the thermoreceptor and two hygroreceptor neurons, respectively. Two hygroreceptor neurons antagonistically responded to a rapid step-change in stimulating air RH. Firing rate of the moist air neuron (MHN) increased and that of the dry air neuron (DHN) decreased with RH increase (later defined as moist-hot neuron and dry-hot neuron), while the thermoreceptor neuron (CHN) showed no sensitivity to humidity stimulations (Fig. 10, **III**) (later defined as cold-hot neuron). On the other hand, at constant absolute humidity (AH) conditions, the CHN was highly sensitive to rapid step-changes in temperature. Its firing rate drastically decreased with temperature increase (Fig. 8A, **III**) and *vice versa*, spike frequency of the neuron increased in response to rapid cooling (Fig. 9A, **III**). Thus, the CHN responded to tested air temperature and humidity stimuli as a typical cold neuron. The MHN and DHN antagonistically responded to rapid warming (Fig. 9B,C, **III**) and cooling (Fig. 8B,C, **III**) stimulations but to a much lesser extent than the CHN. In the warming experiment, MFRs

were correlated negatively and positively with temperature in the MHN and DHN, respectively. The opposite occurred in the cooling experiment, MFR of the MHN increased and that of the DHN decreased with temperature decrease. Changes in MFR of the hygroreceptor neurons in response to changes in temperature could be explained, mostly at least, by the fact that at constant AH, RH inevitably changes with temperature fluctuations. Thus, in the range of moderate temperatures (22–27 °C), the antennal DSS neurons responded to offered thermal and humidity stimuli as typical moist air, dry air and cold neuron in the classical sensory triad of insect thermo- and hygroreceptor neurons.

5.2.2. Dependence of the stationary MFR of the DSS neurons on temperature

MFR of the three DSS neurons was measured in 5 °C increments at different levels of steady temperature ranging from 20 to 35 °C at both constant AH and RH in *P. oblongopunctatus* and at a constant AH in *A. obscurus* only. In *P. oblongopunctatus*, at constant AH conditions, nearly linear decrease from 30.6 to 8.4 spikes s^{-1} with temperature increase from 20 to 35 °C was observed in MFR of the CHN (Fig. 6C, **I**). It appeared that the negative slope of the temperature-MFR curve of the neuron was steeper at the constant AH (fold change 3.6; Fig. 6C, **I**) than at the constant RH (fold change 1.9; Fig. 6F, **I**). In *A. obscurus*, the fold decrease in MFR of the CHN, measured at a constant AH, was smaller (2.1), from 25.8 to 12.2 spikes s^{-1}, and the dynamic range of the temperature-response curve remained between 25 to 35 °C being shifted by 5 °C towards the high end of tested temperatures (Fig. 7A, **III**) compared to that of *P. oblongopunctatus*.

By contrast to the CHN, at a constant AH, MFR of the DHN almost linearly increased from 38.3 to 54.3 spikes s^{-1} (fold change 1.4) with a temperature increase in *P. oblongopunctatus* (Fig. 6B, **I**) and from 38.3 to 54.3 spikes s^{-1} (fold change 1.9) in *A. obscurus* (Fig. 7C, **III**). Expectedly, in the constant RH experiment, MFR of the DHN did not depend on temperature over the all range of 20 to 35 °C (Fig. 6E, **I**).

MFR of the MHN oppositely responded to thermal stimulations at constant AH and constant RH conditions. As predicted, in the constant AH experiment with *P. oblongopunctatus*, MFR of the MHN showed a significant decrease from 23.6 to 6.2 spikes s^{-1} (fold change 3.8), but at

the high end of tested temperatures (30–35 °C) the difference between the MFRs was statistically not significant (Fig. 6A, **I**). Surprisingly, at a constant RH, MFR of the neuron linearly increased from 10.2 to 24.9 spikes s^{-1} (fold change 2.4) as temperature increased from 20 to 35 °C (Fig. 6D, **I**). In the thermal stimulation experiment conducted at constant AH with *A. obscurus*, a negative correlation between temperature and the MFR of the MHN was expected, comparable to that observed in *P. oblongopunctatus*, but that was not the case. Spike production of the neuron remained unchanged over the all range of tested temperatures (Fig. 7B, **III**).

5.2.3. No spiking responses of the CHN to rapid step-warmings

When confronted with a rapid warming the CHN stopped spike firing for a shorter or longer period of time depending on the initial temperature and the extent of temperature increase. For example, exposure of a DSS to a rapid warming by 1 °C from 35 to 36 °C caused the CHN of the *P. oblongopunctatus* to stop its spike production for about 0.5 s (Fig. 8C, **II**). When temperature jumped higher by 5 °C, from 30 to 35 °C, the CHN stopped spike generation during all the 10 s warming period while one or both of the hygrosensitive neurons in the same sensillum, MHN and DHN, respectively, continued spike generation (Figs. 8E, **I**; 9D, **I**). Duration of this no spiking period also depended on a particular neuron. For example, in *A. obscurus*, a 10 s rapid warming by 5 °C at the low end of noxious heat from 30 to 35 °C caused the CHN to stop spiking for 5 s (Fig. 14A, **III**) and 10 s (Fig. 12A, **III**) in two different DSS, respectively. The no spiking response of the CHN was reversible. After cooling to the initial temperature (30 °C), normal spike generation of the neuron recovered (Fig. 12E, **III**).

5.2.4. Spike bursting probability of the antennal DSS neurons at different temperatures

Bursting probability of the neurons was tested and analysed in the broad range of temperatures ranging from 20 to 45 °C at constant AH conditions. At moderate temperatures (20–25 (30) °C), the antennal DSS neurons tend to fire in a regular manner both in *P. oblongopunctatus* (Figs. 2A, **I**; 7A, **I**; 5A, **II**) and *A. obscurus* (Figs. 11A–C, **III**; 14B, **III**). For the first time in insects, it was found that at higher temperatures above 30 (25) °C, the pattern of spike firing of the sensory triad changed.

At different threshold temperatures, they started to generate spike bursts instead of single spikes. In bursty spike trains, the intraburst intervals are shorter than interburst intervals (Fig. 1E, **III**). If regular and burst firing occurs mixed in a spike train of a neuron interspike interval (ISI) analysis allows discrimination between regular and bursty spikes (Fig. 7A–C, **III**). It was observed that in both at constant temperatures as well as in rapid warming experiments, not only the CHN but the MHN and DHN also switched from regular, single spike production to burst firing in both *P. oblongopunctatus* (Figs. 7B,C, **I**; 8B,C, **I**; 5B–D, **II**) and *A. obscurus* (Figs. 12B, **III**; 13A, **III**; 14C,D, **III**; 15A–D, **III**). In a sensillum, the threshold temperatures for spike bursting of the three neurons differed. Usually, the humidity sensitive MHN and DHN started to produce spike bursts at lower temperatures than the CHN in both *P. oblongopunctatus* (Fig. 7B,C, **I**) and *A. obscurus* (Figs. 13A, **III**; 14C,D, **III**). Bursting probability of the neurons was very low at 25 to 30 °C depending on the physiological type of the neuron, but it quickly increased with temperature increase in both *P. oblongopunctatus* (Figs. 10A–D, **I**; 6, **II**) and *A. obscurus* (Fig. 17, **III**). It appeared that in the whole range of tested temperatures, the DHN and MHN had the highest tendency for spike bursting in *P. oblongopunctatus* and *A. obscurus*, respectively. Spike bursting response of the DSS neurons was reversible. The neurons immediately switched from high temperature induced spike bursting to regular firing when temperature dropped by several degrees (Fig. 14A–E, **III**; 15D, **III**).

These results demonstrated that in *P. oblongopunctatus*, a positive correlation exists between the bursting probability of the DHN, CHN and temperature in the range of 20–40 °C and 25–45 °C, respectively (Fig. 6, **II**). Exclusively, for the MHN, the temperature-response curve was calculated at 20 to 35 °C. A positive correlation between the bursting probability of the neuron and temperature was found in the range of 25 to 35 °C (Fig. 10 C, **I**). For comparison, in *A. obscurus*, a positive correlation between temperature and bursting probability of the DHN, MHN and CHN occurred in the ranges of 30–45 °C, 25–45 °C and 30–45 °C, respectively (Fig. 17, **III**). These findings evidenced for the first time that the MHN and DHN, in fact, were bimodal switching from humidity-dependent regular firing mode to the temperature-dependent burst firing mode. Therefore, in this study, a new classification of the DSS neurons was used. According to their response characteristics, the CHN, MHN and DHN were classified as the cold-hot neuron, the bimodal moist-hot neuron and the bimodal dry-hot neuron, respectively.

5.2.5. Dependence of bursty spike train parameters of the CHN and DHN on steady temperatures

Dependence of several parameters of bursty spike trains of the CHN and DHN (MFR, spike burst frequency, the number of spikes per burst, CV of ISIs, percentage of bursty spikes, mean ISI in a burst) on temperature was analysed in detail in the carabid beetle *P. oblongopunctatus*. Since both firing rate and bursting probability of the MHN were very low at the high end of tested temperatures (25–45 C) this neuron was not subjected to further analysis in this study.

It appeared that MFR and spike burst frequency in bursty spike trains of both the CHN and DHN ambiguously depended on temperature. In the reverse V-shape temperature-MFR curve of the DHN, the same values of the measured parameter represented two different temperatures (Fig. 7a, **II**). By contrast, MFR of the CHN linearly increased from 15 to 35 spikes s^{-1} with temperature increase from 35 to 45 °C (Fig. 7a, **II**). Thus, most of the MFR values measured in bursty spike trains at the high end of noxious heat (35–45 °C) overlapped with the MFRs of the neuron measured in regular spike trains at the low end of heat (20–35 °C) (Fig. 6C, F, **I**). Even more, in the two dose-response curves, the sign of the slope was opposite. The temperature-response curve for the spike burst frequency of the DHN was also reverse V-shaped (Fig. 7b, **II**) demonstrating that unambiguous relationship between this response parameter and temperature was absent. By contrast, the spike burst frequency of the CHN increased a little, from 4.2 to about 7 bursts s^{-1} as temperature increased from 35 to 40 °C, and stabilised close to this value at above 40 °C (Fig. 7b, **II**).

Two response parameters of the DHN, the number of spikes in a burst and CV of ISIs significantly increased as temperature increased from 25 to 45 C. The positive slope of the respective temperature-response curves was remarkably steeper above than below 35 °C (Fig. 7c, d, **II**) suggesting that these two parameters were much more sensitive to the high end than to the low end of noxious heat. The two response parameters of the CHN also rapidly increased with temperature increase in the range of 35 to 45 °C (Fig. 7c, d, **II**) demonstrating their remarkable sensitivity to heat above 35 °C.

The fifth parameter of the DHN, the percentage of bursty spikes in a spike train significantly increased with temperature increase following an S-curve with the steepest positive slope between 30 and 40 °C (Fig. 7e, **II**). For comparison, in the CHN, the parameter significantly and nearly linearly increased with temperature increase in the range of 35 to 45 °C (Fig. 7e, **II**). At 45 °C, in both the DHN and CHN, the parameter reached a value close to 100. In most cases, the number of spikes in a burst, CV of ISIs and the percentage of bursty spikes had considerably higher values in the DHN compared to those of the CHN.

A significant, negative, almost linear correlation was found between temperature and the sixth measured response parameter of the neurons, ISI in a burst. In the CHN, the parameter showed a strong, 5.1-fold decrease with temperature increase from 35 to 45 °C (Fig. 7f, **II**). By comparison, in the DHN, the change of the parameter over the all range of 25 to 45 °C was much slower (Fig. 7f, **II**).

5.2.6. Effects of rapid step warming on the spike bursting response of the neurons

Rapid step changes in temperature caused immediate changes in the pattern of bursty spike trains of the DSS neurons as demonstrated by sample recordings for the CHN (Figs. 15, A,B,D, **III**; 16A, **III**), MHN (Figs. 12B, **III**; 15A,C,D, **III**; 16B, **III**) and DHN (Figs. 8C, **I**; 9B, **I**; 8a,b, **II**; 16C, **III**), respectively. It appeared that the response depended not only on the initial temperature and magnitude of the change in temperature but also on the duration of the rapid step warming/cooling (Fig. 9A, B, **I**; 8A,B, **II**; 15A–D, **III**; 16A–C, **III**). Thus, in contrast to what was observed in regular spike trains of the CHN, spike generation in bursting neurons never stopped in response to rapid warming. Typically, burstiness of the spike trains increased with temperature increase.

Response of several bursty spike train parameters of the DHN to rapid step warmings at the high end of noxious heat (from 35 to 36 °C and from 35 to 40 °C) was analysed in *P. oblongopunctatus* in detail (Table 1, **II**). It appeared that four parameters out of six (MFR, CV of ISIs in a spike train, percentage of bursty spikes, and the number of spikes in a burst) significantly increased with temperature increase. One parameter, ISI in a burst, significantly shortened as the temperature jumped to a higher level. Surprisingly, a significant increase in the spike burst

frequency was observed at warming by 1 °C only but not at warming by 5 °C. By contrast, in four parameters, CV of ISIs, percentage of bursty spikes, the number of spikes per burst and ISIs in a burst, a significantly larger change was observed at warming by 5 °C than that at warming by 1 °C. Thus, these four temperature-dependent parameters of bursty spike trains produced by the DHN were capable momentarily to discriminate rapid changes in heat.

5.3. Effects of high temperatures on the LA of the beetles

Behavioural experiments with *A. obscurus* were carried out at constant AH conditions in the range of 20 to 45 °C. Three essential turning points (OELA, CTmax and TP) were determined in the temperature-LA curves (Fig. 2, **III**). It appeared that the threshold temperature for OELA of the beetles was equal to 27.5±0.75 °C (Fig. 18, **III**) well coinciding with the threshold temperature for spike bursting in the MHN and DHN (25–30 °C) (Fig. 17, **III**). A steep decline in high temperature induced, elevated locomotor activity (CTmax) occurred at 39.4±0.37 °C. Thus, observed CTmax of the beetles was higher by 11.9 °C compared to its threshold temperature for OELA. The threshold temperature for TP occurred at 41.8±0.37 °C which was higher by only 2.4 °C than CTmax. The beetles stopped moving and quickly died due to thermoshock. At CTmax, the beetles fully recovered when rapidly cooled down to room temperature (22 °C). By contrast, from TP the beetles never recovered.

6. DISCUSSION

For the first time in the two large group of insects, carabids and elaterids, inner fine structure of the antennal thermo- and hygroreceptive sensilla was analysed using a novel FIB/SEM combined technique. The results of the study enable us to explain innervation specifics and shed light on the confused morphological classification of these sensory structures. Several characteristic features, such as the presence of a prominent cuticular dome protruding above the antennal surface, and a small peg with a non-perforated wall tightly inserted into the peg socket etc. show that by their morphological type these organs are identical in carabids and elaterids (**I**, **II**, **III**). On the other side, these sensilla, termed as the DSSs, fundamentally differ from the classical thermo- and hygroreceptive peg-in-pit organs (coeloconic sensilla) (**II**) widespread in many insect taxons (Altner and Loftus, 1985; Chapman, 1998; Ruchty et al., 2009; Wang et al., 2016; Schneider et al., 2018). They also contrast with all other morphological types of insect thermo- and hygroreceptive sensilla (Chapman, 1998; Piersanti et al., 2011; Nagel and Kleineidam, 2015).

The complex of sensory neurons and auxiliary cells in the DSSs of carabid and elaterid beetles is similar to that of the classical thermo- and hygroreceptive coeloconic sensilla (**II**, **III**). One thermoreceptor neuron and two hygroreceptor neurons innervate these sensilla. The ODS of the two hygroreceptor neurons tightly fill the peg lumen and unbranching reach up to the very tip of the peg. In carabids, the lamellated dendritic branches of the ODS of the thermoreceptor neuron enter deeply into the peg lumen, up to half of its length (**I**, **II**). By contrast, in elaterids, the ODS of the thermoreceptor neuron is unbranched and ends below the peg base (**III**). Below the peg base, three auxiliary cells, the thecogen, trichogen and tormogen cell, respectively, concentrically envelope the dendrites of the sensory neurons, both in carabids (**I**, **II**) and elaterids (**III**) typical for insect thermo- and hygroreceptive sensilla (Altner and Loftus, 1985; Chapman, 1998; Schneider et al., 2018).

A sensory neuron may potentially discriminate environmental temperatures within a dynamic range of its spike train parameters. Electrophysiological extracellular single sensillum recordings, performed at moderate temperatures in the range of 20 to 30 °C, show that by their response modality, firing mode and reaction type the three DSS neurons

behave as typical temperature sensitive cold neuron, moist air neuron and dry air neuron, respectively, both in carabids (Merivee et al., 2003, 2010) and elaterids (**III**). In an insect sensillum, combinations of a single thermoreceptor neuron with chemoreceptor and mechanoreceptor neurons also exist (Altner and Loftus, 1985; Chapman 1998). In some instances, two thermoreceptor neurons innervate one and the same sensillum. For example, in the ant *Campanotus rufipes* (Hymenoptera), two cold neurons in an antennal sensillum coelocapitulum respond to different parameters of the thermal environment (Nagel and Kleineidam, 2015). Two antagonistically responding thermoreceptor neurons, the warm cell and the cold cell, innervate coeloconic sensilla on the antennae of a katydid (Orthoptera) (Schneider et al., 2018). However, the classical sensory triad of a cold neuron, and two antagonistically responding hygroreceptor neurons, the moist air and the dry air neuron, respectively, is the most widespread in various insect taxa including Blattodea, Coleoptera, Hemiptera, Hymenoptera, Lepidoptera, Odonata, Orthoptera and Phasmatodea (Lacher, 1964; Loftus 1968; Waldow, 1970; Yokohari and Tateda, 1976; Tichy, 1979; Yokohari et al., 1982; Altner and Loftus, 1985; Nishikawa et al., 1985; Chapman, 1998; Shields and Hildebrand, 1999; Piersanti et al., 2011). The results of this study support earlier findings that even though MFR of the cold neuron in the classical sensory triad may unambiguously encode moderate temperatures in some insects, it cannot discriminate different levels of noxious heat above 30–35 °C (Must et al., 2010; **III**).

At high temperatures above 25 (30) °C, firing mode of the DSS cold neuron changes by switching from regular spiking to spike bursting in various carabids (Must et al., 2010; **I**, **II**) as well as in elaterids (**III**). The threshold temperature of the cold neuron for spike bursting is much lower in carabids (25 to 30 °C) (Must et al., 2010; **I**, **II**) compared to that of elaterids equal to 35 °C (**III**). Bursting probability of the neuron is very low close to its threshold temperature for burst firing, but it quickly increases with temperature increase both in carabids (**I**, **II**) and elaterids (**III**). ISI analysis shows that several parameters of bursty spike trains of the DSS cold neuron depend on temperature and potentially, may unambiguously encode noxious heat from moderate to lethal levels of 45 °C and higher in a graded manner both in carabids (Must et al., 2010; **I**, **II**) and elaterids (**III**). Thus, different firing modes of the same neuron, regular and burst firing, respectively, encode different ranges of temperature in the thermal environment of the beetles. Therefore, in

this study, the cold neuron of the classical sensory triad in DSS, by its reaction type, is reclassified and termed as the cold-hot neuron (CHN) (**III**).

For the first time, the results of this study demonstrate that the two hygroreceptor neurons of the classical sensory triad also, similarly to that of the cold neuron, start to produce high temperature induced spike bursts instead of regular firing characteristic of the neurons at lower temperatures both in carabids (**I**, **II**) and elaterids (**III**). Even more, ISI analysis performed in the carabid *P. oblongopunctatus* show that several temperature dependent parameters of bursty spike trains of both the moist air neuron and the dry air neuron such as the bursting probability, burst frequency, percentage of bursty spikes in a spike train, the number of spikes per burst, CV of ISIs of the spike trains and ISI in a burst may, in addition to the cold neuron, unambiguously encode high temperatures from moderate to lethal levels in a graded manner (**II**). Thus, the two hygroreceptor neurons of the classical sensory triad are, in fact, bimodal. At moderate temperatures, they fire in regular mode and encode ambient air humidity. At higher temperatures, the sensory modality of the neuron's changes, they switch to burst firing mode encoding noxious heat. For this reason, the moist air neuron and the dry air neuron of the classical sensory triad are reclassified and termed as the moist-hot neuron and the dry-hot neuron, respectively (**III**).

There exists a large variation in threshold temperatures for spike bursting of the CHN, MHN and DHN across different DSSs (Must et al., 2010; **I**, **II**, **III**) which is probably caused, partly at least, by structural variations in their ODSs and cuticular parts of the sensilla (**II**, **III**). Alternative explanations to this phenomenon are possible. According to the phase model of temperature-dependent spike bursting developed on the example of cold neurons in *Aplysia* (Gastropoda) and mammalian CNS, various chemical and electrical processes of the neuron operate on many time scales to produce a fast oscillating system coupled to a slowly oscillating subsystem (Longtin and Hinzer, 1996; Roper et al., 2000; Hyun et al., 2014). These two oscillating systems interact to produce a variety of specific regular and burst firing patterns. Excitability of the neurons is determined by the state of the cell membrane sodium channels, which can be influenced by the ionic composition and pH of extracellular fluids (Brumberg et al., 2000; Hammond, 2015; Viatchenko-Karpinski and Gu, 2018). It is plausible that processes and factors like these may

vary from cell to cell contributing to variation of threshold temperatures of the neurons for bursting.

Neurons capable of generating high-frequency spike bursts occur in various sensory systems (Krahe and Gabbiani, 2004). In insects, besides temperature sensitive DSS neurons of carabids and elaterids, burst firing mode occurs in auditory interneurons of crickets and moths (Boyan and Fullard, 1988; Marsat and Pollack, 2006; Eyherabide et al., 2008). It is related to evasion behaviour. Hunting bats echolocate flying prey insects by means of ultrasonic signals, and crickets respond to these signals with avoidance behaviour triggered by spike bursts in the ultrasound-sensitive interneuron, AN2 (Hoy, 1992). There exists a strict temporal concurrency between ultrasonic signals and bursts produced by the AN2. By contrast, the CHN, MHN and DHN of carabids and elaterids have continuous burst trains, no temporal information is encoded in the timing of the bursts (Must et al., 2010; **I**, **II**, **III**).

It seems that the DSS neurons, as heat detectors, most reliably function in different ranges of high temperatures. Bursting probability of the DHN and MHN, in carabids and elaterids, respectively, is higher remarkably compared to that of the CHN (**II**, **III**). The difference is most prominent at moderate and sublethal ranges of noxious heat (25 to 40 °C). This is probably because the ODSs of the DHN and MHN extend to the tip of the cuticular peg of the DSSs and are more exposed to ambient air compared to that of the cold neuron (**I**, **II**, **III**). In addition, at temperatures close to 45 °C and higher, the ability of the DHN and MHN to produce normal spike waveforms worsens while the CHN continues to produce normal spikes (**II**, **III**). Thus, spike bursts of the two bimodal hygro-thermoreceptor neurons and the CHN are specifically responsible for hierarchically encoding moderate and lethal high temperatures, respectively. In the middle range, at sublethal heat (35–40 °C), all the three neurons of the triad can discriminate temperatures reliably.

The advantage of burst firing is to increase reliability of interneuronal communication because presynaptic, intraburst high-frequency spike firing improves information transmission across unreliable synapses (Lisman, 1997; Krahe and Gabbiani, 2004). Spike bursting neurons release more neurotransmitter molecules compared to those that generate single spikes with larger ISI intervals. Additionally, spike bursts

guarantee more precise information transfer compared to regular spikes because flexible burst patterns can drive higher neurons more efficiently (Dykes, 1975; Roper et al., 2000; Krahe and Gabbiani, 2004). The central neurons are able to discriminate between patterns of bursty spike trains with the same MFR but which correspond to different temperatures.

There is strong evidence that bursts have a distinct function in sensory information transmission. A number of studies on visual and auditory systems support the hypothesis that spike bursts represent a special neural code involved in the detection of specific, external signals of danger or behaviourally important stimulus features (Crick, 1984; Sherman, 2001; Swadlow and Gusev, 2001; Kepecs et al., 2002; Krahe and Gabbiani, 2004; Marsat and Pollack, 2006; Eyherabide et al., 2008). The results of this study show that, threshold temperatures for spike bursting of the neurons in antennal DSSs, and OELA of the beetles well coincide (**III**) suggesting that information on ambient heat coded by bursts of the sensory triad is involved in behavioural thermoregulation of these animals. These findings consider spike bursting as a fundamental quality of the insect thermo- and bimodal hygro-thermoreceptor neurons being a flexible and reliable firing mode of coding unfavourably high temperatures. Its occurrence in two large taxonomic group of Coleoptera – Carabidae and Elateridae, with more than 40,000 and 10,000 species worldwide (Kromp, 1999; Han et al., 2016), respectively, suggests that it is widespread in many if not all insects with the classical sensory triad of antennal thermo- and hygroreceptor neurons.

7. CONCLUSIONS

The results of this study show that morphologically, antennal thermo-hygroreceptive sensilla of carabids and elaterids are identical, and differ from all known types of sensilla described in insects before. They are termed as dome-shaped sensilla (DSSs)

Combined FIB/SEM analysis confirms that DSSs in both carabids and elaterids are innervated by three sensory neurons, one thermoreceptor neuron and two hygroreceptor neurons.

Electrophysiological recordings state that at moderate temperatures, the three DSS neurons of both carabids and elaterids respond to thermal and humidity stimuli as the classical sensory triad composed of a cold neuron, a moist air neuron and a dry air neuron.

ISI analysis underlines that at noxious heat, firing mode of the DSS cold neuron changes, switching from regular spiking to temperature-dependent burst firing enabling unambiguous encoding of high temperatures in a graded manner in both carabids and elaterids. For the first time, in this study, the cold neuron, by its reaction type, is reclassified as the cold-hot neuron (CHN).

Electrophysiological evidence demonstrates that both the moist air neuron and dry air neuron, in fact, are bimodal responding to both air humidity and temperature. It appears, that at high temperatures they switch from humidity dependent regular firing mode to temperature dependent burst firing mode enabling unambiguous encoding of high temperatures in a graded manner in both carabids and elaterids similarly to that of the CHN. For the first time, in this study, the moist air neuron and the dry air neuron of the sensory triad are reclassified as the moist-hot neuron (MHN) and the dry-hot neuron (DHN), respectively.

Coincidence of the threshold temperatures for spike bursting of the DSS neurons and OELA suggests that information coded by burst firing patterns of the classical sensory triad in DSS is involved in behavioural thermoregulation of the beetles.

The results of this study serve as an essential contribution to the theory of insect thermoreception.

8. REFERENCES

Abram, P.K., Boivin, G., Moiroux, J., Brodeur, J., 2017. Behavioural effects of temperature on ectothermic animals: unifying thermal physiology and behavioural plasticity. Biol. Rev. **92**, 1859–1876. https://doi.org/10.1111/brv.12312

Altner, H., Loftus, R., 1985. Ultrastructure and function of insect thermo- and hygroreceptors. Annu. Rev. Entomol. **30**, 273–295. https://doi.org/10.1146/annurev.en.30.010185.001421

Altner, H., Prillinger, L., 1980. Ultrastructure of invertebrate chemo-, thermo-, and hygroreceptors and its functional significance. Int. Rev. Cytol. **67**, 69–139. https://doi.org/10.1016/S0074-7696(08)62427-4

Ameismeier, F., Loftus, R., 1988. Response characteristics of cold cell on the antenna of *Locusta migratoria* L. J. Comp. Physiol. A **163**, 507–516. https://doi.org/10.1007/BF00604904

Becker, C.D., Genoway, R.G., 1979. Evaluation of the critical thermal maximum for determining thermal tolerance of freshwater fish. Environ. Biol. Fish. **4**, 245–256. https://doi.org/10.1007/BF00005481

Bowler, K., Terblanche, J.S., 2008. Insect thermal tolerance: what is the role of ontogeny, ageing and senescense? Biol. Rev. **83**, 339–355. https://doi.org/10.1111/j.1469-185X.2008.00046.x

Boyan, G.S., Fullard, J.H., 1988. Information processing at a central synapse suggests a noise filter in the auditory pathway of the noctuid moth. J. Comp. Physiol. A Neuroethol. Sens. Neural Behav. Physiol. **164**, 251–258. doi: 10.1007/BF00603955

Brown, J., Gillooly, J., Allen, A., Savage, V., West, G., 2004. Toward a metabolic theory of ecology. Ecology, **85**, 1771–1789. https://doi.org/10.1890/03-9000

Brumberg, J.C., Nowak, L.G., McCormick, D.A., 2000. Ionic mechanisms underlying repetitive high-frequency burst firing in supragranular cortical neurons. J. Neurosci., **20**, 4829–4843. https://doi.org/10.1523/JNEUROSCI.20-13-04829.2000

Chapman, R.F., 1998. The Insects. Structure and Function. Cambridge University Press, U.K.

Cherepanov, A.I., 1957 Click Beetles of Western Siberia (Coleoptera, Elateridae). Novosibirsk Publishing House, Russia (in Russian).

Chown, S.L., Nicolson, S.W., 2004. Insect Physiological Ecology. Mechanisms and Patterns. Oxford University Press, Oxford.

Chown, S.L., Terblanche, J.S., 2007. Physiological diversity in insects: ecological and evolutionary contexts. Adv. Insect Physiol. **33**, 50–152. https://doi.org/10.1016/S0065-2806(06)33002-0

Cossins, A.R., Bowler, K., 1987. Temperature biology of animals. Chapman & Hall, U.K.

Cowles, R.B., Bogert, C.M., 1944. A preliminary study of the thermal requirements of desert reptiles. Bull. Am. Mus. Nat. Hist. **83**, 261–296. https://doi.org/10.1086/394795

Crick, F., 1984. Function of the thalamic reticular complex: the searchlight hypothesis. Proc. Natl. Acad. Sci. U.S.A. **81**, 4586–4590. https://doi.org/10.1073/pnas.81.14.4586

Davis, E.E., Sokolove, P.G., 1975. Temperature responses of antennal receptors of the mosquito, *Aedes aegypti*. J. Comp. Physiol. **96**, 223–236. https://doi.org/10.1007/BF00612696

DeLong, J.P., Gibert, J.P., Luhring, T.M., Bachman, G., Reed, B., Neyer, A., Montooth K.L., 2017. The combined effects of reactant kinetics and enzyme stability explain the temperature dependence of metabolic rates. Ecol. Evol. **7**, 3940–3950. https://doi.org/10.1002/ece3.2955

Denlinger, D.L., Yocum, G.D., 1998. Physiology of heat sensitivity. In: Hallman, G.J., Denlinger, D.L. (Eds.), Temperature Sensitivity in Insects and Application in Integrated Pest Management. Westview Press, Boulder, CO, USA, pp. 7–57.

DeVries, Z.C., Kells, S.A., Appel, A.G., 2016. Estimating the critical thermal maximum (CT_{max}) of bed bugs, *Cimex lectularius*: Comparing thermolimit respirometry with traditional visual methods. Comp. Biochem. Physiol. Part A **197**, 52–57. doi: 10.1016/j.cbpa.2016.03.003

Dhaka, A., Viswanath, V., Patapoutian, A., 2006. TRP ion channels and temperature sensation. Annu. Rev. Neurosci. **29**, 135–161. DOI: 10.1146/annurev.neuro.29.051605.112958

Di Giulio, A., Maurizi, E., Rossi Stacconi, M.V., Romani, R., 2012. Functional structure of antennal sensilla in the myrmecophilous

beetle *Paussus favieri* (Coleoptera, Carabidae, Paussini). Micron **43**, 705–719. doi: 10.1016/j.micron.2011.10.013

Dolin, V.G., 1978. Guide for Identification of Elaterid Larve of USSR Fauna. Urozhai, Ukraine (in Russian).

Dykes, R.W., 1975. Coding of steady, transient temperatures by cutaneous "cold" fibers serving the hand of monkeys. Biophys. J. **98**, 485–500. https://doi.org/10.1016/0006-8993(75)90368-6

Ehn, R., Tichy, H., 1996. Response characteristics of a spider warm cell: temperature sensitivities and structural properties. J. Comp. Physiol. A **178**, 537–542. https://doi.org/10.1007/BF00190183

Eyherabide, H.G., Rokem, A., Herz, A.V.M., Samengo, I., 2008. Burst firing is a neural code in an insect auditory system. Front. Comput. Neurosci. **2**, 1–17. doi: 10.3389/neuro.10.003.2008

Fusser, M.S., Pfister, S.C., Entling, M.H., Schirmel, J. 2017. Effects of field margin type and landscape composition on predatory carabids and slugs in wheat fields. Agric. Ecosyst. Environ. **247**, 182–188. https://doi.org/10.1016/j.agee.2016.04.007

Gilbert, B., Tunney, T.D., McCann, K.S., DeLong, J.P., Vasseur, D.A., Savage, V., Shurin, J.B., Dell, A.I., Barton, B.T., Harley, C.D.G., Kharouba, H.M., Kratina, P., Blanchard, J.L., Clements, C., Winder, M., Greig, H.S., O'Connor, M.I. (2014). A bioenergetic framework for the temperature dependence of trophic interactions. Ecol. Lett. **17**, 902–914. https://doi.org/10.1111/ele.12307

Gingl, E., Tichy, H., 2001. Infrared sensitivity of thermoreceptors. J. Comp. Physiol. A **187**, 467–475. doi: 10.1007/s003590100221

Gurjeva, E.L., 1979. The Elaterid Beetles (Elateridae). Subfamily Elaterinae. Tribes Megapenthini, Physorhinini, Ampedini, Elaterini, Pomachilini. Fauna of USSR. The Beetles XII, Vol. 4. Nauka, Leningrad, Russia (in Russian).

Hammond, C., 2015. Cellular and Molecular Neurophysiology. Academic Press. Amsterdam, Boston, Heidelberg, London, New York, Oxford, Paris, San Diego, San Francisco, Singapore, Sydney, Tokyo.

Han, T., Lee, W., Lee, S., Park, I.G., Park, H., 2016. Reassessment of species diversity of the subfamily Denticollinae (Coleoptera: Elateridae) through DNA barcoding. PLoS ONE 11(2): e0148602. doi:10.1371/journal.pone.0148602

Hess, E., Loftus, R., 1984. Warm and cold receptors of two sensilla on the foreleg tarsi of the tropical bont tick *Amblyomma variegatum*. J. Comp. Physiol. A **155**, 187–195. https://doi.org/10.1007/BF00612636

Hochachka, P.W., Somero, G.N., 2002. Biochemical Adaptation: Mechanism and Process in Physiological Evolution. Oxford University Press, Oxford, UK.

Hoy, R.R., 1992. The evolution of hearing in insects as an adaptation to predation from bats. In: Webster, D.B., Fay, R.R., Popper, A.N. (Eds.), The Evolutionary Biology of Hearing. Springer, New York. pp. 115–130. https://doi.org/10.1007/978-1-4612-2784-7_8

Huey, R.B., Kearney, M.R., Krockenberger, A., Holtum, J.A., Jess, M., Williams, S.E., 2012. Predicting organismal vulnerability to climate warming: roles of behaviour, physiology and adaptation. Philos. Trans. R. Soc. London B Biol. Sci. **367**, 1665–1679. doi: 10.1098/rstb.2012.0005

Hyun, N.G., Hyun, K.-H., Hyun, K.-B., Lee, K., 2014. Temperature-dependent bursting pattern analysis by modified plant model. Mol. Brain **7**, 50. doi: 10.1186/s13041-014-0050-5

Kepecs, A., Wang, X.J., Lisman, J., 2002. Bursting neurons signal input slope. J. Neurosci. **22**, 9053–9062. https://doi.org/10.1523/JNEUROSCI.22-20-09053.2002

Krahe, R., Gabbiani, F., 2004. Burst firing in sensory systems. Nat. Rev. Neurosci. **5**, 13–23. https://doi.org/10.1038/nrn1296

Kromp, B., 1999. Carabid beetles in sustainable agriculture: a review on pest control efficacy, cultivation aspects and enhancement. Agric. Ecosyst. Environ. **74,** *187–228.* doi:10.1016/S0167-8809(99)00037-7

Lacher, V., 1964. Elektrophysiologische Untersuchungen an einzelnen Rezeptoren für Geruch, Kohlendioxyd, Luftfeuchtigkeit und Temperatur auf den Antennen der Arbeitsbiene und der Drohne (*Apis mellifera* L.). Z. Vgl. Physiol. **48**, 587–623.

Li, C., Fang, Y., Caldeira, K., Zhang, X., Diffenbaugh, N.S., Michalak, A.M., 2018. Widespread persistent changes to temperature extremes occurred earlier than predicted. Sci. Rep. **8**:1007. https://doi.org/10.1038/s41598-018-19288-z

Lindroth, C.H., 1986. The Carabidae (Coleoptera) of Fennoscandia and Denmark. Fauna Entomologica Scandinavica, **15**(2), 233–497.

Lisman, J.E., 1997. Bursts as a unit of neural information: making unreliable synapses reliable. Trends Neurosci. **20**, 38–43. doi: 10.1016/S0166-2236(96)10070-9

Löbl, I., Smetana, A. (eds.), 2003. *Catalogue of Palaearctic Coleoptera. Volume I. Archostemata-Myxophaga-Adephaga*. Apollo Books, Stenstrup, Denmark.

Loftus, R., 1968. The response of the antennal cold receptor of *Periplaneta americana* to rapid temperature changes and steady temperature. Z. Vgl. Physiol. **59**, 413–455.

Loftus, R., 1976. Temperature-dependent dry receptor on antenna of *Periplaneta*. Tonic response. J. Comp. Physiol. **111**, 153–170.

Loftus, R., Corbière-Tichané, G., 1981. Antennal warm and cold receptors of the cave beetle, *Speophyes lucidulus* Delar., in sensilla with a lamellated dendrite. I. Responses to sudden temperature change. J. Comp. Physiol. A **143**, 443–452.

Longtin, A., Hinzer, K., 1996. Encoding with bursting, subthreshold oscillations, and noise in mammalian cold receptors. Neural Comput. **8**, 215–255. https://doi.org/10.1162/neco.1996.8.2.215

Lövei, G.L., Magura, T., Sigsgaard, L., Ravn, H-P., 2002. Patterns in ground beetle (Coleoptera: Carabidae) assemblages in single-row hedgerows in a Danish agricultural landscape. In: Szyszko J, den Boer P, Bauer T (Eds.) How to protect or what we know about Carabid Beetles. Proceedings of the 10th European Meeting of Carabidologists. Agricultural University Press, Warsaw, Poland, pp. 201–212.

Lövei, G.L., Sunderland, K.D., 1996. Ecology and behavior of ground beetles (Coleoptera: Carabidae). Annu. Rev. Entomol. **41,** 231–256. doi: 10.1146/annurev.en.41.010196.001311

Lutterschmidt, W.I., Hutchison, V.H., 1997. The critical thermal maximum: history and critique. Can. J. Zool. **75**, 1561–1574. https://doi.org/10.1139/z97-783

Magura, T., 2002. Carabids and forest edge: spatial pattern and edge effect. For. Ecol. Manag., **157**, 23–37. doi: 10.1016/S0378-1127(00)00654-X

Marsat, G., Pollack, G.S., 2006. A behavioural role for feature detection by sensory bursts. J. Neurosci. **26**, 10542–10547. doi: 10.1523/JNEUROSCI.2221-06.2006

Merivee, E., Must, A., Luik, A., Williams, I., 2010. Electrophysiological identification of hygroreceptor neurons from the antennal dome shaped sensilla in the ground beetle *Pterostichus oblongopunctatus*. J. Insect Physiol. **56**, 1671–1678. doi: 10.1016/j.jinsphys.2010.06.017

Merivee, E., Ploomi, A., Luik, A., Rahi, M., Sammelselg, V., 2001. Antennal sensilla of the ground beetle *Platynus dorsalis* (Pontoppidan, 1763) (Coleoptera, Carabidae). Micros. Res. Tech. **55**, 339–349. https://doi.org/10.1002/jemt.1182

Merivee, E., Ploomi, A., Rahi, M., Bresciani, J., Ravn, H.P., Luik, A., Sammelselg, V., 2002. Antennal sensilla of the ground beetle *Bembidion properans* Steph. (Coleoptera, Carabidae). Micron **33**, 429–440. https://doi.org/10.1016/S0968-4328(02)00003-3

Merivee, E., Ploomi, A., Rahi, M., Luik, A., Sammelselg, V., 2000. Antennal sensilla of the ground beetle *Bembidion lampros* Hbst. (Coleoptera, Carabidae). Acta Zool. **81**, 339–350. doi: 10.1046/j.1463-6395.2000.00068.x

Merivee, E., Rahi, M., Bresciani, J., Ravn, H.L., Luik, A., 1998. Antennal sensilla of the click beetle, *Limonius aeruginosus* (Oliver) (Coleoptera: Elateridae). Int. J. Insect Morphol. Embryol. **27**, 311–318. doi: 10.1016/S0020-7322(98)00023-3

Merivee, E., Rahi, M., Luik, A., 1997. Distribution of olfactory and some other antennal sensilla in the male click beetle *Agriotes obscurus* L. (Coleoptera: Elateridae). Int. J. Insect Morphol. Embryol. **26**, 75–83. https://doi.org/10.1016/S0020-7322(97)00013-5

Merivee, E., Rahi, M., Luik, A., 1999. Antennal sensilla of the click beetle, *Melanotus villosus* (Geoffroy) (Coleoptera: Elateridae). Int. J. Insect Morphol. Embryol. **28**, 41–51. https://doi.org/10.1016/S0020-7322(98)00032-4

Merivee, E., Vanatoa, A., Luik, A., Rahi, M., Sammelselg, V., Ploomi, A., 2003. Electrophysiological identification of cold receptors on the antennae of the ground beetle *Pterostichus aethiops*. Physiol. Entomol. **28**, 88–96. https://doi.org/10.1046/j.1365-3032.2003.00320.x

Molles, M., 2012. Ecology: Concepts and Applications. McGraw-Hill, New York, NY.

Morak, S., Hegerl, G.C., Christidis, N., 2013. Detectable changes in the frequency of temperature extremes J. Clim., **26**, 1561–1574. https://doi.org/10.1175/JCLI-D-11-00678.1

Must, A., Merivee, E., Luik, A., Williams, I., Ploomi, A., Heidemaa, M., 2010. Spike bursts generated by the thermosensitive (cold) neuron from the antennal campaniform sensilla of the ground beetle *Platynus assimilis*. J. Insect Physiol. **56**, 412–421. https://doi.org/10.1016/j.jinsphys.2009.11.017

Must, A., Merivee, E., Mänd, M., Luik, A., Heidemaa, M., 2006a. Electrophysiological responses of the antennal campaniform sensilla to rapid changes of temperature in the ground beetles *Pterostichus oblongopunctatus* and *Poecilus cupreus* (Tribe Pterostichini) with different ecological preferences. Physiol. Entomol. **31**, 278–285. https://doi.org/10.1111/j.1365-3032.2006.00518.x

Must, A., Merivee, E., Mänd, M., Luik, A., Heidemaa, M., 2006b. Responses of antennal campaniform sensilla to rapid temperature changes in ground beetles of the tribe Platynini with different habitat preferences and daily activity rhythms. J. Insect Physiol. **52**, 506–513. https://doi.org/10.1016/j.jinsphys.2006.01.010

Nagel, M., Kleineidam, C.J., 2015. Two cold-sensitive neurons within one sensillum code for different parameters of the thermal environment in the ant *Camponotus rufipes*. Front. Behav. Neurosci. **9,** 240. doi: 10.3389/fnbeh.2015.00240

Neven, L.G., 2000. Physiological responses of insects to heat. Postharvest Biol. Technol. **21**, 103–111. https://doi.org/10.1016/S0925-5214(00)00169-1

Nishikawa, M., Yokohari, F., Ishibashi, T., 1985. The antennal thermoreceptor of the camel cricket, *Tachycines asynamorus*. J. Insect Physiol. **31**, 517–524. https://doi.org/10.1016/0022-1910(85)90107-6

Nishikawa, M., Yokohari, F., Ishibashi, T., 1992. Response characteristics of two types of cold receptors on the antennae of the cockroach, *Periplaneta americana*. J. Comp. Physiol. A **171**, 299–307. doi:10.1007/BF00223960

Piersanti, S., Rebora, M., Almaas, T.J., Salerno, G., Gaino, E., 2011. Electrophysiological identification of thermo- and hygro-sensitive

receptor neurons on the antennae of the dragonfly *Libellula depressa*. J. Insect Physiol. **57**, 1391–1398. doi: 10.1016/j.jinsphys.2011.07.005

Price, P.W., Denno, R.F., Eubanks, M.D., Finke, D.L., Kaplan, I., 2011. Insect Ecology: Behavior, Populations and Communities. Cambridge University Press, UK.

Roper, P., Bressloff, P.C., Longtin, A., 2000. A phase model of temperature-dependent mammalian cold receptors. Neural Comput. **12**, 1067–1093. DOI: 10.1162/089976600300015510

Ruchty, M., Romani, R., Kuebler, L.S., Ruschioni, S., Roces, F., Isidoro, N., Kleineidam, C.J., 2009. The thermo-sensitive sensilla coeloconica of leaf-cutting ants (*Atta vollenweideri*). Arthropod Struct. Dev. **38**, 195–205. doi: 10.1016/j.asd.2008.11.001

Schneider, E.S., Kleineidam, C.J., Leitinger, G., Römer, H., 2018. Ultrastructure and electrophysiology of thermosensitive sensilla coeloconica in a tropical katydid of the genus *Mecopoda* (Orthoptera, Tettigoniidae). Arthropod Struct. Dev. **47**, 482–497. https://doi.org/10.1016/j.asd.2018.08.002

Schulte, P.M., 2015. The effects of temperature on aerobic metabolism: Towards a mechanistic understanding of the responses of ectotherms to a changing environment. J. Exp. Biol. **218**, 1856–1866. doi: 10.1242/jeb.118851.

Sherman, S.M., 2001. Tonic and burst firing: dual modes of thalamocortical relay. Trends Neurosci. **24**, 122–126. https://doi.org/10.1016/S0166-2236(00)01714-8

Shields, V.D.C., Hildebrand, J.G., 1999. Fine structure of antennal sensilla of the female sphinx moth, *Manduca sexta* (Lepidoptera: Sphingidae). II. Auriculate, coeloconic, and styliform complex sensilla. Can. J. Zool. **77**, 302–313. https://doi.org/10.1139/z99-003

Steinbrecht, R.A., 1989. The fine structure of thermo-/hygrosensitive sensilla in the silkmoth *Bombyx mori*: receptor membrane substructure and sensory cell contacts. Cell Tissue Res. **255**, 49–57. https://doi.org/10.1007/BF00229065

Stocker, T.F., Qin, D., Plattner, G.K., Tignor, M.T., Allen, S.K., Boschung, J., Nauels, A., Xia, Y., Bex, B., Midgley, B.M., 2013. IPCC, 2013: Climate Change 2013: The Physical Science Basis. Contribution of Working Group I to the Fifth Assessment Report of the Intergovernmental Panel on Climate Change. Cambridge University Press, Cambridge.

Sunday, J.M., Bates, A.E., Kearney, M.R., Colwell, R.K., Dulvy, N.K., Longino, J.T., Huey, R.B., 2014. Thermal-safety margins and the necessity of thermoregulatory behavior across latitude and elevation. Proc. Natl. Acad. Sci. U.S.A. **111**, 5610–5615. https://doi.org/10.1073/pnas.1316145111

Swadlow, H.A., Gusev, A.G., 2001. The impact of 'bursting' thalamic impulses at a neocortical synapse. Nat. Neurosci. **4**, 402–408. https://doi.org/10.1038/86054

Thiele, H.U., 1977. Carabid Beetles in Their Environment. Zoophysiology and Ecology, vol. 10. Springer, Berlin, Germany. https://doi.org/10.1007/978-3-642-81154-8

Tichy, H., 1979. Hygro- and thermoreceptive triad in antennal sensillum of the stick insect, *Carausius morosus*. J. Comp. Physiol. **132**, 149–152. https://doi.org/10.1007/BF00610718

Tichy, H., 1987. Hygroreceptor identification and response characteristics in the stick insect *Carausius morosus*. J. Comp. Physiol. **160**, 43–53. https://doi.org/10.1007/BF00613440

Tichy, H., Kallina, W., 2010. Insect hygroreceptor responses to continuous changes in humidity and air pressure. J. Neurophysiol. **103**, 3274–3286. doi: 10.1152/jn.01043.2009

Tichy, H., Loftus, R., 1987. Response characteristics of a cold receptor in the stick insect, *Carausius morosus*. J. Comp. Physiol. A **160**, 33–42. https://doi.org/10.1007/BF00613439

Traugott, M., Benefer, C., Blackshaw, R., van Herk, W., Vernon, R., 2015. Biology, ecology, and control of elaterid beetles in agricultural land. Annu. Rev. Entomol. **60**, 313–334. doi: 10.1146/annurev-ento-010814-021035

Viatchenko-Karpinski, V., Gu, J.G., 2018. Effects of cooling temperatures and low pH on membrane properties and voltage-dependent currents of rat nociceptive-like trigeminal ganglion neurons. Mol. Pain **14**, 1–11. https://doi.org/10.1177/1744806918814350

Waldow, U., 1970. Elektrophysiologische untersuchungen an feuchte-, troken- und kälterezeptoren auf der antenne der wanderheuschrecke locusta. Z. Vgl. Physiol. 69, 249–283. https://doi.org/10.1007/BF00297962

Wang, Y., Li, D., Liu, Y., Li, X.-J., Cheng, W.-N., Zhu-Salzman, K. 2016. Morphology, ultrastructure and possible functions of antennal

sensilla of *Sitodiplosis mosellana* Géhin (Diptera: Cecidomyiidae). Journal of Insect Science, 16, 1–12. DOI: 10.1093/jisesa/iew080

Yokohari, F., 1978. Hygroreceptor mechanism in the antenna of the cockroach *Periplaneta.* J. Comp. Physiol. **124**, 53–60. https://doi.org/10.1007/BF00656391

Yokohari, F., Tateda, H., 1976. Moist and dry hygroreceptors for relative humidity of the cockroach, *Periplaneta americana* L. J. Comp. Physiol. **106**, 137-152. https://doi.org/10.1007/BF00620495

Yokohari, F., Tominaga, Y., Tateda, H., 1982. Antennal hygroreceptors of the honey bee, *Apis mellifera* L. Cell Tissue Res. **226**, 63–73. https://doi.org/10.1007/BF00217082

Yvon-Durocher, G., Caffrey, J.M., Cescatti, A., Dossena, M., Giorgio, P.D., Gasol, J.M., Allen A.P., Montoya, J.M., Pumpanen, J., Staehr, P.A., Trimmer, M., Woodward, G., 2012. Reconciling the temperature dependence of respiration across timescales and ecosystem types. Nature, **487**, 472–476. doi:10.1038/nature11205

Zauli, A., Maurizi, E., Carpaneto, G.M., Chiari, S., Merivee, E., Svensson, G., Di Giulio, A., 2016. Scanning electron microscopy analysis of the antennal sensilla in the rare saproxylic beetle *Elater ferrugineus* (Coleoptera: Elateridae). Ital. J. Zool. **83**, 338–350. doi: 10.1080/11250003.2016.1211766

9. KOKKUVÕTE

Ümbritseva keskkonna temperatuur mõjutab kõiki elusloodus organiseerituse tasemeid – geenidest ökosüsteemini. Temperatuuri tõusuga kiirenevad nii biokeemilised (Hochachka and Somero, 2002) kui ka ainevahetuslikud protsessid (Schulte, 2015), mis kutsuvad esile muutusi nii organismi füsioloogias kui ka käitumises (Denlinger and Yocum, 1998; Chown and Terblanche, 2006; Abram et al., 2017) ning erinevates ökosüsteemi protsessides (Brown et al., 2004; Yvon-Durocher et al., 2012). Eluprotsesside sõltuvus ümbritseva keskkonna termilisetest tingimusetest on lihtsamini prognoositav väikestel kõigusoojalistel loomadel nagu näiteks putukatel, kes erinevalt püsisoojalistest ei suuda oma kehatemperatuuri homöostaasi kaudu säilitada. Viimasel kümnendil on sellekohaste teadustööde maht kasvanud (e.g. Must et al., 2010; Huey et al., 2012; Gilbert et al., 2014; Sunday et al., 2014; Abram et al., 2017; DeLong et al., 2017). Suures osas on see huvi antud teema vastu tingitud vajadusest selgitada kuidas kliimasoojenemisega kaasnevad temperatuuri ekstreemumid ja keskmisest kõrgemad temperatuurid mõjutavad üksikorganisme ja ökosüsteeme (Morak et al., 2013; Stocker et al., 2013; Li et al., 2018). Samas põhimehhanismid ja viisid, kuidas kõigusoojalised organismid kõrgete temperatuuridega toime tulevad, pole veel päris täpselt teada.

Temperatuuril on oluline roll kõigusoojaliste organismide geograafilisel ja ökoloogilisel levikul (Price et al., 2011; Molles, 2012). Suurema viljasaagi saamiseks tuleb põllumajandusmaadel efektiivsemalt manipuleerida nii kasur- kui ka kahjurputukate käitumisega, selleks aga on vaja põhiteadmisi sensoorsetest mehhanismidest, mis on nende putukate (mikro-) elupaikade valiku, otsingulise käitumise ja termoregulatsiooni aluseks. Väikeste kõigusoojaliste jaoks, võivad mikroklimaatilised tingimused olla ebasoodsad ja isegi surmavad, seepärast peavad nad saama kiiret ja adekvaatset informatsiooni välistemperatuuride, eriti kõrgete temperatuuride kohta (Denlinger and Yocum, 1998; Chown and Terblanche, 2006; Abram et al., 2017). Kahjuks pole teada, kuidas putukad sh. põllumajanduslikult tähtsad jooksiklased ja naksurlased, ohtlikult kõrgeid temperatuure kodeerivad (Dhaka et al., 2006).

Temperatuuri tajumiseks kasutavad putukad ehituslikult erinevaid antennaalseid sensille, nt tsölokoonilisi, basikoonilisi, trihhoidseid jpt (Altner and Loftus, 1985; Merivee et al., 2003; Ruchty et al., 2009; Nagel and Kleineidam, 2015; Schneider et al., 2018). Kõige klassikalisemal juhul asetseb neis sensillides neuronite triaad, mis koosneb ühest termoneuronist ja kahest antagonistlikust hügroneuronist, niiske ja kuivaõhu neuronist (Altner and Loftus, 1985; Chapman, 1998; Piersanti et al., 2011). Eelnevate morfoloogiliste ja elektrofüsioloogiliste katsetega on näidatud, et jooksiklaste termo- ja hügroneuronid on innerveeritud antennaalsetes kupli kujulistes sensillides. Väliskujult sarnaseid sensille on täheldatud ka naksurlastel, kuid elektrofüsioloogilised katseandmed seni veel puuduvad. Varasemates töödes ja erinevatel putukaliikidel on ehituselt sarnaseid sensille nimetatud mitmeti. Selleks, et likvideerida terminoloogiline segadus, viiakse käesolevas töös läbi põhjalik morfoloogiline analüüs koos toetava elektrofüsioloogilise uuringuga.

Laboratoorsed katsed viidi läbi metsa-süsijooksiku (Pterostichus oblongopunctatus) ja tume-viljanaksuriga (Agriotes obscurus). Elektrofüsioloogilistes katsetes mõõdeti katsemardikate antenaalsetes kuppeljates sensillides paiknevate neuronite nii reaktsiooni erinevatele püsitemperatuuridele vahemikus 20–45 °C kui ka järskudele temperatuuri muutustele nii konstantse absoluutse kui relatiivse õhuniiskuse tingimustes. Närvimpulsside salvestused analüüsiti tarkvaraga Spike 2, impulsside valangulisus määratleti valangusiseste impulsside vahelise kauguse histogrammi meetodit kasutades. Antennaalsete kuppeljate sensillide siseehituse ja innervatsiooni iseärasuste väljaselgitamiseks kasutati elektronmikroskoopia SEM/FIB kombineeritud meetodit. Peenmorfoloogilised uuringud teostati Rooma Tre Ülikooli elektronmikroskoopialaboris (L.I.M.E.). Käitumiskatsed lineaarselt kasvavas temperatuuri tingimustes 20–45 °C (1 °C min^{-1}) viidi läbi tume-viljanaksuriga. Mardikate lokomotoorset aktiivsust videofilmiti USB veebikaameratega (Logitech Inc., USA) 5 kaadrit sekundis, kasutades arvutitarkvara Debut Video Capture (NCH Software, USA). Saadud videofilme analüüsiti programmiga Ethovion 11XT.

Doktoritööle püstitati järgmised hüpoteesid:

- Jooksiklaste ja naksurlaste tundlatel paiknevad kuplikujulised termo-hügrosensillid on kutikulaarosa siseehituselt ja innervatsioonilt sarnased.

- Elektrofüsioloogiliselt on naksurlaste antennaalses kuppeljas sensillis klassikaline neuronite triaad, mis koosneb külmaneuronist ja kahest antagonistlikust hügroneuronist.
- Ohtlikult kõrgetel temperatuuridel lülituvad naksurlaste temperatuuritundlikud külmaneuronid regulaarsete impulsside genereerimiselt temperatuurist sõltuvatele impulss-valangute genereerimisele.
- Jooksiklaste ja naksurlaste antagonistlikud hügroneuronid kodeerivad ainult niiskust ja on reaktsioonitüübilt unimodaalsed, neuronite reaktsioonid ei ole temperatuuri sõltuvuslikud.
- Antennaalsete külmaneuronite impulssvalangud on seotud mardikate käitumusliku termoregulatsiooniga.

Lähtuvalt hüpoteesidest olid käesoleva doktoritöö eesmärgid:
- Uurida metsa-süsijooksiku ja tume-viljanaksuri antennaalsete termo-hügrosensillide siseehitust kasutades FIB/SEM kombineeritud meetodit.
- Elektrofüsioloogilistes katsetes teha kindlaks tume-viljanaksuri termo-hügrosensillis paiknevate neuronite reaktsioonid temperatuurile ja niiskusele ning määrata nende modaalsus ja reaktsioonitüüp.
- Elektrofüsioloogiliste katseandmete põhjal määrata seos neuronite statsionaarse impulss-sageduse ja temperatuuri (20 kuni 45 °C) vahel.
- Elektrofüsioloogiliste katseandmete põhjal määrata metsa-süsijooksiku külmaneuroni impulss-valangulisuse tõenäosus erinevatel temperatuuridel (20–45 °C).
- Määrata seos metsa-süsijooksiku külmaneuroni erinevate valanguparameetrite (valangute sagedus, impulsside arv valangus, valangusiseste impulsside vahelise kauguse variatsioonikordaja, impulsi valangu tõenäosus, keskmine valangusiseste impulsside vaheline kaugus) ja temperatuuri (25–45 °C) vahel.
- Mardikate lokomotoorse aktiivsuse/temperatuuri kõveratelt määrata kindlaks kolm olulist lävitemperatuuri, millal toimus muutus mardikate käitumises: suurenenud lokomotoorse aktiivsuse algus (OELA), kriitiline termaalne maksimum (CTmax) ja täieliku halvatuse künnistemperatuur (TP).

Töö tulemused kinnitasid, et morfoloogiliselt on jooksiklaste ja naksurlaste tundla termo- ja hügrotundlikud sensillid identsed ning erinevad morfoloogiliselt putukate kõigist seni tuntud sensillitüüpidest. FIB/SEM andmetele tuginedes nimetati sensill antud töös kuppeljaks sensilliks (DSS, inglise keeles dome shaped sensilla).

FIB/SEM analüüs kinnitas, et nii jooksiklaste kui ka naksurlaste kuppeljaid sensille innerveerivad kolm neuronit: üks termo ja kaks niiskusneuronit. Mõõdukatel temperatuuridel teostatud elektrofüsioloogilised katsed näitasid, et kuppeljas sensillis paiknevad neuronid reageerivad temperatuurile ja niiskusele nagu tüüpilised külma-, niiske- ja kuivaõhu neuronid. Ohtlikult kõrgetel temperatuuridel (alates 35 (40) °C), aga muudab külmaneuron oma närviimpulsi tootmise rütmi regulaarselt valangulisele, mis võimaldab nii jooksikutel kui naksuritel üheselt kodeerida kõrgeid temperatuure. Oma bimodaalse loomuse tõttu nimetati külmaneuron käesolevas töös esmakordselt külma-kuumaneuroniks.

Elektrofüsioloogilised katsed näitasid, et jooksiklaste ja naksurlaste kuppeljate sensillide hügroneuronid (kuiva ja niiske õhu neuron) reageerivad nii niiskusele kui ka temperatuurile ja on oma olemuselt bimodaalsed. Sarnaselt külma-kuumaneuronile, lülitusid mõlemad hügroneuronid kõrgetel temperatuuridel 25 (30)°C regulaarsete närviimpulsside genereerimiselt ümber temperatuurisõltuvuslike impulss-valangute genereerimisele. Katsed näitasid, et mitmed valangute parameetrid on temperatuurisõltuvuslikud ja võivad hierarhiliselt ja ühemõtteliselt kodeerida ohtlikult kõrgeid temperatuure. Eelnevat arvesse võttes nimetati käesolevas doktoritöös mardikate kuppeljas sensillis paiknevad kuiva ja niiskeõhu neuron ümber kuiva-kuumaneuroniks ja niiske-kuumaneuroniks.

Käitumiskatsed näitasid, et mardikate kõrgendatud lokomotoorse aktiivsuse algus langeb kokku kuppeljate sensillide hügro-termoneuronite impulss-valangutele ümberlülitumise lävitemperatuuriga. Seega termo-hügroneuronite triaadi poolt genereeritud impulss-valangud on seotud mardikate käitumusliku termoregulatsiooniga.

10. ACKNOWLEDGMENTS

The study was supported by institutional research funding IUT36-2 of the Estonian Ministry of Education and Research; Estonian target financing project SF0170057s09, Estonian Science Foundation Grant No. 8685; Estonian State Forest Management forest protection project (T12115MIMK) and by the Development Fund of the Estonian University of Life Sciences (8PM170157PKTK).

I

PUBLICATIONS

Nurme, K., Merivee, E., Must, A., Sibul, I., Muzzi, M., Di Giulio, A., Williams, I., Tooming, E. 2015. Responses of the antennal bimodal hygroreceptor neurons to innocuous and noxious high temperatures in the carabid beetle, Pterostichus oblongopunctatus. Journal of Insect Physiology, 81, 1−13.

Journal of Insect Physiology 81 (2015) 1–13

Contents lists available at ScienceDirect

Journal of Insect Physiology

journal homepage: www.elsevier.com/locate/jinsphys

Responses of the antennal bimodal hygroreceptor neurons to innocuous and noxious high temperatures in the carabid beetle, *Pterostichus oblongopunctatus*

Karin Nurme [a,*], Enno Merivee [a], Anne Must [a], Ivar Sibul [b], Maurizio Muzzi [c], Andrea Di Giulio [c], Ingrid Williams [a], Ene Tooming [a]

[a] Institute of Agricultural and Environmental Sciences, Estonian University of Life Sciences, Kreutzwaldi Street 1, 51014 Tartu, Estonia
[b] Institute of Forestry and Rural Engineering, Estonian University of Life Sciences, Kreutzwaldi Street 1, 51014 Tartu, Estonia
[c] Department of Science, University of Roma Tre, Viale G. Marconi 446, I-00146 Rome, Italy

ARTICLE INFO

Article history:
Received 19 November 2014
Received in revised form 18 June 2015
Accepted 19 June 2015
Available online 20 June 2015

Keywords:
Electrophysiology
Peripheral spike bursting
FIB/SEM technique
Dome-shaped sensilla
Inner structure
Behavioural thermoregulation

ABSTRACT

Electrophysiological responses of thermo- and hygroreceptor neurons from antennal dome-shaped sensilla of the carabid beetle *Pterostichus oblongopunctatus* to different levels of steady temperature ranging from 20 to 35 °C and rapid step-changes in it were measured and analysed at both constant relative and absolute ambient air humidity conditions. It appeared that both hygroreceptor neurons respond to temperature which means that they are bimodal. For the first time in arthropods, the ability of antennal dry and moist neurons to produce high temperature induced spike bursts is documented. Burstiness of the spike trains is temperature dependent and increases with temperature increase. Threshold temperatures at which the two neurons switch from regular spiking to spike bursting are lower compared to that of the cold neuron, differ and approximately coincide with the upper limit of preferred temperatures of the species. We emphasise that, in contrast to various sensory systems studied, the hygroreceptor neurons of *P. oblongopunctatus* have stable and continuous burst trains, no temporal information is encoded in the timing of the bursts. We hypothesise that temperature dependent spike bursts produced by the antennal thermo- and hygroreceptor neurons may be responsible for detection of noxious high temperatures important in behavioural thermoregulation of carabid beetles.

1. Introduction

Temperature and humidity conditions are undoubtedly the most important environmental factors influencing geographical distribution and habitat selection in insects (Thiele, 1977; Lövei and Sunderland, 1996; Holland, 2002). Ground dwelling carabid beetles are very vulnerable to desiccation and high temperature injury (Thiele, 1977; Denlinger and Yocum, 1998; Hochachka and Somero, 2002; Robertson, 2004; Klose and Robertson, 2004; Chown and Terblanche, 2007). On entering direct sunlight, due to solar IR radiation, a 10-mg insect can heat up by 10 °C in only 10 s (Heinrich, 1993). The temperature at which total heat paralysis begins in various carabids lies in a narrow range between 47.4 and 51.7 °C (Thiele, 1977). Steep temperature gradients are common both above and below the ground surface, and the microclimatic conditions can be greatly modified, especially in areas with vegetation. In Estonia, on sunny summer days with air temperatures above 22 °C, maximum soil surface temperatures in sunlit areas may reach lethal high values above 50 °C while minimum soil surface temperatures in shaded areas below the foliage remain 30–40 °C lower (Must et al., 2006a). Brief forays into sunlit high temperature zones are readily tolerated, however, as long as the animal has the option of retreating frequently to a more moderate environment to prevent overheating and desiccation (Thiele, 1977; Denlinger and Yocum, 1998; Chown and Nicolson, 2004). Behavioural thermoregulation is a complex process that includes sensing of temporal and spatial variation in the thermal environment, and subsequent processing of environmental information (Cooper, 2002; Seebacher and Shine, 2004; Seebacher and Franklin, 2005). In *Pterostichus oblongopunctatus* (Fabricius, 1787) (Coleoptera, Carabidae), the subject of the current experiments, temperature preference depends on ambient air humidity and lies between 10 and 25 °C (Thiele, 1977). As a eurytopic forest species with a palaearctic distribution, the adults are more or less euryhygric to dry-preferring (Lindroth, 1986).

* Corresponding author.
E-mail address: karin.nurme@emu.ee (K. Nurme).

http://dx.doi.org/10.1016/j.jinsphys.2015.06.010
0022-1910/

In carabid beetles, the sensory neurons responsible for detection of ambient temperature are located on the surface of the antennae within dome-shaped or campaniform sensilla. These sensilla occur pairwise on the ventral surface of all nine flagellomeres, and in addition, 5–6 of them lie at the distal margin of the terminal flagellomere (Merivee et al., 2000, 2001, 2002). Both outer and inner structure of the dome-shaped sensilla has been described in the myrmecophilous carabid beetle *Paussus favieri* (Di Giulio et al., 2012). These sensilla are innervated by three neurons, one thermoreceptor (TN) and two hygroreceptor neurons. Electrophysiological experiments confirm the existence of two physiologically different types of hygroneurons: the dry neuron (DN) and the moist neuron (MN) (Merivee et al., 2010), and one thermoreceptor (cold) neuron (CN) (Merivee et al., 2003) in the antennal dome-shaped sensilla in various carabids. A similar triad of thermo- and hygroneurons has been found in various insects and spiders (Waldow, 1970; Tichy, 1979; Altner and Prillinger, 1980; Altner and Loftus, 1985; Tichy and Loftus, 1996; Tichy and Gingl, 2001).

Our knowledge on insect thermoreception is incomplete. Though, the firing rate of the CN increases with rapid temperature decrease and vice versa (Loftus, 1968; Merivee et al., 2003), it does not measure ambient temperature correctly. In the honeybee *Apis mellifera* L. and some carabid beetles, the firing rate of the CN decreases with temperature increase and, at high temperatures above 30–40 °C, spike production may fall to zero, especially when stimulated with a rapid temperature increase (Lacher, 1964; Merivee et al., 2003; Must et al., 2006a,b), making precise detection of dangerously high temperatures impossible. Second, in the American cockroach *Periplaneta americana* and some carabids, the stationary firing rate of the CN does not depend on temperature ranging from 20 to 35 (40) °C at all (Loftus, 1968; Must et al., 2006a,b). Third, the CN fires a high frequency phasic spike train (peak frequency burst) in response to a rapid temperature drop and adapts after several seconds to a frequency determined by the new steady temperature (Loftus, 1968; Merivee et al., 2003; Must et al., 2006a). The peak frequency of the initial spike burst depends primarily upon the initial temperature when the antenna is exposed to 25–32 °C, but above or below this range the extent of temperature change becomes prevalent. Thus, a particular peak frequency can be achieved by several different combinations of initial temperature and magnitude of temperature drop. This ambiguity and significant fluctuations in frequency at steady temperature make it unlikely that the CN is a useful thermometer (Loftus, 1968). These results suggest that additional noxious high temperature encoding mechanisms should be hidden in the spike trains of the neuron triad. In this context, it is of interest that at high temperatures the antennal CNs of the carabid beetle *Platynus assimilis* switch from regular spiking to a bursting manner of firing (Must et al., 2010). The threshold temperature of spike bursting varies in different neurons from 25 to 47 °C. Interspike interval (ISI) analysis showed that the burstiness of the spike trains are temperature dependent and may precisely encode noxious high temperatures in a graded manner.

Hygroneurons may also be involved in thermoreception of insects. In *P. americana* and *Locusta migratoria*, the DN responds to both temperature and humidity resulting in such excessive ambiguity that the unit has been termed bimodal (Waldow, 1970; Loftus, 1976; Altner and Loftus, 1985). The MN of *Carausius*, *Apis* and *Locusta* is another bimodal unit whose firing rate is affected by both humidity and temperature (Lacher, 1964; Waldow, 1970; Altner and Loftus, 1985; Tichy, 1987). By contrast, relative humidity alone has been shown to be an adequate stimulus for the antennal MN of *P. americana* (Yokohari and Tateda, 1976; Yokohari, 1978). No research has been conducted on the temperature sensitivity of the hygroneurons in carabids. The biological significance of bimodality of the hygroneurons remains unclear.

The aim of this study was to test the sensitivity of the antennal DN and MN to temperature in *P. oblongopunctatus*. The electrophysiological experiments were carried out in the range of air temperatures from 20 to 35 °C which approximately falls within the range of preferred temperatures of the species (Thiele, 1977). The responses of the hygroneurons to temperature were measured in two ambient humidity situations: at constant relative (RH) and absolute humidity (AH) conditions, respectively. Results of the experiments are presented in this paper.

2. Materials and methods

2.1. Test beetles

Adult beetles were collected from a local population in southern Estonia before they left their preferred overwintering sites in brown-rot decayed wood in spring 2014. The beetles were kept in 20 × 30 × 10 cm plastic boxes filled with moist pieces of brown-rotted wood and moss at 5 °C for a couple of weeks until they were used in tests. Three to four days prior to experiments, the beetles were exposed to room temperature (20 °C), fed with larvae of *Tenebrio molitor* and given tap water to drink every day.

For electrophysiological experiments, each test beetle was immobilised by placing it firmly into a conical tube made of thin sheet-aluminium of a size that allowed its head and antennae to protrude from the narrower end of the tube. The wider rear end of the tube was blocked with a piece of plasticine to prevent the beetle from retreating out of the tube. The antennae of the beetle were fastened horizontally onto the edge of a special aluminium stand with tiny amounts of beeswax so that dome-shaped sensilla at the tip of the terminal flagellomere were visible from above under a light microscope, were well exposed to stimulating airstreams, and were readily accessible for microelectrode manipulation from the side.

2.2. Electrophysiology

2.2.1. Single sensillum recordings

Tungsten wire (0.08 mm diameter) microelectrodes were sharpened electrolytically in a concentrated KOH solution. The indifferent electrode was inserted into the antennal lumen at the base of the antennal flagellum. The recording electrode was thrust into the base of the dome-shaped sensillum at the distal margin of the terminal flagellomere using the micromanipulator DC-3KS with push-button control (Stoelting CO., USA) under visual control with the upright electrophysiological light microscope Eclipse FN1 (Nikon, Japan) at a magnification 500–1000×. The microscope was equipped with the ITS-FN1 Physiostage (Nikon, Japan) consisting of the X-Y Translator and stainless steel Stage mounted on the Passive Anti-Vibration ScienceDesk (ThorLabs, UK). All experiments were performed in the 100 × 120 × 100 cm Faraday Cage FAR01 (ThorLabs, UK).

Spikes picked up by the recording electrode and initially amplified (input impedance 10 GΩ) by a custom-made Preamplifier Board (Interspectrum, Estonia) were led to input of the main amplifier ISO-DAM 8A (World Precision Instruments, USA), filtered with a bandwidth set at 10–3000 Hz, monitored on an oscilloscope screen, and relayed to a computer via an A/D input board DAS-1401 (Keithley, Taunton, Massachusetts) for data acquisition and storage using testpoint software (Capital Equipment Corp., Billerica, Massachusetts) at a sampling rate of 10 kHz (channel 1). The recordings were made from one sensillum of each test beetle. The number of tested beetles (*N*) is shown directly everywhere

in the text (Section 3) and in the legends of figures together with the results of statistical analysis. For analysis of recorded spike trains Spike 2 software (Cambridge Electronic Design Ltd, UK) was used.

2.2.2. Stimulation and control of air humidity and temperature

The stimuli were presented by way of one or two airstreams depending on the experiment, initially driven through separate units U1 and U2 to be set at a wide range of RH levels (Fig. 1). Thereafter, the airstream from U1 or U2 was led to the terminal outlet tubes TOT1 or TOT2 which were heated by the heating coils HC1 and HC2 to a necessary level of temperature. Finally, the airstreams flowed out of 8-mm nozzles at a velocity of 2 m s^{-1}. An electromagnetic air valve (Model 062 4E1, Humphrey Products, MI, USA) EMV and a digital timer (Model 4030, Kaiser, Germany) were used for rapid switching between the airstreams from units U1 and U2. When firing rates of the antennal thermo- and hygroreceptor neurons were measured at different steady temperatures, the dome-shaped sensilla to be adapted before each recording were exposed to each tested temperature for 10 min. The thermo- and two hygroreceptor neurons from each tested sensillum were subjected to an electrophysiological identification by differences between their responses to a rapid change in RH (Fig. 2). A custom made electronic airflow hygrometer (Interspectrum, Estonia) based on the LinPicco™ capacitive humidity analogue module A01 (response time < 5 s, accuracy < ±3% RH) (Innovative Sensor Technology, Switzerland) was used for measurements of the airstreams RH at 20 °C. RH decreases with ambient temperature increase. To hold the airstream RH in TOT1 and TOT2 at the same constant level (35% in our constant RH experiments) at various higher temperatures from 20 to 35 °C it was necessary to increase the airstream RH at 20 °C directly before the heating coil, respectively (Fig. 1). Respective recalculations were made for 25, 30 and 35 °C. For example, to set RH 35% at 35 °C in TOT1 and TOT2 the measured RH at 20 °C should be 80.16%. Signals from the hygrometers were led to the second and third channel of the DAQ board DAS-1401.

For stimulation of the dome-shaped sensilla, the orifices of TOT1 and TOT2 were placed 10 mm from the tip of the terminal flagellomere. Both the terminal dome-shaped sensilla and a copper-constantan thermocouple made of 0.08 mm wire were located at the intersection of the two air streams, with the thermocouple junction 1 mm away from the inserted recording microelectrode. The signal generated and amplified by a thermocouple circuit, led to the fourth channel of the DAQ board DAS-1401 and was stored on a PC hard disc for further data management and calculation of the temperatures.

2.2.3. Focused ion beam/scanning electron microscope (FIB/SEM)

The dome-shaped sensilla on antennae of *P. oblongopunctatus* were analysed with the Dualbeam (FIB/SEM) Helios Nanolab (FEI Company, Eindhoven, The Netherlands) at the L.I.M.E. (Roma Tre University, Rome, Italy). The FIB/SEM is equipped with two columns including one electron beam (SEM column) and one ion beam (FIB column), oriented at 52°, and focused on the same point of the sample. This apparatus is capable of selectively ablating (milling process) a previously marked region of the sample by using a focused ion current from a gallium source. The milling process can be interrupted every few nanometers to take high-resolution images to the cross sections by the SEM column.

This instrument was used for both, (1) obtaining high resolution SEM images of the dome-shaped sensilla from critical point dried and gold sputtered antennae, and (2) analysing the sensillum ultrastructure from antennae previously fixed and embedded in epoxy resin. The two procedures are reported in the following:

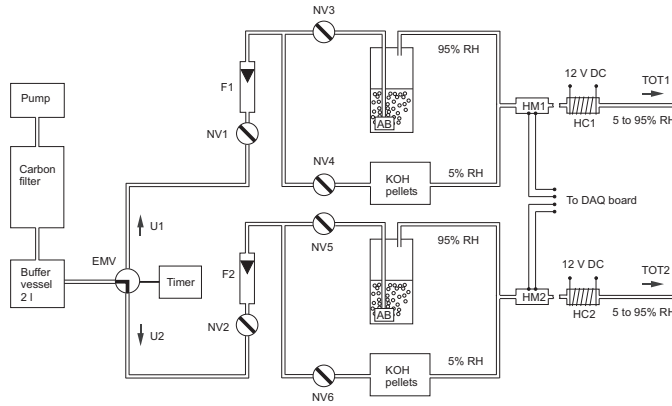

Fig. 1. Flow diagram illustrating the production of two airstreams with pre-adjustable air temperature and humidity levels. The air from a diaphragm gas pump Fp 09 (VEB Elmet, Hettstedt, Germany) was cleaned by a 0.5 L carbon filter. A 2 L buffer vessel served to smooth fluctuations in air pressure caused by the pump. Further, the air was divided into two streams and driven through two separate identical units U1 and U2. The flow rates were adjusted by needle valves NV1 and NV2, and monitored by flowmeters F1 and F2. In both units, the air stream was divided in two substreams. One substream was bubbled out through an aquarium bubbler immersed in water in a 1 L wash bottle. The water level above the bubbler was minimal (10 mm) and kept constant. RH of the bubbled air stream was approximately 95%. The second substream was conducted through the 0.5 L air dryer filled with KOH pellets as desiccant. RH of the dried air stream was almost 5%. The two substreams were mixed by the needle valves NV3, NV4, NV5 and NV6 in a single stream enabling adjustment of RH in the outlet tube of U1 and U2 from 5% to 95%. Direct current heating coils HC1 and HC2 enabled adjustment of air temperature in the metal (aluminium) part of the terminal outlet tubes TOT1 and TOT2 from room temperature (20 °C) to 50 °C. EMV, electromagnetic air valve; AB, aquarium bubbler; DC, direct current from a current source; HM1 and HM2, air flow hygrometers; DAQ board, A/D data aquisition board connected to a computer.

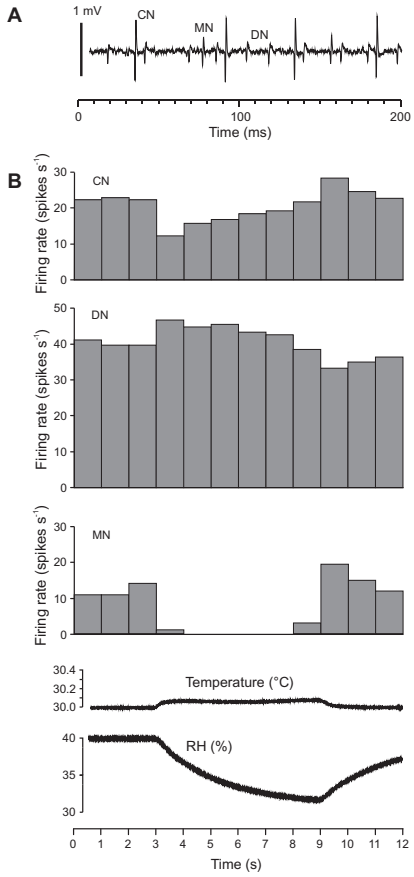

Fig. 2. Electrophysiological identification of the spikes generated by the temperature sensitive neuron and two antagonistically responding hygroreceptor neurons in the antennal dome-shaped sensillum. (A) A 200 ms fragment of the original 12 s sample recording from an antennal dome-shaped sensillum of *P. oblongopunctatus* at 30 °C, RH 40%. Usually, activity of three neurons with different spike amplitudes were observed. The spikes with the largest amplitude are produced by the temperature sensitive (cold) neuron (CN). Small spikes arise from two hygroreceptor neurons (moist and dry air neurons). (B) Antagonistic response of the two hygroreceptor neurons with small spike amplitude to a rapid change in RH. Firing rate of the dry air neuron (DN) increased with decrease in RH. The opposite was observed in the moist air neuron (MN) response, its firing rate drastically decreased when RH decreased. For comparison, the upper diagram shows simultaneous response of the CN of the same sensillum. To discriminate between the small spikes produced by the MN and DN the response of the neurons to a rapid change in air humidity was tested for each dome-shaped sensillum studied.

1. For the high resolution SEM images of the sensilla the antennae, once removed from dried specimens, were re-hydrated, kept overnight in a detergent water solution, cleaned by ultrasounds for 15 s, rinsed 3 times in distilled water, dehydrated by passing through a graded ethanol series, critical point-dried in a Balzer Union CPD 030 unit, gold coated in an Emitech K550 unit, and finally examined by using the field emission SEM column of the dualbeam FIB/SEM, with secondary electrons (SE) and an operating voltage of 5 kV.
2. For FIB ultrastructural analysis of the antennal sensilla embedded in Epon-Araldite resin we followed a procedure similar to the one normally used for TEM preparation (Di Giulio et al., 2012). Ten specimens (5 males and 5 females) were CO_2 anesthetized and immediately immersed in Karnovsky's glutaraldehyde. The antennae were removed from the head; each antennal flagellum was cut transversally in 3 parts, to improve penetration, and held in Karnovsky's fixative for 2 h at 4 °C. They were then rinsed overnight in cacodylate buffer, post-fixed in 1% osmium tetroxide for 1 h at 4 °C and rinsed in a cacodylate buffer. Samples were stained en bloc with 2% aqueous uranyl acetate for about 2 h at 4 °C and dehydrated in a graded ethanol series followed by embedding in Epon-Araldite with propylene oxide as a bridging solvent. Thick sequential antennal slices of about 15–20 μm were cut with a glass knife on a Leica Ultracut T ultramicrotome, and mounted on a stub by using self-adhesive carbon disks. Antennal slices were gold coated in an Emitech K550 unit and analysed at FIB/SEM. Dome-shaped sensilla present on each thick slice were cross sectioned by the focused gallium ion beam (FIB) operated at 30 kV and 0.92 nA; SEM pictures were taken by using backscattered electrons (BSE) and a through-the-lens (TDL) detector to the cross section approximately every 100 nm of milling (horizontal feed), with an operating voltage of 2 kV, at a working distance of 2 mm, and an applied current of 0.17 nA.

2.2.4. Data management and analysis

The spikes from several sensory neurons innervating antennal dome-shaped sensilla were distinguished by differences in their amplitude and shape using Spike 2 software (Cambridge Electronic Design Ltd, UK). The spikes with the largest amplitude were produced by the cold neuron (CN). To discriminate between the small spikes produced by the two hygroreceptor neurons the response of the neurons from each tested sensillum to a rapid change in RH was recorded and analysed as shown in Fig. 2. The firing rate of the DN was usually higher compared to that of the MN. Its firing rate increased with RH decrease in contrast to the MN in which the firing rate decreased with RH decrease. Usually spikes of the MN were larger compared to those of the DN but frequently the opposite was observed. When two spikes from two different neurons were superimposed a special option of Spike 2 software (Collision analysis) and visual inspection were involved in spike sorting. The instantaneous frequency (Hz) of spikes was calculated as the reciprocal of the period between two successive spikes. Interspike intervals (ISI) of the recorded spike trains were analysed. An interspike interval histogram was used to detect critical interval values (ISI threshold) in the distribution represented by the gap between short intervals within a burst and the longer intervals between bursts (Cocatre-Zilgien and Delcomyn, 1992; Bakkum et al., 2014). Coefficient of variation of ISIs (CV), mean number of spikes in a burst (NSB), mean ISI in a burst (ISIB), mean number of bursts per second (NBS) and the percentage of bursty spikes (PBS) were used to compare burstiness of the recorded spike trains. One way ANOVA and Fisher LSD tests were used to evaluate the effect of temperature on the responses of the thermo- and hygroreceptor neurons and to calculate the significance of different

means, respectively. All mean responses were accompanied by a standard error bar (SE).

3. Results

3.1. General morphology of the antennal dome-shaped sensilla using SEM/FIB technology

Electrophysiological recordings were made from the dome-shaped sensilla located in a row at the apical margin of the terminal flagellomere in *P. oblongopunctatus* (Fig. 3A and B). The diameter of the low dome was typically 6.5 μm (Fig. 3C). Externally, it consists of the dome base, central cap and a tiny tip (diameter 0.5 μm; height 0.3 μm) of the aporous conical peg approximately 3 μm in length located at the bottom of the narrow sensillum socket with the base diameter of 3.3 μm (Fig. 3D). Directly below the peg base, perikarya of two hygroreceptor neurons of equal size (diameter 1.6 μm) were located (Fig. 3C) sending their unbranched dendrites through the peg cavity up to the tip of the peg (Fig. 3E and F). In addition to the dendrites from two hygroreceptor neurons, numerous dendritic branches of a thermoreceptor neuron also entered deeply into the peg cavity (Fig. 4A). The branches were strongly lamellated at the base of the peg (Fig. 4B). A generalised diagram of the antennal dome-shaped sensillum of *P. oblongopunctatus* is represented in Fig. 5.

3.2. Response of the thermo- and hygroreceptor neurons from antennal dome-shaped sensilla to different levels of steady temperature at constant AH conditions

In the constant AH experiment, firing rates displayed by the antennal thermo- and hygroreceptor neurons at various steady temperatures were measured at AH 12.15 g m^{-3} which is equal to RH 70% at 20 °C (Fig. 6A–C). A 3.8-fold decrease in firing rate, from 23.6 to 6.2 spikes s^{-1}, was observed in the MN with temperature increase from 20 to 35 °C (Fig. 6A; one way ANOVA: $F_{3,53} = 22.69$; $p < 0.05$; $N = 15$). However, the difference between the firing rates measured at 30 and 35 °C, was statistically not significant (Fisher LSD, $p > 0.05$, $N = 15$).

By contrast, the firing rate of the DN significantly increased with temperature increase (Fig. 6B; one way ANOVA: $F_{3,53} = 3.51$; $p < 0.05$; $N = 15$) from 38.3 to 54.3 spikes s^{-1} which indicates a 1.4-fold change in neural activity only. However, the firing rates displayed at 20 and 25 °C did not differ significantly (Fisher LSD: $p > 0.05$, $N = 15$). The firing rate of the CN almost linearly decreased from 30.6 to 8.4 spikes s^{-1} when temperature increased from 20 to 35 °C (Fig. 6C; one way ANOVA: $F_{3,53} = 21.48$; $p < 0.05$; $N = 15$). The 3.6-fold change in neural activity was almost equal to that observed in the MN.

3.3. Response of the antennal thermo- and hygroreceptor neurons to steady temperature in the constant RH experiment

In this experiment, firing rates produced by the antennal thermo- and hygroreceptor neurons at various steady temperatures were constantly recorded at RH 35%. Both of the hygroreceptor neurons showed very different temperature/response curves compared to those which were observed in the constant AH experiment. In the MN, a linear, 2.4-fold increase in firing rate from 10.2 to 24.9 spikes s^{-1} was observed when temperature increased from 20 to 35 °C (Fig. 6D; one way ANOVA: $F_{3,53} = 15.16$; $p < 0.05$; $N = 15$). On the other hand, no changes were observed in firing rate of the DN (Fig. 6E). Its firing rate was close to 45 spikes s^{-1} independent of temperature (one way ANOVA: $F_{3,53} = 0.15$; $p = 0.92$; $N = 15$).

Spike production of the CN showed an 1.9-fold decrease from 30.8 to 16.0 spikes s^{-1} when temperature was increased from 20 to 35 °C (Fig. 6F; one way ANOVA: $F_{3,53} = 13.06$; $p < 0.05$; $N = 15$). Thus, its firing rate decreased significantly more slowly with temperature increase in constant RH conditions compared to that which was observed at constant AH (one way ANOVA: $F_{4;25} = 4{,}81$; $p = 0.005$). The difference between the firing rates shown by the CN at constant AH and RH grew remarkably larger towards higher temperatures (Fig. 6C and F).

3.4. Preliminary observations on high temperature induced spike bursting in the antennal hygroreceptor neurons

At a steady 20 °C, antennal thermo- and hygroreceptor neurons of *P. oblongopunctatus* fired in a regular manner. The ISIs of the neurons varied to a greater or lesser extent but no spike bursts were observed (Fig. 7A). The first indications of spike bursting in the hygro- and thermoreceptor neurons were observed at a steady temperature of 25 °C. In the case of spike bursting, intra- and interspike intervals form two separate maxima in the ISI histograms. Usually, spike bursting in hygroreceptor neurons started at lower temperatures compared to that in the CN (Fig. 7B). When air temperature was increased by 5 °C steps from 20 to 35 °C it was the DN which was the first of the three neurons to switch from regular spiking to a bursting manner of firing. When the two hygroreceptor neurons started to produce spike bursts at the same temperature burstiness of the DN was higher compared to that of the MN i.e. CV of ISIs, NSB and NBS of the DN were higher and ISIB of the DN was shorter compared to those of the MN (Fig. 7B). It was also observed that burstiness of the spike trains generated by the two hygroreceptor neurons increased with temperature increase (Fig. 7B and C), i.e. CV of ISIs, NSB and NBS increased and ISIB decreased when temperature increased.

In the experiments when air temperature was rapidly increased from one high temperature level above 30 °C to another it was frequently observed that the antennal CN stopped to fire as demonstrated by a sample recording in Fig. 8A, B and E. At the same time, temperature dependent spike production by the hygroreceptor neurons or by the DN alone continued in a bursting manner (Fig. 8A–D). As demonstrated by Fig. 8C, high temperature induced change in burstiness of the spike train generated by the DN was a rearrangement of the pattern of spiking without any considerable changes in firing rate of the neuron. However, in this case, no clear indications of spike bursting were observed in the spike train produced by the MN (Fig. 8D). Both high temperature induced spike bursting and termination of spike production observed in the antennal thermo- and hygroreceptor neurons were reversible responses. The initial pattern of spike generation recovered immediately when temperature after the heating was lowered to the initial level again (Fig. 9A–D).

The percentage of bursting thermo- and hygroreceptor neurons increased with stepwise increase of steady temperatures especially quickly at temperatures above 30 °C (Fig. 10A–C). It appeared that the percentage of bursting DNs was noticeable higher compared to the percentage of the bursting MNs and CNs, at a steady temperature of 35 °C, 30.1%, 8.1% and 9.3%, respectively. In the experiment with rapid temperature increase from 30 to 35 °C, the percentages of bursting hygro- and thermoreceptor neurons were even higher, 73.3%, 34.5% and 44.1% in the DN, MN and CN, respectively (Fig. 10D). These results show that high temperature induced temperature dependent spike bursting in antennal hygroreceptor neurons was common enough to be ignored. Our results suggest that high temperature induced spike bursts of hygroreceptor neurons could contribute to quick and precise sensing of high temperatures

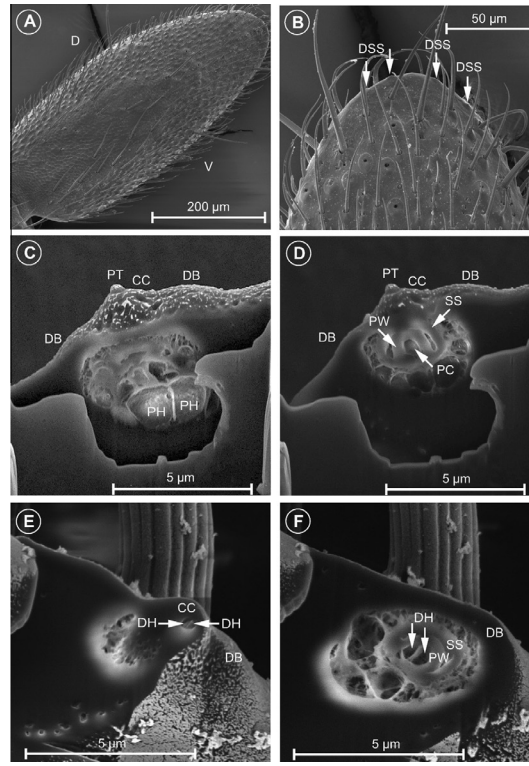

Fig. 3. Location and fine structure of the antennal dome-shaped sensilla in *P. oblongopunctatus* demonstrated by the SEM-FIB combined technique. (A) General view of the terminal flagellomere. (B) Side view of the apex of the terminal flagellomere with a group of dome-shaped sensilla at a higher magnification. (C) Side view of the dome-shaped sensillum. The cut made at 45° below the sensillum demonstrates two hygroreceptor neurons innervating the small central peg. (D) Side view of the same sensillum. The cut made at the height of the peg base demonstrates the cuticular walls of the sensillum socket and non-perforated peg base. Inside the conical peg a cavity with a diameter of 0.44 µm is visible. Note that the peg base and the bottom of the peg socket fuse. (E) An oblique section through the upper part of the central cap of the dome-shaped sensillum demonstrating that two dendrites from the hygroreceptor neurons reach up to the tip of the conical peg. (F) An oblique section through the peg base at the level where the two dendrites of the hygroreceptor neurons enter inside the peg cavity. Abbreviations: D, dorsal side of the flagellomere; DB, dome base; DH, dendrite of the hygroreceptor neuron; DSS, dome-shaped sensillum; CC, central cap of the dome; PC, peg cavity; PH, perikarya of the hygroreceptor neurons; PT, tip of the conical peg; PW, peg wall; SS, wall of the sensillum socket; V, ventral side of the flagellomere.

in *P. oblongopunctatus* especially in those dangerous situations when spiking activity of the CN is low or absent.

4. Discussion

The inner structure of the antennal dome-shaped sensilla in *P. oblongopunctatus* has been described for the first time. As shown by the SEM-FIB combined technique, two hygroneurons and one thermoneuron reside in these sensilla. Specific ultrastructural features show that the antennal dome-shaped sensilla of *P. oblongopunctatus* resemble the antennal thermo- and hygroreceptive sensilla of the carabid *P. favieri* (Di Giulio et al., 2012) and many other insects though variously named by different authors (Altner and Prillinger, 1980; Altner and Loftus, 1985; Chapman, 1998; Nation, 2002).

Insect peripheral thermo- and hygroneurons may respond to stimuli of more than one modality. Our results show that temperature also strongly affects spike production of the two hygroneurons but differently in the DN and MN. At a constant RH, firing rate of the MN strongly increases with temperature increase, in the range of 20–35 °C, at least. In contrast, the mean firing rate of the DN is hardly affected by temperature which makes it a better hygrometer than the ambiguous MN. Hygroneurons responding to both air humidity and temperature have been termed bimodal (Loftus, 1976) and they are widely distributed in various insects

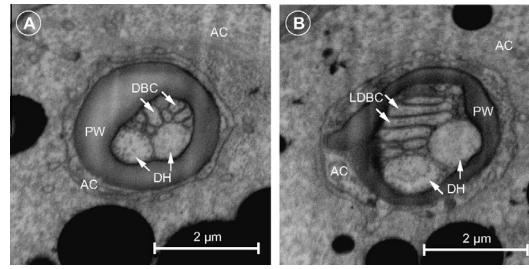

Fig. 4. Innervation of the antennal dome-shaped sensillum demonstrated by combined SEM-FIB technique. (A) Cross section through the peg base. (B) Cross section through the peg base somewhat deeper than (A). Abbreviations: AC, auxiliary cell; DBC, dendritic branches of the cold neuron; DH, unbranched dendrites of the hygroreceptor neurons; LDBC, lamellated dendritic branches of the cold neuron; PW, peg wall at the level where the peg base and the bottom of the peg socket fuse.

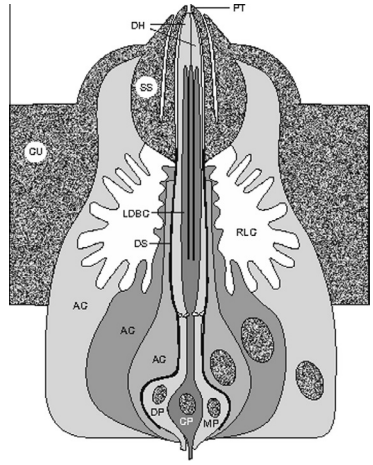

Fig. 5. Diagram of the antennal dome-shaped sensillum in adults of *P. oblongopunctatus*. AC, auxiliary cells; CU, cuticle; CP, DP and MP, perikarya of the cold neuron, dry neuron and moist neuron, respectively; DH, unbranched dendrites of the two hygroreceptor neurons (dry and moist neuron); LDBC, lamellated dendritic branches of the cold neuron; DS, dendritic sheath; RLC, receptor lymph cavity; PT, tip of the peg; SS, sensillum socket.

(Waldow, 1970; Altner and Prillinger, 1980; Altner and Loftus, 1985; Tichy, 1987; Tichy and Loftus, 1990; Chapman, 1998; Tichy and Kallina, 2013). The occurrence of bimodal CNs have been established on the antennae of the stick insect *Carausius morosus*. They respond with an increase in activity when either the temperature or the partial pressure of water vapour in ambient air is suddenly reduced (Tichy, 2007). In contrast, at constant 23 °C, over a wide range of ambient air humidity levels (RH 20–80%), the CN of *P. oblongopunctatus* does not respond to changes in RH (Merivee et al., 2010), but its spike production may be significantly affected by air humidity conditions at temperatures above 30 °C.

At constant air AH conditions, the responses of the antennal hygroneurons of *P. oblongopunctatus* to temperature considerably differ from those observed at a constant RH. Reputedly, when ambient air AH is held constant, air RH decreases with temperature increase. Therefore, air temperature and RH in opposite directions affect spike production of the MN, and the effect of RH change is prevalent, the stimulus/response curve is falling. In contrast, firing rate of the DN increases with temperature increase probably due to the concurrent RH decrease alone.

Neural pathways and central processes of temperature sensation underlying behavioural thermoregulation of insects remain poorly understood. Also, it remains an open question what is the biological relevance of bimodality widely distributed in insect thermo- and hygroneurons. Conclusive identification of the receptor neurons by which insects monitor innocuous and noxious environmental temperatures, and even whether and how they routinely use such information in their behavioural activities, is tentative or sparse (Nation, 2002; Dhaka et al., 2006; Dillon et al., 2009; Must et al., 2010).

Vertebrates can sense environmental temperature via specialised neurons in the peripheral nervous system that project to the skin. Temperature sensitive neurons divide into two classes: innocuous and noxious thermoreceptors. ThermoTRPs, a subset of the transient receptor potential family of ion channels, are expressed in sensory neurons and in keratinocytes of skin epithelial cells. There exist four heat-activated channels (TRPV1–4) and two cold activated channels (TRPM8 and TRPA1). Each thermoTRP has unique characteristics, highlighted by a distinct temperature threshold of activation (Dhaka et al., 2006; Talavera et al., 2008). TRPV1 (43 °C) and TRPV2 (52 °C) have properties consistent with noxious heat sensors. Both TRPV3 (33 °C) and TRPV4 (25–34 °C) are required for innocuous warm sensation. In mice, TRPV3 and TRPV4 are both involved in thermotaxis response for selection of preferred warm temperatures whereas all three, TRPV1, TRPV3 and TRPV4, seem to have a role in avoidance of noxious hot temperatures (Dhaka et al., 2006). Various thermoTRP channels are also implicated in thermosensation and in thermotaxis behaviour of the nematode *Caenorhabditis elegans* and the fruit fly *Drosophila melanogaster* (Dhaka et al., 2006; McKemy, 2007; Dillon et al., 2009).

In insects, the occurrence of separate peripheral thermoreceptor neurons for innocuous and noxious high temperatures have been demonstrated in rare cases only (Dillon et al., 2009). Adult *D. melanogaster* has two thermosensors, one in fly antennae that mediates the preference for 24 °C and a second that drives flies away from noxious high temperatures above 31 °C (Sayeed and

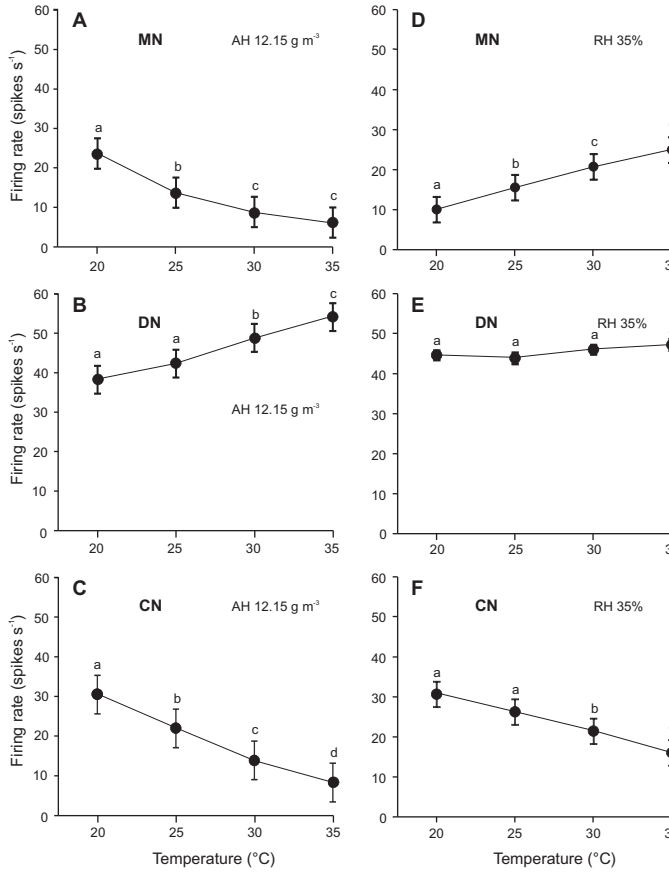

Fig. 6. Stationary firing rates of the antennal hygro- and thermoreceptor neurons of *P. oblongopunctatus* at different air temperatures. (A–C) Neural activity measurements performed at constant absolute humidity condition (12.15 g m^{-3}). Remember that under constant AH conditions, RH decreases when temperature increases. (D–F) Neural activity measured at constant relative humidity (35%). Different letters indicate significantly different means at $p < 0.05$ (Fisher LSD test, $N = 15$). Vertical bars show standard errors of the means. MN, DN and CN refer to the moist air, dry air, and temperature sensitive (cold) neurons, respectively.

Benzer, 1996). However, the location of the second temperature sensitive unit remains unknown. Anatomically, *Drosophila* larvae probably detect painfully high temperatures above 39 °C in both the central nervous system and in highly arborized peripheral neurons beneath the thin epidermis (Tracey et al., 2003). No specialised thermoreceptors for noxious high temperatures have been reported in other insects, including carabid beetles.

Behavioural responses to rising temperature have been well documented in the arctic-alpine seed bug *Nysius groenlandicus* (Böcher and Nachman, 2001). This thermophilous insect displays a wide spectrum of behavioural responses induced by various temperatures. It is unlikely that all the repertoire of various behaviours is guided by different levels of the mean firing rate of one type of thermoreceptor (cold) neurons only. Probably, in insects, there exist different neural pathways and mechanisms for coding innocuous and noxious ambient temperatures similar to that of vertebrate animals.

Existing data suggest that in some carabids, stationary firing rate of the antennal CN mainly codes innocuous temperatures and spike bursts of the same neuron code noxious high temperatures. The range of preferred temperatures for adults of eurythermic *P. oblongopunctatus* is rather wide, reaching from 10 to 25 °C

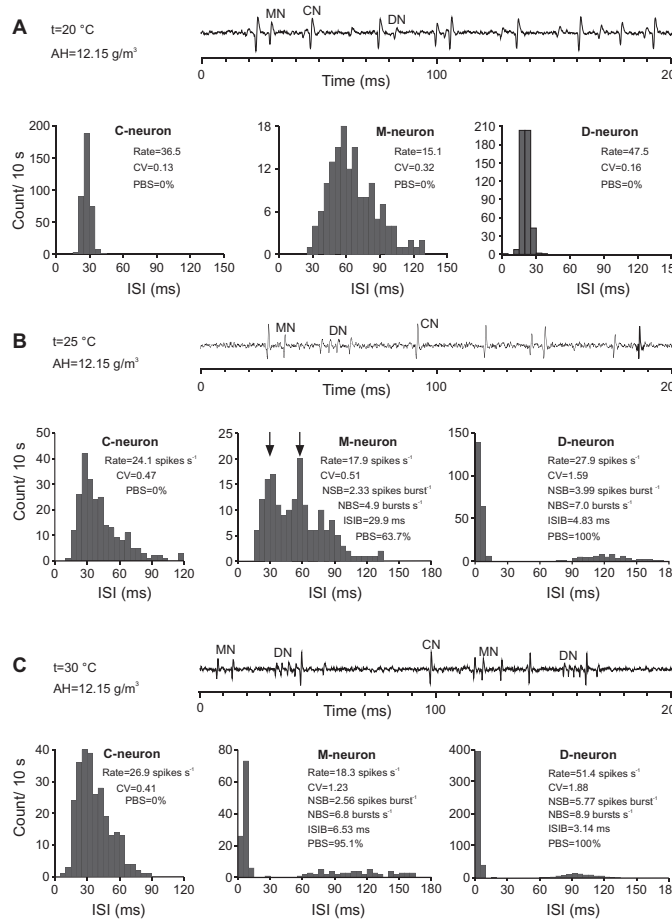

Fig. 7. Sample recordings from the antennal dome-shaped sensilla of *P. oblongopunctatus* demonstrating high temperature induced spike bursting produced by the hygroreceptor neurons at constant temperature and AH. (A) At 20 °C, moist air, dry air, and cold neuron always discharged in a regular manner. ISI histograms showed one maximum which is an indication that no spike bursting occurred. CV values of ISIs were low. (B) At 25 °C, first indications of spike bursting generated by the hygroreceptor neurons were observed. ISI histograms of the MN and DN had two maxima and high CV values. Left and right maxima in the histograms show maxima for intra- and interburst intervals, respectively. Threshold ISI values for intraburst intervals were 42.5 and 15 ms for MN and DN, respectively. Note that burstiness of the DN was higher than that of the MN. CN was firing in a regular manner. (C) At 30 °C, burstiness of MN and DN increased compared to that at 25 °C i.e. CV of ISIs, NSB, NBS and PBS increased, and ISIB decreased with temperature increase. Threshold ISI values for intraburst intervals were 15 and 10 ms for MN and DN, respectively. No spike bursts were observed in the CN. Recordings (B) and (C) were obtained from the same sensillum. The fragments with duration of 200 ms from original 10 s recordings were added to each set of ISI histograms. Bin size for ISI histograms 5 ms. Abbreviations: ISI, interspike interval; CV, coefficient of variation of ISIs; NBS, the mean number of bursts per second; NSB, the mean number of spikes per burst; ISIB, mean ISI in a burst; PBS, percentage of bursty spikes in the spike train; CN, MN and DN show spikes from cold neuron, and moist air and dry air neuron, respectively.

in males, and from 10 to 27 °C in females (Paarmann, 1966; Thiele, 1977). Above upper limits of the preferred temperatures choice percentages fall quickly to zero. Electrophysiological experiments in the carabid beetle *P. assimilis* (Platynini) have shown that one

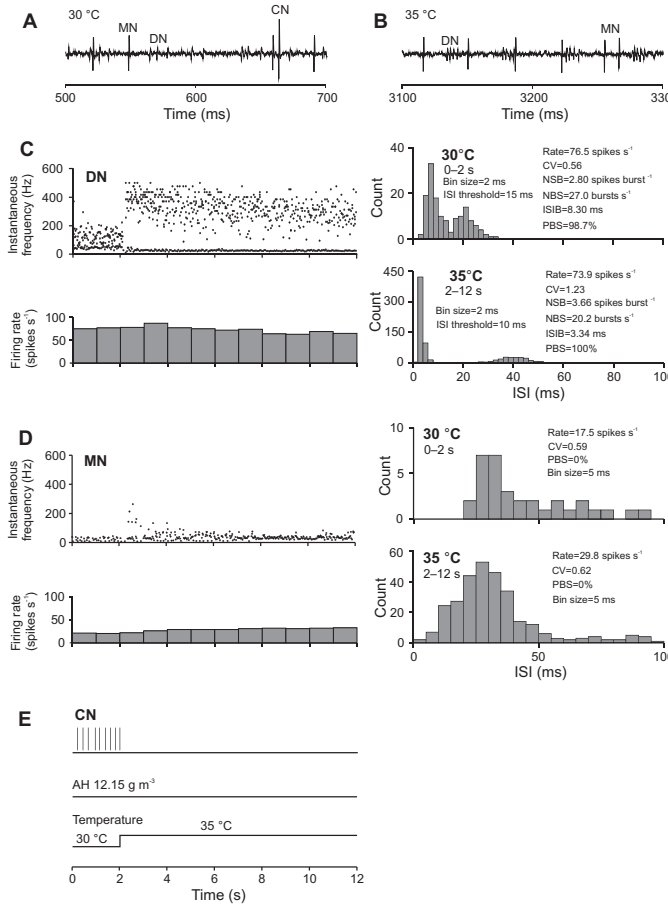

Fig. 8. Sample response of the neurons from an antennal dome-shaped sensillum of *P. oblongopunctatus* to a rapid increase in temperature at constant AH. (A) and (B), sample 200 ms fragments of the original 12 s recording before and after the rapid increase in temperature, respectively. (C) Burstiness of the DN strongly increased (CV, NSB and PBS increased, and ISIB decreased) when temperature increased whereas its firing rate did not change very much. (D) The pattern of spike firing in the MN was regular before as well as after the jump in temperature. ISI histograms had only one maximum and instantaneous frequency plot did not show separated high and low frequency data points as demonstrated for the DN in (C). (E) Extracted spikes of the CN from the same original recording. Initially, at 30 °C, firing rate of the CN was low and when temperature increased to 35 °C spikes from the CN disappeared altogether.

and the same antennal CN may precisely code innocuous and noxious steady temperatures switching from temperature dependent regular spiking to temperature dependent spike bursting. (Must et al., 2006b, 2010). Antennal CN of *P. oblongopunctatus* (Pterostichini) responds to moderate and high ambient temperatures in a similar way. Its stationary firing rate linearly decreases from 24 to 10 spikes s^{-1} with temperature increase from 23 to 39 °C (Must et al., 2006a) allowing precise detection of ambient temperatures in the range of thermo-preference of the species. First indications of spike bursting in the CNs of *P. assimilis* (Must et al., 2010) and *P. oblongopunctatus* occur at about 25–30 °C. In both cases, the percentage of spike bursting neurons and burstiness of their spike trains increase with temperature increase. Even more, the percentage of spike bursting CNs increases with

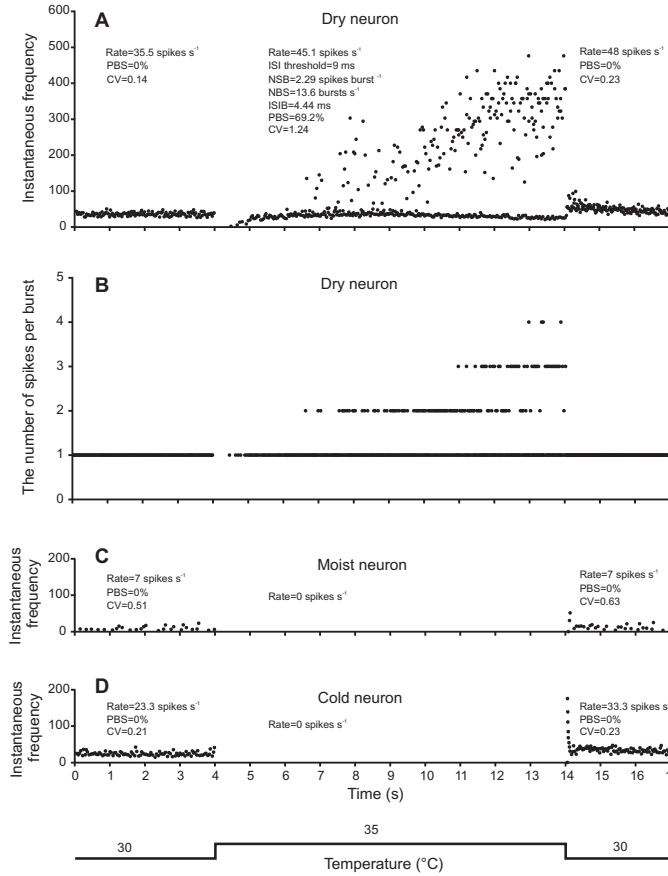

Fig. 9. Reversibility of the responses of antennal thermo- and hygroreceptor neurons to a rapid increase in temperature. (A–D) Simultaneous sample recording from the CN and two hygroreceptor neurons belonging to the same sensillum. Note that only the DN produced high frequency spike bursts in response to temperature increase from 30 to 35 °C (A and B). Spike bursting stopped immediately and regular spiking recovered when temperature dropped back to the initial level. In contrast, during the period of 10 s warming (35 °C), no spikes were generated by either the MN or the CN (C and D). Spikes from the MN and CN appeared again when temperature was lowered to the initial level (30 °C).

different speed in these two carabid species. For example, at 35 °C, the percentages of bursty CNs are 36 and 12 in *P. assimilis* and *P. oblongopunctatus*, respectively. These results are in accordance with the fact that, compared to *P. oblongopunctatus*, the stenothermic *P. assimilis* prefers lower temperatures ranging from 5 to 20 °C with a maximum preference of about 10 °C (Thiele, 1977). Thus, to induce the same proportion of CNs to switch from regular spiking to spike bursting, higher temperatures are required in the species with a higher temperature preference. In *P. oblongopunctatus*, temperatures at which spike bursting of the antennal CNs begins approximately coincides with the upper limit of its preferred temperatures (Paarmann, 1966; Thiele, 1977).

For the first time in arthropods, both at constant RH and constant AH conditions, we have demonstrated that, in addition to the CN, antennal hygroneurons of *P. oblongopunctatus* may also generate high temperature induced spike bursts starting at 25–30 °C and higher. Both burstiness of the spike trains produced by the hygroneurons and the percentage of spike bursting

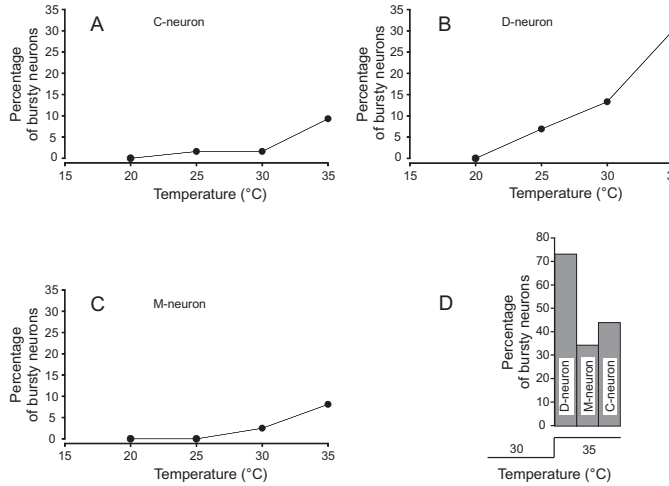

Fig. 10. Percentage of bursting neurons in antennal dome-shaped sensilla of *P. oblongopunctatus* at various steady temperatures (A–C) and at a rapid increase in temperature from 30 to 35 °C (D). $N = 120$ (A–C) and 40 (D); AH 12.15 g m^{-3}. When two spikes from two different neurons were superimposed a special option of Spike 2 software (Collision analysis) and visual inspection were involved in spike sorting.

hygroneurons increase with temperature increase. Thus, bursty spike trains of the DN and MN may also carry useful information on noxious high temperatures for the beetle. Moreover, threshold temperatures at which spike bursting begins in the thermo- and hygroneurons innervating one and the same antennal dome-shaped sensillum differ. Typically, when ambient air temperature increases step-wise, it is the DN which starts to produce spike bursts at the lowest temperature. When temperature increases further, the MN and CN of the sensillum, after each other, also switch from regular spiking to spike bursting. On the other hand, at a steady 23 °C, antennal hygroneurons of *P. oblongopunctatus* never show any bursty spike trains independent of ambient air RH ranging from 5% to 95% (Merivee et al., 2010).

The role of the spike bursting hygroneurons in behavioural thermoregulation of *P. oblongopunctatus* may be even more important in rapid temperature increase conditions, especially when initial temperatures are close to 30 °C and higher. The first event observed in the response of the CN to a rapid increase in temperature is a very long interspike period (LP) (Merivee et al., 2003; Must et al., 2006a,b). Thereafter, the spikes appear again, but with considerably lower frequencies than before warming at the initial temperature. The duration of long interspike period depends on both initial temperature and the magnitude of temperature increase. Higher initial temperatures and larger rises in temperature cause longer LPs in the spike train of the cold neuron. For example, in *P. oblongopunctatus*, an LP of 4 s is elicited by a temperature increase of only 4–5.5 °C from an initial 23 °C (Must et al., 2006a). At initial temperatures above 30 °C, a rapid warming by several degrees may stop spike production by the CN completely, in the 10 s observation period, at least. At the same time, spike production by the DN continues in a bursting manner. Frequently, both the DN and MN produce temperature dependent spike bursts in the absence of the spikes from the CN, whereby burstiness of the spike train of the DN is higher compared to that of the MN. These results suggest that thermal information coded by spike bursts in the antennal thermo- and hygroneurons of P. oblongopunctatus may play an important role in an early threefold warning system of the beetles, and potentially, may be used to avoid overheating and noxious high temperatures when confronted.

To improve our knowledge on insect thermosenstation and behavioural thermoregulation, further studies are needed to compare threshold temperatures and specifics of high temperature induced spike bursting in thermo- and bimodal hygroreceptor neurons of insects with different thermal requirements. However, the most important question, how are the regular spikes and spike bursts from antennal thermo- and hygrosensory input processed by the CNS, remains.

5. Conclusions

Our results show that antennal DNs and MNs of the carabid beetle *P. oblongopunctatus* are bimodal responding to changes in both air humidity and temperature.

For the first time in arthropods, the ability of antennal DNs and MNs of *P. oblongopunctatus* to produce high temperature induced spike bursts is documented.

Our results suggest that burstiness of the spike trains of both hygroneurons is temperature dependent and increases with temperature increase.

We have shown that threshold temperatures at which the DNs, MNs and CNs switch from regular spiking to spike bursting differ and approximately coincide with the upper limit of preferred temperatures of the species.

We hypothesise that high temperature induced spike bursts of antennal thermo- and hygroreceptor neurons may be responsible for detection of noxious high temperatures in carabid beetles.

Acknowledgements

The study was supported by Estonian target financing project SF0170057s09, Estonian Science Foundation Grant No. 8685, Estonian State Forest Management forest protection project (2012–2015) (T12115MIMK) and institutional research funding IUT36-2 of the Estonian Ministry of Education and Research.

References

Altner, H., Loftus, R., 1985. Ultrastructure and function of insect thermo- and hygroreceptors. Annu. Rev. Entomol. 30, 273–295.
Altner, H., Prillinger, L., 1980. Ultrastructure of invertebrate chemo- thermo-, and hygroreceptors and its functional significance. Int. Rev. Cytol. 67, 69–139.
Bakkum, D.J., Radivojevic, M., Frey, U., Franke, F., Hierlemann, A., Takahashi, H., 2014. Parameters for burst detection. Front. Comput. Neurosci. 7, 193. http://dx.doi.org/10.3389/fncom.2013.00193.
Böcher, J., Nachman, G., 2001. Temperature and humidity responses of the arctic-alpine seed bug *Nysius groenlandicus*. Entomol. Exp. Appl. 99, 319–330.
Chapman, R.F., 1998. The Insects. Structure and Function, fourth ed. Cambridge University Press, U.K.
Chown, S.L., Nicolson, S.W., 2004. Insect Physiological Ecology. Mechanisms and Patterns. Oxford University Press, Oxford.
Chown, S.L., Terblanche, J.S., 2007. Physiological diversity in insects: ecological and evolutionary contexts. Adv. Insect Physiol. 33, 50–152.
Cocatre-Zilgien, J.H., Delcomyn, F., 1992. Identification of bursts in spike trains. J. Neurosci. Methods 41, 19–30.
Cooper, K.E., 2002. Molecular biology of thermoregulation. Some historical perspectives on thermoregulation. J. Appl. Physiol. 92, 1717–1724.
Denlinger, D.L., Yocum, G.D., 1998. Physiology of heat sensitivity. In: Hallman, G.J., Denlinger, D.L. (Eds.), Temperature Sensitivity in Insects and Application in Integrated Pest Management. Westview Press, Boulder, CO, USA, pp. 7–57.
Dhaka, A., Viswanath, V., Patapoutian, A., 2006. TRP ion channels and temperature sensation. Annu. Rev. Neurosci. 29, 135–161.
Di Giulio, A., Maurizi, E., Rossi Stacconi, M.V., Romani, R., 2012. Functional structure of antennal sensilla in the myrmecophilous beetle *Paussus favieri* (Coleoptera, Carabidae, Paussini). Micron 43, 705–719.
Dillon, M.E., Wang, G., Garrity, P.A., Huey, R.B., 2009. Thermal preference in *Drosophila*. J. Therm. Biol. 34, 109–119.
Heinrich, B., 1993. The Hot-Blooded Insects: Strategies and Mechanisms of Thermoregulation. Harvard Univ. Press, Cambridge, MA.
Hochachka, P.W., Somero, G.N., 2002. Biochemical Adaptation. Mechanisms and Processes in Physiological Evolution. Oxford University Press, New York.
Holland, J.M., 2002. Carabid beetles: their ecology, survival and use in agroecosystems. In: Holland, J.M. (Ed.), The Agroecology of Carabid Beetles. Intercept, Andover, Hampshire, pp. 1–40.
Klose, M.K., Robertson, R.M., 2004. Stress-induced thermoprotection of neuromuscular transmission. Integr. Comp. Biol. 44, 14–20.
Lacher, V., 1964. Elektrophysiologische Untersuchungen an einzelnen Rezeptoren für Geruch, Kohlendioxyd, Luftfeuchtigkeit und Temperatur auf den Antennen der Arbeitsbiene und der Drohne (*Apis mellifica* L.). Z. Vergl. Physiol. 48, 587–623.
Lindroth, C.H., 1986. The Carabidae (Coleoptera) of Fennoscandia and Denmark. Fauna Entomologica Scandinavica, 15(2), 233–497.
Loftus, R., 1968. The response of the antennal cold receptor of *Periplaneta americana* to rapid temperature changes and steady temperature. Z. Vergl. Physiol. 59, 413–455.
Loftus, R., 1976. Temperature-dependent dry receptor on antenna of *Periplaneta*. Tonic response. J. Comp. Physiol. 111, 153–170.
Lövei, G.L., Sunderland, K.D., 1996. Ecology and behavior of ground beetles (Coleoptera: Carabidae). Annu. Rev. Entomol. 41, 231–256.
McKemy, D.D., 2007. Temperature sensing across species. Eur. J. Physiol. 454, 777–791.
Merivee, E., Ploomi, A., Luik, A., Rahi, M., Sammelselg, V., 2001. Antennal sensilla of the ground beetle *Platynus dorsalis* (Pontoppidan, 1763) (Coleoptera, Carabidae). Microsc. Res. Tech. 55, 339–349.
Merivee, E., Ploomi, A., Rahi, M., Luik, A., Sammelselg, V., 2000. Antennal sensilla of the ground beetle *Bembidion lampros* Hbst. (Coleoptera, Carabidae). Acta Zool. 81, 339–350.
Merivee, E., Ploomi, A., Rahi, M., Bresciani, J., Ravn, H.P., Luik, A., Sammelselg, V., 2002. Antennal sensilla of the ground beetle *Bembidion properans* Steph. (Coleoptera, Carabidae). Micron 33, 429–440.
Merivee, E., Vanatoa, A., Luik, A., Rahi, M., Sammelselg, V., Ploomi, A., 2003. Electrophysiological identification of cold receptors on the antennae of the ground beetle *Pterostichus aethiops*. Physiol. Entomol. 28, 88–96.
Merivee, E., Must, A., Luik, A., Williams, I., 2010. Electrophysiological identification of hygroreceptor neurons from the antennal dome-shaped sensilla in the ground beetle *Pterostichus oblongopunctatus*. J. Insect Physiol. 56, 1671–1678.
Must, A., Merivee, E., Mänd, M., Luik, A., Heidemaa, M., 2006a. Electrophysiological responses of the antennal campaniform sensilla to rapid changes of temperature in the ground beetles *Pterostichus oblongopunctatus* and *Poecilus cupreus* (Tribe Pterostichini) with different ecological preferences. Physiol. Entomol. 31, 278–285.
Must, A., Merivee, E., Luik, A., Mänd, M., Heidemaa, M., 2006b. Responses of antennal campaniform sensilla to rapid temperature changes in ground beetles of the tribe Platynini with different habitat preferences and daily activity rhythms. J. Insect Physiol. 52, 506–513.
Must, A., Merivee, E., Luik, A., Williams, I., Ploomi, A., Heidemaa, M., 2010. Spike bursts generated by the thermosensitive (cold) neuron from the antennal campaniform sensilla of the ground beetle *Platynus assimilis*. J. Insect Physiol. 56, 412–421.
Nation, J.L., 2002. Insect Physiology and Biochemistry. CRC Press, Boca Raton, London, New York, Washington, D.C.
Paarmann, W., 1966. Vergleichende Untersuchungen über die Bindung zweier Carabidenarten (*Pterostichus angustatus* Dft. und *Pterostichus oblongopunctatus* F.) an ihre verschiedenen Lebensräume. Z. Wiss. Zool. 174, 83–176.
Robertson, R.M., 2004. Modulation of neural circuit operation by prior environmental stress. Integr. Comp. Biol. 44, 21–27.
Sayeed, O., Benzer, S., 1996. Behavioural genetics of thermosensation and hygrosensation in *Drosophila*. Proc. Natl. Acad. Sci. U.S.A. 93, 6079–6084.
Seebacher, F., Franklin, C.E., 2005. Physiological mechanisms of thermoregulation in reptiles: a review. J. Comp. Physiol. B 175, 533–541.
Seebacher, F., Shine, R., 2004. Evaluating thermoregulation in reptiles: the fallacy of the inappropriately applied method. Physiol. Biochem. Zool. 77, 688–695.
Talavera, K., Nilius, B., Voets, T., 2008. Neuronal TRP channels: thermometers, pathfinders and life-savers. Trends Neurosci. 31, 287–295.
Thiele, H.U., 1977. Carabid beetles in their environment. Zoophysiology and Ecology, vol. 10. Springer, Berlin.
Tichy, H., 1979. Hygro- and thermoreceptive triad in antennal sensillum of the stick insect, *Carausius morosus*. J. Comp. Physiol. 132, 149–152.
Tichy, H., 1987. Hygroreceptor identification and response characteristics in the stick insect *Carausius morosus*. J. Comp. Physiol. 160, 43–53.
Tichy, H., 2007. Humidity-dependent cold cells on the antenna of the stick insect. J. Neurophysiol. 97, 3851–3858.
Tichy, H., Gingl, E., 2001. Problems in hygro-and thermoreception. In: Barth, F.G., Schmid, A. (Eds.), Ecology of Sensing. Springer, Berlin, Heidelberg, New York, pp. 271–287.
Tichy, H., Kallina, W., 2013. The evaporative function of cockroach hygroreceptors. PLoS One 8 (1), e53998. http://dx.doi.org/10.1371/journal.pone.0053998.
Tichy, H., Loftus, R., 1990. Response of the moist-air receptor on antenna of the stick insect, *Carausius morosus*, to step changes in temperature. J. Comp. Physiol. A 166, 507–516.
Tichy, H., Loftus, R., 1996. Hygroreceptors in insects and a spider: humidity transduction models. Naturwissenschaften 83, 255–263.
Tracey, W.D., Wilson, R.I., Laurent, G., Benzer, S., 2003. Painless, a *Drosophila* gene essential for nociception. Cell 113, 261–273.
Waldow, U., 1970. Elektrophysiologische Untersuchungen an Feuchte-, Troken- und Kälterezeptoren auf der Antenne der Wanderheuschrecke *Locusta*. Z. Vergl. Physiol. 69, 249–283.
Yokohari, F., 1978. Hygroreceptor mechanism in the antenna of the cockroach *Periplaneta*. J. Comp. Physiol. 124, 53–60.
Yokohari, F., Tateda, H., 1976. Moist and dry hygroreceptors for relative humidity of the cockroach, *Periplaneta americana* L. J. Comp. Physiol. 106, 137–152.

II

Must, A., Merivee, E., **Nurme, K.**, Sibul, I., Muzzi, M., Di Giulio, A., Williams, I., Tooming, E. 2017. Encoding noxious heat by spike bursts of antennal bimodal hygroreceptor (dry) neurons in the carabid Pterostichus oblongopunctatus. Cell and Tissue Research, 368 (1), 29-46.

Cell Tissue Res
DOI 10.1007/s00441-016-2547-y

REGULAR ARTICLE

Encoding noxious heat by spike bursts of antennal bimodal hygroreceptor (dry) neurons in the carabid *Pterostichus oblongopunctatus*

Anne Must[1] · Enno Merivee[1] · Karin Nurme[1] · Ivar Sibul[2] · Maurizio Muzzi[3] · Andrea Di Giulio[3] · Ingrid Williams[1] · Ene Tooming[1]

Received: 23 February 2016 / Accepted: 23 November 2016

Abstract Despite thermosensation being crucial in effective thermoregulation behaviour, it is poorly studied in insects. Very little is known about encoding of noxious high temperatures by peripheral thermoreceptor neurons. In carabids, thermo- and hygrosensitive neurons innervate antennal dome-shaped sensilla (DSS). In this study, we demonstrate that several essential fine structural features of dendritic outer segments of the sensory neurons in the DSS and the classical model of insect thermo- and hygrosensitive sensilla differ fundamentally. Here, we show that spike bursts produced by the bimodal dry neurons in the antennal DSS may contribute to the sensation of noxious heat in *P. oblongopunctatus*. Our electrophysiological experiments showed that, at temperatures above 25 °C, these neurons switch from humidity-dependent regular spiking to temperature-dependent spike bursting. Five out of seven measured parameters of the bursty spike trains, the percentage of bursty dry neurons, the CV of ISIs in a spike train, the percentage of bursty spikes, the number of spikes in a burst and the ISIs in a burst, are unambiguously dependent on temperature and thus may precisely encode both noxious high steady temperatures up to 45 °C as well as rapid step-changes in it. The cold neuron starts to produce temperature-dependent spike bursts at temperatures above 30–35 °C. Thus, the two neurons encode different but largely overlapping ranges in noxious heat. The extent of dendritic branching and lamellation of the neurons largely varies in different DSS, which might be the structural basis for their variation in threshold temperatures for spike bursting.

Keywords Insect · Bimodal neuron · Spike burst · High temperature · Encoding · Behavioural thermoregulation · *Pterostichus oblongopunctatus*

✉ Anne Must
anne.must@emu.ee

[1] Institute of Agricultural and Environmental Sciences, Estonian University of Life Sciences, Kreutzwaldi Street 1, 51014 Tartu, Estonia

[2] Institute of Forestry and Rural Engineering, Estonian University of Life Sciences, Kreutzwaldi Street 1, 51014 Tartu, Estonia

[3] Department of Science, University of Roma Tre, Viale G. Marconi 446, I-00146 Rome, Italy

Introduction

External temperature conditions strongly affect the physiology, ecology and fitness of ectotherms. Small-bodied insects are particularly sensitive to heat, so solar radiation can quickly elevate their body temperature to lethal levels (Heinrich 1993; Denlinger and Yocum 1998; Chown and Terblanche 2007). Noxious high temperatures at which total heat paralysis begins in various carabid beetles lie in a narrow range between 47.4 and 51.7 °C (Thiele 1977). The first indications of partial paralysis (of the hind legs) have been observed at 44.4 ± 0.6 °C (Must et al. 2010), offering additional thermal challenges for ground-dwelling arthropods such as carabid beetles. An array of abnormalities is evident at the cellular level in response to heat stress at noxious high temperatures above the upper limit of a species specific range of thermal preference (Denlinger and Yocum 1998; Neven 2000; Hochachka and Somero 2002; Klose and Robertson 2004); in most carabid beetles, this lies between 10 and 30 °C

Published online: 28 December 2016

(Thiele 1977). Noxious heat also has deleterious effects on insect metabolism, respiration, endocrine and nervous systems, behaviour, reproduction, development and growth (reviewed by Cossins and Bowler 1987; Denlinger and Yocum 1998; Neven 2000; Chown and Terblanche 2007).

Ectothermic insects are not entirely at the mercy of noxious high temperatures. Various physiological and behavioural mechanisms help resist noxious heat (Denlinger and Yocum 1998; Chown and Terblanche 2007). For example, carabid beetles can avoid overheating and maintain their body temperature at a remarkably narrow, species-specific range of preferred temperatures via behavioural thermoregulation, e.g., shuttling between sunshine and shade (Thiele 1977; Lövei and Sunderland 1996). Despite thermosensation being crucial in effective thermoregulation behaviour, it is poorly studied in insects. Very little is known of the neural pathways and coding of noxious high temperatures by peripheral thermoreceptor neurons in these small arthropods (Dhaka et al. 2006; Tang et al. 2013).

Through electrophysiological recordings, thermoreceptor neurons have been found in various morphological types of cuticular sensilla on the antennae of insects and the legs of ticks and spiders (Altner and Prillinger 1980; Hess and Loftus 1984; Ehn and Tichy 1996; Merivee et al. 2003; Ruchty et al. 2009; Wang et al. 2009). In a sensillum, they usually form a sensory triad with two hygro-receptor neurons (Waldow 1970; Tichy 1979; Altner et al. 1981; Yokohari et al. 1982; Altner and Loftus 1985; Piersanti et al. 2011). The classical, most widely distributed thermo-hygroreceptive sensillum type on insect antennae is a kind of peg-in-pit organ classified as a sensillum coeloconicum (Altner and Loftus 1985; Chapman 1998) (Fig. 1). It consists of a short peg concealed in a cavity in the antennal cuticle and an inflexible socket usually surrounded by an inflated cuticular collar. The peg wall lacks pores except for a single terminal molting pore plugged by electron-dense material. In the cavity, the entire peg wall is exposed to the ambient air. The number of these sensilla on the insect antennae is not large. Usually, there is a group of peg-in-pit sensilla on the terminal antennomere and one or two on each of the proximal antennomeres. Typically, coeloconic sensilla are innervated by three sensory neurons. However, the physiologically defined modality of the neurons cannot be distinguished simply by morphological criteria (Altner and Loftus 1985; Steinbrecht 1989; Chapman 1998; Tichy and Kallina 2010); only when electrophysiological data are available can functional types and subtypes be determined. Two neurons possess unbranched outer dendritic segments extending up to the apex of the cuticular peg and tightly fill the peg lumen; these are possible hygroreceptor neurons. The third dendrite is lamellated and terminates below the peg base. The presence of a lamellated dendrite appears to correspond to thermoreceptor activity. Below the peg base, the sensory neurons are concentrically surrounded by three auxiliary cells,

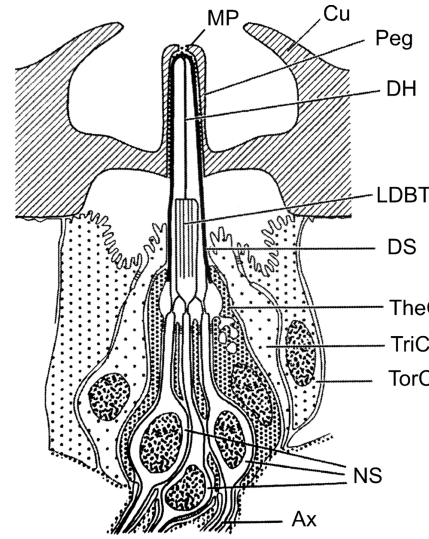

Fig. 1 Diagrammic longitudinal section through the classical thermo- and hygroreceptive peg-in-pit organ (sensillum coeloconicum) (by Chapman 1998). *Ax* axon; *Cu* cuticle; *DH* unbranched dendrites of the hygroreceptor neurons; *DS* dendritic sheath, *LDBT* lamellated dendritic branches of the thermoreceptor neuron, *MP* moulting pore, *NS* neuron somata, *Peg* cuticular peg in a pit, *TheC* thecogen cell, *TorC* tormogen cell, *TriC* trichogen cell

the innermost is the thecogen cell followed by the trichogen and tormogen cells.

The antennal hygro- and thermosensitive dome-shaped sensilla (DSS) of the carabid beetle *Pterostichus oblongopunctatus* (Must et al. 2006a; Merivee et al. 2010; Nurme et al. 2015) are non-perforated peg-in-dome sensory organs with an inflexible socket (Nurme et al. 2015) distributed on the antennae of various beetles, for example in other Carabidae (Merivee et al. 2000, 2001, 2002; Di Giulio et al. 2012) and Elateridae (Merivee 1992; Merivee et al. 1997, 1998, 1999). The SEM/FIB combined fine morphological analysis made by Nurme et al. (2015) showed that they differ from insect peg-in-pit sensory organs like sensilla coeloconica, sensilla ampullacea, sensilla coelocapitula and sensilla coelosphaerica (Altner and Loftus 1985; Zacharuk 1985; Yokohari 1999; Nakanishi et al. 2009; Ruchty et al. 2009) by a couple of characteristic structural features. The principal differences include the characteristic cuticular dome bulging above the antennal surface and well exposed to ambient air. Secondly, no pit exists in the carabid DSS and the peg is situated in a very tight cuticular socket. Only the tiny tip of the peg, protruding over the dome, is directly exposed to

environmental air conditions. These morphological specifics suggest that both the cuticular dome and the sensillum socket might have importance as stimulus-mediating structures in these sensilla. Therefore, it might be supposed that the location of dendritic lamellae and possible branches of the sensory neurons inside the dome-shape sensillum might strongly affect their exposure to external temperature and humidity. In earlier literature, due to the characteristic large dome, these sensilla have been sometimes incorrectly termed as sensilla campaniformia (Merivee et al. 1998, 2000, 2001, 2002), which they externally resemble most. However, internally, true sensilla campaniformia with the purely mechanoreceptive function (Snodgrass 1935; Keil and Steinbrecht 1984; McIver 1985; Chapman 1998) and DSS differ completely. Though DSS are widely distributed on the antennae of various insects, their internal fine structure is not well known in detail.

Both electrophysiological (Merivee et al. 2003, 2010; Must et al. 2006a; Nurme et al. 2015) and fine morphological studies (Nurme et al. 2015) have demonstrated that antennal DSS of carabid beetles, including *P. oblongopunctatus*, are innervated by three neurons. By reaction type, they are classified as the dry air, the moist air and the cold neuron, respectively. A similar physiological triad of sensory neurons is typical of classical poreless peg-in pit sensilla with an inflexible socket in many insect groups (Altner et al. 1978, 1981; Tichy 1979, 1987, 2007; Altner and Loftus 1985; Shanbhag et al. 1995; Yokohari 1999; Rebora et al. 2007).

The peculiar feature of the thermo- and hygroreceptor neurons in antennal DSS of carabid beetles is the large variation in threshold temperatures at which they switch from regular spiking to spike bursting. Moreover, the threshold temperature for spike bursting of the neurons varies greatly in different sensilla (Must et al. 2010; Nurme et al. 2015) implying that sensitivity of the neurons to temperature differs in different sensilla. Similar, conspicuous variation in threshold temperatures for spike bursting has also been observed in the CNs of mammals (Dykes 1975; Gallar et al. 2003). The underlying fine structural basis of that functional variation is not known. In this context, the opinion of Steinbrecht (1989) is of interest stating that the lamellation, which greatly increases the surface area of the receptor membrane, might contribute to increasing sensitivity of the insect thermoreceptor neuron, an idea that has never been investigated specifically. Thus, it might be hypothesised that possible variation in the extent of dendritic lamellation and branching may lead to variation in temperature sensitivity of individual thermoreceptor neurons in different sensilla. However, dendritic lamellation and branching have never been observed in insect hygroreceptor neurons but due to insufficient investigation this possibility cannot be ruled out in some bimodal thermo-hygrosensitive neurons like the dry and moist air neuron in the antennal DSS of carabids (Merivee et al. 2010; Nurme et al. 2015).

By reaction type, thermoreceptor neurons of most arthropods studied, including carabids, are cold receptors responding with a phasic-tonic increase in firing rate to rapid cooling and a decline in firing rate after temperature increase. Spike production by the cold neurons temporarily stops immediately after a rapid temperature increase. The duration of this long interspike period depends on the amplitude of temperature jump and may continue up to several seconds or longer at 28–37 °C (Merivee et al. 2003; Must et al. 2006a, b; Nurme et al. 2015). During this non-spiking period, cold neurons are not able to respond to subsequent rise in temperature. On the other hand, the peak frequency of the initial spike burst depends on both the initial temperature and the magnitude of temperature drop (Loftus 1968). Thus, a particular peak frequency can be achieved by several different combinations of initial temperature and magnitude of rapid step-decrease in temperature. This ambiguity makes it unlikely that instantaneous spike frequencies of the antennal cold neuron can precisely encode rapid step-increases in temperature.

The stationary firing rate of the cold neuron depends on temperature and, hence, can unambiguously encode the full range of steady physiological temperatures in some insect species but not in others (Lacher 1964; Loftus 1968; Waldow 1970; Davis and Sokolove 1975; Ameismeier and Loftus 1988; Must et al. 2006a, b). For example, in the carabids *Pterostichus oblongopunctatus* and *Platynus assimilis*, a strong negative correlation has been found between the mean firing rate of the cold neuron and temperature at 23–39 °C (Must et al. 2006a, b). By contrast, no relationship between the stationary firing rate and temperature has been observed in *Pterostichus cupreus* (Must et al. 2006a). In *Anchomenus dorsalis* and *Agonum muelleri*, the firing rate does not depend on temperature at 23–27 °C and 23–33 °C, respectively but plots of firing versus temperature show rapid declines when the temperature increases further (Must et al. 2006b). Cold neurons of insects have a relatively high stationary firing rate, usually 10–40 spikes s^{-1}, at temperatures of 20–30 °C. However, they have remarkable individual variability (Lacher 1964; Loftus 1968; Davis and Sokolove 1975; Tichy 1979; Ameismeier and Loftus 1988; Gingl and Tichy 2001; Merivee et al. 2003; Must et al. 2006a, b). Large individual variability of the cold neurons and inconsistency between their stationary firing rate and temperature leads to the assumption that the stationary firing rate does not contain adequate information for insects on external temperature important in thermoregulation behaviour. These results on the physiology of cold neurons suggest that additional peripheral temperature encoding mechanisms should be involved in precise thermosensation of various insects including carabids.

In this context, the discovery that, during warming, insect cold neurons may switch from regular spiking to high temperature induced spike bursting, is of interest. This response was first demonstrated in the cold neurons innervating antennal

DSS of the carabid beetle *P. assimilis* (Must et al. 2010) and later in another carabid beetle *P. oblongopunctatus* (Nurme et al. 2015).

In these neurons, the number of spikes in the burst and interspike intervals within the burst are temperature-dependent and may precisely encode noxious high temperatures in a graded manner. In *P. assimilis*, the threshold temperature of spike bursting varies in different neurons from 25 to 47 °C. As a result, the number of bursting cold neurons increases with temperature increase. Thus, in addition to the burst characteristics, the total number of bursting neurons may also contain useful information on environmental thermal conditions.

Certain patterns in the spike train of antennal bimodal thermo-hygroreceptor neurons of insects may also encode unfavourably high temperatures. Antennal DSS of carabid beetles house, in addition to the cold neuron, two antagonistically responding hygroreceptor neurons, the dry and moist air neuron, as electrophysiologically and anatomically demonstrated in *P. oblongopunctatus* (Merivee et al. 2010; Nurme et al. 2015). A similar set of thermo- and hygroreceptor neurons, as a triad, is located in various types of sensilla on the antennae of many insects (Altner and Prillinger 1980; Altner and Loftus 1985; Chapman 1998; Di Giulio et al. 2012). Recently, it was found that the two hygroreceptor neurons of *P. oblongopunctatus* are in fact bimodal responding to both air humidity and temperature (Nurme et al. 2015), as found in other insects (Lacher 1964; Waldow 1970; Loftus 1976; Altner and Loftus 1985; Tichy 1987). Nurme et al. (2015) discovered, for the first time in arthropods, the ability of the antennal dry and moist neurons to produce spike bursts at noxious high temperatures above 25–30 °C, as in *P. oblongopunctatus*, for example. The percentage of bursting neurons increases with temperature increase. At 35 °C, 30 % of the dry neurons and 8 % of the moist neurons produce bursty spike trains. Thus, heat induced spike bursting in antennal bimodal hygroreceptor neurons is common enough to be ignored. Even more, the results of rather preliminary, qualitative experiments have shown that burstiness of the spike trains in these two hygroreceptor neurons also increases with temperature increase. With increasing temperature, relative air humidity (RH) decreases but spike bursting in the two hygroreceptor neurons is not caused by humidity stress. It has been convincingly demonstrated that, at moderate temperatures close to 23 °C and at RH levels ranging from 5 to 95 %, both the moist and dry neurons of *P. oblongopunctatus* never fire in a bursting manner, even at RH extremes (Merivee et al. 2010). Based on these results, we hypothesise that, in addition to the spike bursts of the antennal cold neuron (Must et al. 2010), temperature-dependent spike bursts produced by the antennal bimodal hygroreceptor neurons may also contribute to the sensation of noxious high temperatures in insects. More precisely, however, quantitative experiments are needed to prove this novel concept of thermosensation.

To test this hypothesis, we concentrate on the spike bursting response to heat in the antennal dry neuron of *P. oblongopunctatus* for two reasons: (1) unlike the low spike production of the moist neuron (approximately 6 spikes s^{-1} at 35 °C), the stationary firing rate of the dry neuron remains at a relatively high level (above 40 spikes s^{-1}) even at the noxious heat of 35 °C (Nurme et al. 2015); and (2) the threshold temperature for spike bursting in the dry neuron is considerably lower than that of the moist neuron (Nurme et al. 2015).

The aims of this study were: (1) to explain variability in the location and extent of dendritic lamellation of the thermoreceptor (cold) neuron in different antennal DSS of *P. oblongopunctatus*; (2) to explain possible occurrence of dendritic branching in the two bimodal thermo-hygroreceptor neurons in the antennal DSS; (3) to measure threshold temperatures for spike bursting in antennal dry and cold neurons of the species; and (4) to explain the dependence of bursty spike trains parameters on temperature. To this end, several important characteristics of spike bursting were measured and analysed: the firing rate, the percentage of bursty dry neurons and cold neurons on the antenna, the percentage of bursty spikes in a spike train (PBS), the coefficient of variance of interspike intervals of the spike train (CV of ISI), the number of spikes per burst (NSB), the mean interspike interval in a burst (ISIB) and the number of bursts per second (NBS). Results of the experiments are presented in this paper.

Materials and methods

Test beetles

Adult *P. oblongopunctatus* carabid beetles originated from a local population in southern Estonia. They were collected from their preferred overwintering sites in brown-rotted wood lying on the ground in spring 2014 and 2015. They were placed in 20 cm × 30 cm × 10 cm plastic boxes filled with small pieces of moist brown-rotted wood, 50 specimens in each box and kept at 5 °C until they were used in experiments. Three to four days prior to tests, they were placed singly in 110-mm glass Petri dishes with moistened filter paper (Whatman International, UK) and kept at room temperature (20 °C) in the Versatile Environmental Test Chamber MLR-35 1H (SANYO Electric, Japan) at 16 h light and 8 h dark (16L:8D) photoperiod and 70 % relative humidity (RH) necessary for good electrophysiological recordings.

For electrophysiological recordings, intact test beetles were used. They were immobilised and fixed with special clamps (for details, see Merivee et al. 2010; Must et al. 2010; Nurme et al. 2015). Their antennae were fastened horizontally with beeswax at the edge of a special aluminium stand so that the terminal DSS were visible from above under a light microscope, were well exposed to stimulating airstreams and readily accessible for microelectrode manipulation from the side.

For the morphological analysis of the sensilla, we followed the procedure described in detail in Nurme et al. (2015). Antennae from 10 beetles were removed from specimens (previously CO_2 anesthetised), promptly immersed in Karnovsky's glutaraldehyde and dissected to facilitate penetration of the fixative. Specimens were rinsed in cacodylate buffer, post-fixed in 1 % osmium tetroxide and rinsed again in cacodylate buffer, en bloc stained with 2 % aqueous uranyl acetate, dehydrated in a graded ethanol series and embedded in epoxy resin with propylene oxide as a bridging agent.

Focused ion beam/scanning electron microscope (FIB/SEM) combined technique

Ultrastructural analysis of the DSS was performed with the Dualbeam (FIB/SEM) Helios Nanolab (FEI, Eindhoven, The Netherlands) at L.I.M.E. (Roma Tre University, Rome, Italy). In the FIB/SEM, a focused gallium ion beam (FIB column) is combined with one electron beam (SEM column); the two columns are oriented at 52° and focus on the same point of the specimen. The FIB/SEM proved to be a highly effective instrument capable of replacing the classical ultrastructural TEM analysis for the precise and complete serial sectioning of delicate arthropod structures surrounded by thickly sclerotised cuticle usually prone to fracture during the ultramicrotome cut (Di Giulio et al. 2015). We used the FIB column to cross-section the surface of the DSS, acquiring serial high-resolution micrographs every 200 nm with the SEM column (equipped with a Field Emission Gun).

The embedded antennomeres were extracted from the epoxy resin, mounted on a stub by using a self-adhesive carbon disk and gold sputtered by an Emithech K550. This procedure allows easy localisation of the target DSS and makes it possible to analyse both its external and internal morphology. DSS were cross-sectioned by the focused gallium ion beam operated at 30 kV and 2.8 nA; SEM pictures of each cross-section were acquired using backscattered electrons (BSE) and a through-the-lens (TDL) detector, approximately every 150 nm of milling (horizontal feed), with an operating voltage of 2 kV, an applied current of 0.17 nA, at a working distance of 2 mm.

Electrophysiology

Single sensillum recordings

Our set-up of single sensillum recordings has been described earlier (Nurme et al. 2015). Tungsten wire (0.08 mm in diameter) microelectrodes were sharpened electrolytically to a point in a concentrated potassium alkali solution. The grounded indifferent electrode was inserted into the antennal lumen at the base of the flagellum. The recording electrode was thrust into the base of a DSS located at the tip of the terminal flagellomere using the micromanipulator DC-3KS (Stoelting, USA) under visual control with the upright microscope Eclipse FN1 (Nikon, Japan) at a magnification of ×1000. The microscope was equipped with the ITS-FN1 Physiostage (Nikon) consisting in the X-Y Translator and stainless steel Stage mounted on the Passive Anti-Vibration ScienceDesk (ThorLabs, UK). All experiments were performed in a 100 cm × 120 cm × 100 cm Faraday Cage FAR01 (ThorLabs). Spike trains picked up by the recording electrode through a custom-made Preamplifier Board (input impedance 10 GΩ) (Interspectrum, Estonia) were led to input of the main amplifier ISO-DAM 8A (World Precision Instruments, USA), filtered with a bandwidth set at 10–3000 Hz, monitored on an oscilloscope screen and relayed to a PC via an A/D input board DAS-1401 (Keithley Instruments, USA) for data acquisition and storage using Testpoint software (Capital Equipment, USA) at a sampling rate of 10 kHz. The recordings were made from one sensillum of each test beetle. The number of beetles tested (N) is shown directly everywhere in the text (see "Results") together with the results of statistical analysis.

Stimulation and control of air humidity and temperature

Our thermo- and hygrostimulation and control set-up were described in detail by Nurme et al. (2015), so here the main principles of the set-up are explained in brief. Steady as well as rapid, jump-wise warming stimuli were presented by way of one or two preheated airstreams depending on the experiment. Initially, the airsteams were driven through separate units to be set at a wide range of RH levels by mixing dried air (RH 5 %) and moistened air (RH 95 %) in an appropriate ratio. Then, the airstreams were heated by two separate heating coils to the required temperature. Finally, the airstreams flowed out of 8-mm nozzles of terminal outlet tubes at a velocity of 2 m s^{-1} at a distance of 10 mm from the terminal flagellomere of the test beetle. An electromagnetic air valve (Model 062 4E1; Humphrey Products, USA) EMV and a digital timer (Model 4030; Kaiser Fototechnik, Germany) were used to switch rapidly between the two airstreams. A thermocouple circuit was used to measure airstream temperature. Both the DSS at the tip of the antenna and a copper–constantan thermocouple made of 0.08 mm wire were located at the intersection of the two air streams, with the thermocouple junction 1 mm from the inserted recording microelectrode. The signal, generated and amplified by a thermocouple circuit, led to the second channel of the DAQ board DAS-1401 and was stored on a PC hard disc for further data management and calculation of airstream temperature. A custom-made electronic airflow hygrometer (Interspectrum) based on the LinPicco™ capacitive humidity analogue module A01 (response time <5 s, accuracy <±3 % RH) (Innovative Sensor Technology, Switzerland) was used to measure

airstream RH at 20 °C. Signals from the two hygrometers were led to the third and fourth channel of the DAQ board, respectively. When responses of the antennal thermo- and hygroreceptor neurons were measured at different steady temperatures, the DSS to be adapted before each recording were exposed to each tested temperature for 10 min. The experiments were carried out at constant absolute humidity conditions (AH 10.39 g m^{-3}).

Data management

For analysis of recorded spike trains, Spike 2 software (Cambridge Electronic Design, UK) was used. The spikes from one thermo- and two hygroreceptor neurons from each tested sensillum were subjected to an electrophysiological identification by differences between their shapes and by differences between their responses to a rapid change in ambient air humidity (for details, see Nurme et al. 2015). To decide if a certain spike in a spike train was "regular" or "bursty", interspike interval histogram (ISIH) analysis and visual inspection were used (for details, see Must et al. 2010; Nurme et al. 2015).

Statistical analyses

The overall temperature effect on the measured parameters of the bursty spike trains produced by the DN and CN was evaluated using the Kruskal–Wallis test. To compare spike burst parameters of DN and CN at various temperatures, the Wilcoxon signed rank test was used. In rapid step-warming experiments, the Wilcoxon signed rank test and Mann–Whitney *U* test were used to compare spike burst responses of the DN before and after the warming, within and between the treatments, respectively. All test results were considered statistically significant at $p < 0.05$ and all analyses were performed with the statistical software STATISTICA 11 (StatSoft, USA).

Results

Outer structure of the antennal DSS

DSS, very few in numbers, were observed in two locations on the antennae of *P. oblongopunctatus*. Two of them occurred close to each other on the ventral side of each flagellomere and they were surrounded by punctured cuticle (Fig. 2a, b); additionally, five or six DSSs were located at the tip of the terminal flagellomere with corrugated cuticle (Fig. 2d, e). DSS, 4–8 μm in diameter had the shape of a small dome consisting of three externally distinguishable structures, the dome base, the central cap and the protruding tip of the peg (Fig. 2b, e). Two outermost layers of the dome cuticle, the light and dark cuticle, were continuous with and formed the tight peg socket sunk into the dome (Fig. 2c).

Inner fine structure and innervation of the antennal DSS sensilla

A cross-section through an apical DSS at the level of the central cap showed that the sensillum peg had a small apical pore, 0.09 μm in diameter, at its tip with 0.6 μm diameter (Fig. 3a). Deeper, at the level of the dome base, the peg lumen, 0.5 μm in diameter, contained numerous (approximately 20) tiny dendritic apical branches, (0.09–0.13 μm in diameter and mostly round in cross-section) from two hygroreceptor neurons (Fig. 3b). The restricted gap between the peg and peg socket was filled with an extracellular material. In the middle part of the peg, the dendrites of unequal diameter from the hygroreceptor neurons were unbranched and tightly filled the peg lumen, 0.5 μm in diameter (Fig. 3c). Thus, a rough estimation shows that, due to extensive apical branching, the total surface area of the dendritic membrane in these neurons at the peg tip was increased by 2.5 times, at least, compared to that of the unbranched dendrites in the middle part of the peg. The extent of dendritic apical branching of the hygroreceptor neurons varied considerably in different sensilla. For example, in another DSS at the tip of the terminal flagellomere, one of the hygroreceptor neurons had one large and two tiny dendritic branches (0.11 μm in diameter and round in cross-section) while the other neuron had no apical branches at all (Fig. 2c). No dendritic branching also occurred in the hygroreceptor neurons innervating a ventral DSS (Fig. 4a, b). We also observed that numerous (close to 20) filamentous dendritic branches of the thermoreceptor neuron, highly variable in shape and diameter ranging between 0.05 and 0.18 μm, entered deeply into the peg lumen, up to half of its length (Fig. 3d). The peg socket was surrounded by an auxiliary cell (Fig. 3c–e). At the level of the peg base with 2.5 μm diameter, the walls of the peg and peg socket fused together, the peg lumen widened up to 1.2 μm in diameter and the unbranched dendrites of the hygroreceptor neurons became thicker, approximately 0.6 μm in diameter (Fig. 3e). Inside the peg base, a common dendritic sheath enveloped the dendrites of all three sensory neurons. Below the peg base, the number of filamentous dendritic branches of the thermoreceptor neuron was much larger compared to that inside the peg lumen. They were highly variable in size (Fig. 3f, h) and in some locations, the branches were slightly lamellated (Fig. 3g). Perikaria of the three sensory neurons, enveloped by three auxiliary cells, the thecogen, trichogen and tormogen cells, respectively, lay directly below the cuticle (Fig. 3i). The extent of dendritic filamentous branching and lamellation in observed thermoreceptor neurons largely varied in different DSS. For example, in

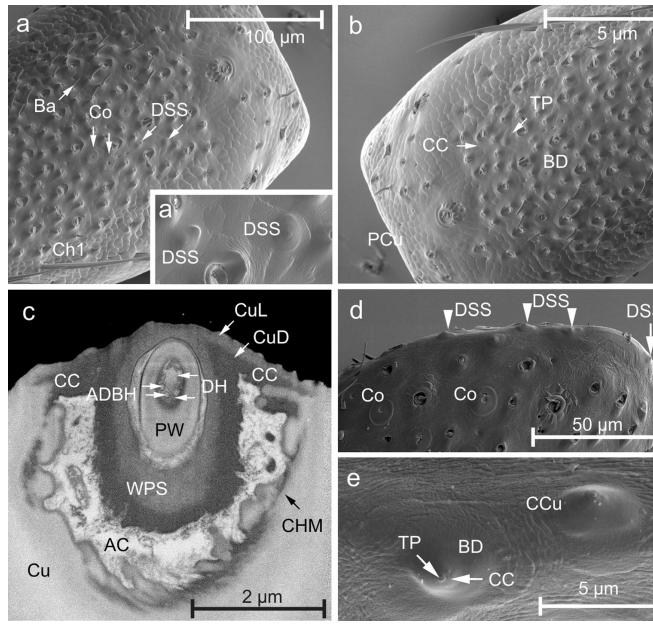

Fig. 2 Antennal DSS: external structure. **a** Location of the DSS as a couple amongst other sensilla on the ventral side of the eighth flagellomere. *Inset* (*a'*) shows the same sensilla at a higher magnification. **b** External shape of a ventral DSS. **c** Oblique section through the tip of the apical DSS. One of the two hygroreceptor neurons has a couple of tiny apical dendritic branches, round in cross-section and 0.11 µm in diameter, in addition to the large, unbranched part of its dendrite. Note that two outermost layers of the dome cuticle (*CuL* and *CuD*) are continuous with and form the peg socket. **d** Location of the DSS in a row at the apical margin of the terminal (ninth) flagellomere (side view). **e** Two apical DSS at a higher magnification (top view). *AC* auxiliary cell, *ADBH* apical dendritic branches of the hygroreceptor neuron, *Ba* sensillum basiconicum, *BD* dome base, *CC* central cap, *CCu* corrugated cuticle, *Ch1* sensillum chaeticum type 1, *CHM* cuticular hole margin, *Co* sensillum coeloconicum, *Cu* cuticle, *CuD* dark cuticle, *CuL* light cuticle, *DH* dendritic outer segment of the hygroreceptor neuron, *DSS* dome-shaped sensillum, *PCu* punctured cuticle, *PW* peg wall, *TP* tip of the peg, *WPS* cuticular wall of the peg socket

another apical DSS, lamellation of dendritic branches of the thermoreceptor neuron was strongly expressed (Fig. 3j). Even more, in a ventral DSS, high extent of lamellation of the dendritic branches occurred inside the peg base as well as below the peg base (Fig. 4e, f). Comparing the cross-sections of the dendritic outer segments at their maximum lamellation (Figs. 3g, 4e), a roughly 10-fold variation in the extent of dendritic lamellation of the thermoreceptor neurons from different DSS was observed. Deeper in the peg lumen, the lamellated dendritic branches were replaced with the filamentous branches. The extent of filamentous branching of the dendrites from the thermoreceptor neuron was lower (the number of branches varied from 3 to 6) and the branches were thicker (0.2–0.4 µm in diameter) compared to those observed in the apical DSS (Fig. 4b–d). The fine structural characters of the DSS are summarised in the schematic drawing (Fig. 9).

Percentage of bursty dry neurons (DN) and cold neurons (CN) at various steady temperatures

Spike trains of the antennal DNs and CNs were recorded and analysed in the range of steady ambient air temperatures from 20 to 45 °C. At 20 °C, all DNs fired in a highly regular manner (firing rate 49.5 ± 2.65 spikes s^{-1}; CV of ISIs 0.19 ± 0.01; $N = 20$) resembling regular spike generation of the CNs at the same temperature (firing rate 32.6 ± 2.09 spikes s^{-1}; mean CV of ISIs 0.22 ± 0.01; $N = 20$). Regular sample spike trains of the DN and CN are demonstrated in Fig. 5a. At higher temperatures, the pattern of spike generation changed in a part of the neurons switching from regular spiking to spike bursting (Fig. 5b–d). First indications of spike bursting were observed at 25 °C in 6.3 % of the DNs (Fig. 6). The proportion of spike bursting DNs increased with temperature increase reaching

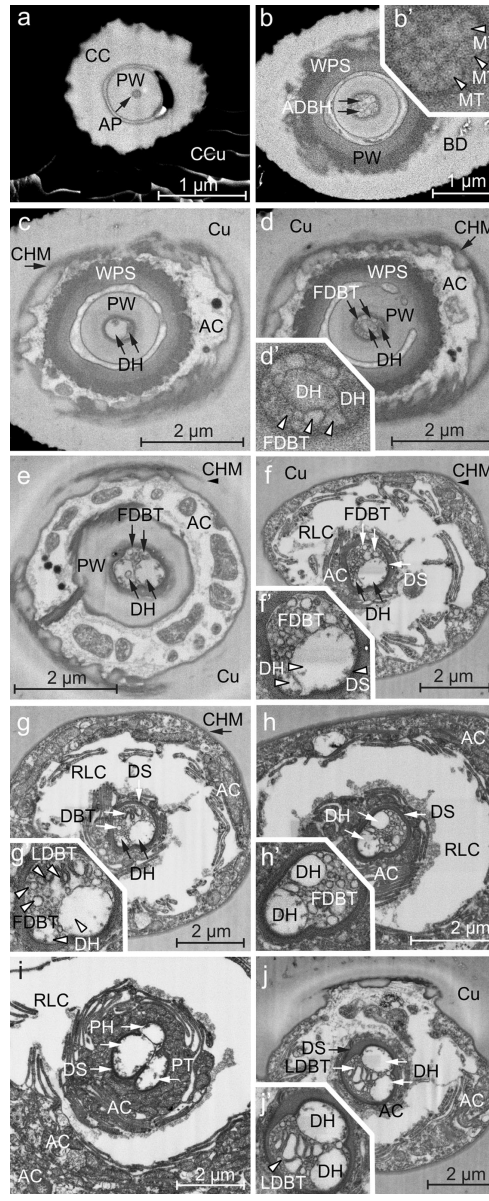
a
CC
PW
AP
CCu
1 µm
b
WPS
ADBH
PW
1 µm
b'
MT
MT
MT
BD
c
Cu
CHM
WPS
PW
AC
DH
2 µm
d
Cu
CHM
WPS
FDBT
PW
AC
DH
d'
DH
DH
FDBT
2 µm
e
CHM
FDBT
AC
PW
DH
2 µm
Cu
f
Cu
CHM
FDBT
RLC
AC
DS
DH
f'
FDBT
DH
DS
2 µm
g
CHM
RLC
DS
AC
DBT
DH
g'
LDBT
FDBT
DH
2 µm
h
AC
DH
DS
RLC
h'
DH
AC
FDBT
DH
2 µm
i
RLC
PH
DS
PT
AC
AC
AC
2 µm
j
Cu
DS
LDBT
DH
AC
AC
j'
DH
LDBT
DH
2 µm

◀ **Fig. 3** Cuticular and cellular parts of the apical DSS. Inserts show the same sensilla at a higher magnification **a** Cross-section through the central cap of the sensillum. **b** Cross-section through the sensillum at the level of the dome base. Note numerous dendritic branches of the hygroreceptor neurons and a restricted gap between the peg and peg socket walls filled with an extracellular material. **c** Cross-section through the peg middle indicating that no dendritic branching takes place at this level. **d** Cross-section through the middle part of the sensillum somewhat deeper than in (**c**). Inside the peg lumen, note numerous dendritic branches of the thermoreceptor neuron. **e** Cross-section through the peg base demonstrating fused walls of the peg and the peg socket. **f** Cross-section through the sensillum below the peg base. Note numerous dendritic branches of various sizes of the thermoreceptor neuron. **g** Cross-section through the sensillum below the peg base a little deeper than in (**f**) indicating few minor lamellated dendritic branches of the thermoreceptor neuron. **h** Cross-section through the sensillum below the antennal cuticle. Note numerous dendritic branches of the thermoreceptor neuron. **i** Cross-section through the sensillum somewhat deeper than in (**h**) demonstrating that three neurons innervate these sensilla. **j** Cross-section through another apical DSS a little below the peg base. Note numerous large lamellated dendritic branches of the thermoreceptor neuron. *AC* auxiliary cell, *ADBH* apical dendritic branches of the hygroreceptor neuron, *AP* apical pore, *BD* dome base, *CC* central cap, *CCu* corrugated cuticle, *CHM* cuticular hole margin, *Cu* cuticle, *DBT* dendritic branches of the thermoreceptor neuron, *DH* dendritic outer segment of the hygroreceptor neuron, *DS* dendritic sheath, *FDBT* filamentous dendritic branches of the thermoreceptor neuron, *LDBT* lamellated dendritic branches of the thermoreceptor neuron, *MT* microtubules, *PH* perikaria of the hygroreceptor neurons, *PT* perikarion of the thermoreceptor neuron, *PW* peg wall, *RLC* receptor lymph cavity, *WPS* cuticular wall of the peg socket

73.3 % at 40 °C. When temperature was increased further, the percentage of bursty DNs rapidly dropped to 42.2 % due to degradation of normal spike bursts in a large part of the DNs at high temperature extremes. Only the first spike in degraded spike bursts was of normal amplitude, followed by a series of waves with decreasing amplitude up to the level of baseline noise (Fig. 5d). In this study, malfunctioning DNs producing degraded spike bursts were not classified as bursty. In addition, at temperatures above 40 °C, one part of the DNs stopped production of normal as well as degraded spike bursts and generated rare single spikes instead, or stopped firing at all. Compared to the DNs, spike bursting of the CNs started at remarkably higher temperatures. None of the CNs were bursty at 25 °C and only 2.05 % of the CNs were bursty at 30 °C (Fig. 6). Again, the percentage of CNs producing bursty spike trains became larger in accordance with temperature increase and at 45 °C, spike trains produced by 83.3 % of the CNs were classified as bursty. It became evident that, at the same temperatures, percentages of bursty DNs were 2.4- to 8.2-fold higher compared to those of the CNs. However, the opposite was observed at the highest temperature of 45 °C, when the percentage of bursty CNs was almost twice that of the DNs (Fig. 6). Further, only the spike trains containing normal spike bursts were analysed.

Spike bursts produced by the DN and CN encode different ranges of noxious heat

Next, we comparatively analysed dependence of several parameters of bursty spike trains (mean firing rate, percentage of bursty spikes, coefficient of variation of inter-spike intervals for bursty spike trains (CV of ISIs), the number of spikes per burst, the number of bursts per second (spike burst frequency) and mean ISI in a burst) on steady temperature in both DNs and CNs. We found that both mean firing rate and the spike burst frequency in the DNs did not unambiguously depend on temperature (Fig. 7a, b). First, its firing rate varied from 53.6 to 67.4 spikes s^{-1} with a temperature increase from 25 to 35 °C but the changes were statistically not significant ($H_{2,48} = 1.83$; $p > 0.05$). However, when the temperature was increased further, up to 45 °C, the firing rate of the DN dropped to 41.5 spikes s^{-1} ($H_{2,48} = 7.61$; $p < 0.05$). The curve shape of spike burst frequency for the DN followed that of its firing rate. At the range of 25 to 35 °C, this parameter showed a rise from 10.8 to 21.6 spike bursts s^{-1} with temperature increase but the change was statistically not approved ($H_{2,48} = 5.04$; $p > 0.05$). At further temperature increase, it showed a nearly three-fold fall to the level of 7.2 spike bursts s^{-1} ($H_{2,48} = 7.56$; $p < 0.05$). Thus, either these two parameters did not depend on temperature (at certain ranges of temperature, at least) or the same values of these parameters represented two different temperatures.

Three parameters of bursty spike trains in the DNs unambiguously increased with temperature increase ranging from 25 to 45 °C (Fig. 7c–e) as verified for the number of spikes per burst ($H_{4,90} = 48.81$; $p < 0.05$), CV of ISIs ($H_{4,90} = 56.55$; $p < 0.05$) and percentage of bursty spikes ($H_{4,90} = 50.62$; $p < 0.05$). For the first two parameters, the change was more rapid at temperatures above 35 °C than below 35 °C. For example, when temperature increased from 25 to 35 °C, the number of spikes in a burst increased by 18.4 % only, from 2.07 to 2.45 ($H_{2,48} = 10.02$; $p < 0.05$), while with further temperature increase from 35 to 45 °C the mean number of spikes per burst increased by 215.1 %, from 2.45 to 7.72 ($H_{2,64} = 24.15$; $p < 0.05$). CV of ISIs/temperature curve behaved in a nearly similar way. At the range of lower temperatures (25–35 °C) this parameter increased by 80 %, from 0.41 to 0.74 ($H_{2,48} = 12.48$; $p < 0.05$) while at higher temperatures (35–45 °C) the change was much more rapid, 233.1 % ($H_{2,64} = 28.07$; $p < 0.05$). The third parameter of spike bursting in this group, the percentage of bursty spikes in a spike train, followed a S-curve increasing from 42.4 % at 25 °C to 97.5 % at 45 °C ($H_{4,90} = 50.62$; $p < 0.05$). Mean ISI in a burst was the only measured parameter of bursty spike trains that showed a nearly linear, three-fold decrease from 9.1 to 3.0 ms ($H_{4,90} = 49.19$; $p < 0.05$) when the temperature increased from 25 to 45 °C (Fig. 7f).

Compared to DN, the firing rate of the CN in bursty spike trains was much lower being equal to 14.9 spikes s^{-1} at

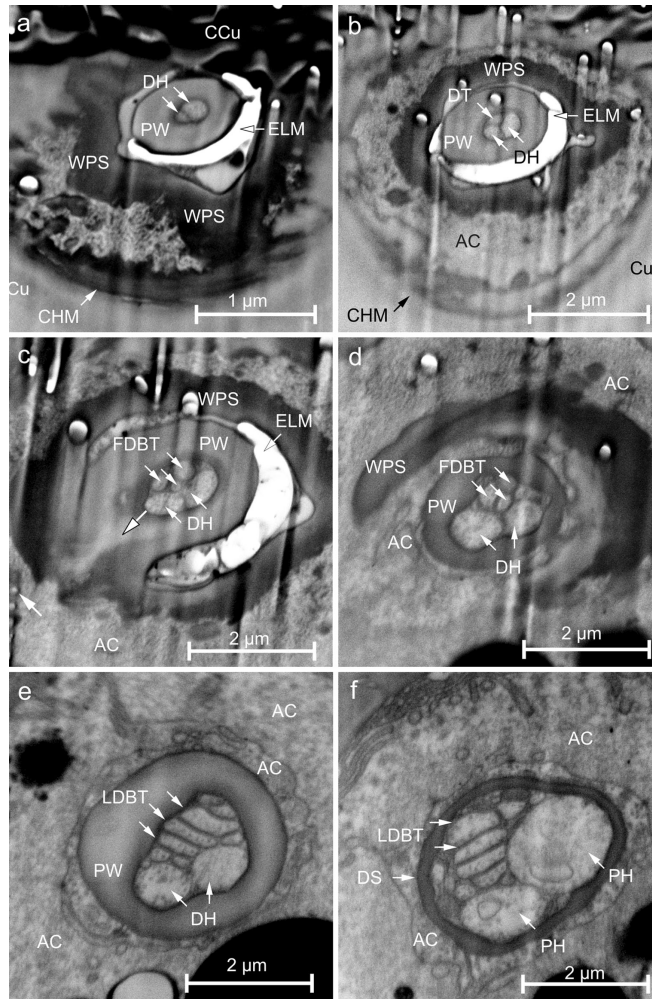

Fig. 4 Inner structure of the antennal ventral DSS. **a** Cross-section through the peg tip. Note that two unbranched dendrites of the hygroreceptor neurons reach the tip of the peg with an aporous wall. **b** Cross-section through the middle part of the peg illustrating that a dendrite from the thermoreceptor neuron enters deep into the peg lumen. **c** Cross-section through the middle of the peg somewhat deeper than (**b**). Note dendritic branches of the thermoreceptor neuron. **d** Cross-section through the sensillum at the level of the peg base. **e** Cross-section through the peg base somewhat deeper than (**d**). Note the wide peg lumen, the fused bases of the peg and the peg socket and lamellated dendritic branches of the thermoreceptor neuron. **f** Cross-section through the sensillum below the peg base. Note large perikarya of two hygroreceptor neurons and lamellated dendritic branches of the thermoreceptor neuron. *AC* auxiliary cell, *CCu* corrugated cuticle, *CHM* cuticular hole margin, *Cu* cuticle, *DH* dendritic outer segment of the hygroreceptor neuron, *DS* dendritic sheath, *DT* dendritic outer segment of the thermoreceptor neuron, *ELM* extracellular electron lucent material, *FDBT* filamentous dendritic branches of the thermoreceptor neuron, *LDBT* lamellated dendritic branches of the thermoreceptor neuron, *PH* perikaria of the hygroreceptor neurons, *PW* peg wall, *WPS* cuticular wall of the peg socket

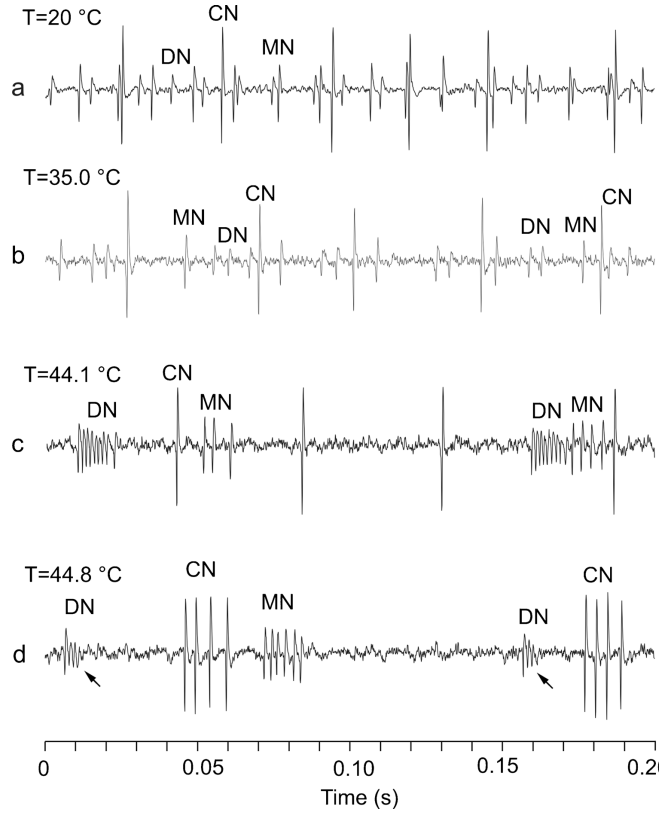

Fig. 5 Sample spike trains of the antennal hygro- and thermoreceptor neurons recorded at various temperatures. All recordings belonged to the neurons of the same DSS. Note that burstyness of the neurons increased with temperature increase. Threshold temperature at which the neurons switched from regular spiking to spike bursting differed and it was the lowest in the DN and the highest in the CN. At high temperature extremes (**d**), spike bursts of the DN began to degrade, only the first spike in a burst was of normal amplitude followed by spikes with gradually diminishing amplitude up to the noise level

35 °C (Fig. 7a) and in contrast to the DN, its firing rate quickly became larger at higher temperatures ($H_{2,54} = 23.3$; $p < 0.05$). Due to the comparatively low firing rate, the spike burst frequency of the CN at 35–45 °C was also considerably (2.2–5.1 times) lower than in the DN (Fig. 7b), equalling only 4.2 spike bursts per second at 35 °C. Above 35 °C, the spike burst frequency increased a little ($H_{2,54} = 8.30$; $p < 0.05$) and at 40–45 °C, stabilised at the level of about 7 spike bursts per second ($p > 0.05$). An unambiguous, 1.6-, 2.5- and 2.7-fold increase was observed in the percentage of bursty spikes ($H_{2,54} = 31.65$; $p < 0.05$), the number of spikes per burst ($H_{2,54} = 34.7$; $p < 0.05$) and CV of ISIs in a spike train ($H_{2,54} = 34.18$; $p < 0.05$) of the CN, respectively, when temperature increased from 35 to 45 °C (Fig. 7c–e) but in most cases, all three

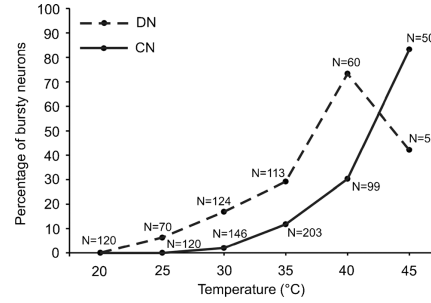

Fig. 6 Percentage of bursty DNs and CDs observed at various temperatures. The number of tested beetles (*N*) is shown along with each data point

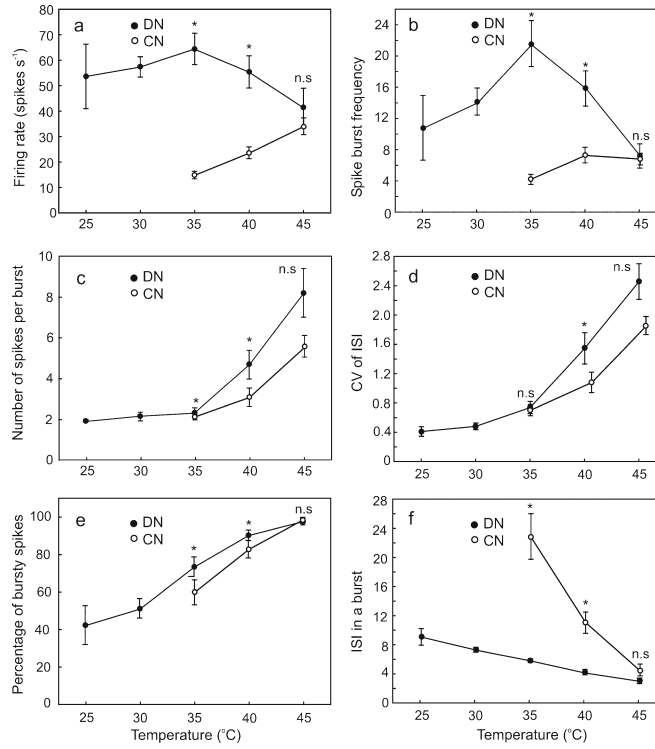

Fig. 7 Dependence of various bursty spike train parameters (mean ± SE) on temperature. The number of tested beetles producing bursty spike trains (*N*) varied between 18 and 23 except for the recordings at 25 °C (*N* = 4). *Asterisks* show significant differences between the spike burst parameters of DN and CN at the same temperatures (Wilcoxon signed rank test; $p < 0.05$)

parameters were considerably lower compared to those of the DN (Fig. 7c–e). However, the most prominent temperature-dependent changes in bursty spike trains of the CN were observed in mean ISIs within the spike bursts (Fig. 7f). This parameter decreased 5.1 times when temperature increased from 35 to 45 °C ($H_{2,54} = 33.62$; $p < 0.05$). Compared to that of the DN, the change was much more rapid.

Rapid step-changes in high temperatures evoke immediate changes in bursty spike trains of the DN

Dependence of spike train burstiness of the DN on ambient temperature was also observed in rapid step-warming conditions (Figs. 8 and 9). In these experiments, six parameters of bursty spike trains of the DN were measured within 10 s before and 10 s after the rapid temperature increase by 1 and 5 °C from the initial temperature of 35 °C, respectively. It was found that four response parameters (firing rate, CV of ISIs of the spike trains, percentage of bursty spikes and the number of spikes in a burst) significantly increased and one response parameter (ISIs in a burst) significantly decreased with a temperature increase of both 1 and 5 °C (Table 1). By contrast, spike burst frequency ambiguously increased with temperature increase so that the change was statistically significant at warming by 1 °C but not at warming by 5 °C. Also the larger change in temperature (by 5 °C) induced significantly larger changes in four measured response parameters, CV of ISIs of the spike trains, percentage of bursty spikes, the number of spikes in a burst and ISIs in a burst compared to those observed at a smaller step-change in temperature (1 °C). Thus, these four temperature-dependent spike

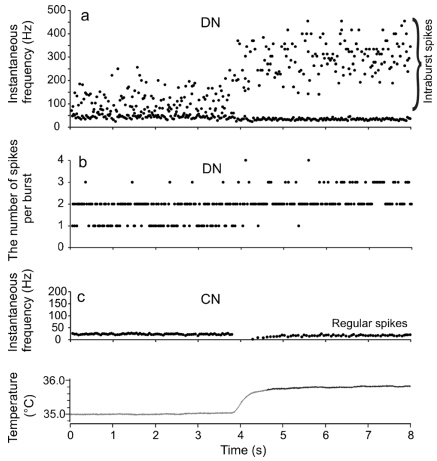

Fig. 8 Reflection of a rapid temperature step-increase in spike trains of the DN and CN belonging to the same sensillum. Note immediate increases in intraburst spike frequencies, percentage of bursty spikes in a spike train and the number of spikes in a burst produced by the DN

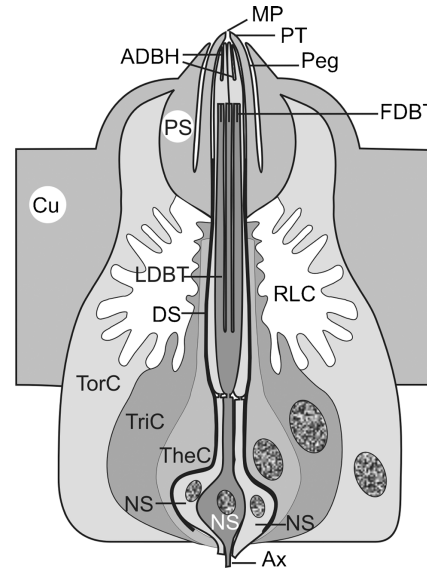

Fig. 9 Schematic reconstruction (not in scale) of an antennal DSS of *P. oblongopunctatus* (by Nurme et al. 2015, modified). *Ax* axon, *Cu* cuticle, *ADBH* apical dendritic branches of the hygroreceptor neurons, *DS* dendritic sheath, *FDBT* filamentous dendritic branches of the thermoreceptor neuron, *LDBT* lamellated dendritic branches of the thermoreceptor neuron, *MP* moulting pore, *NS* neuron somata, *Peg* cuticular peg, *PS* peg socket, *PT* peg tip, *RLC* receptor lymph cavity, *TheC* thecogen cell, *TorC* tormogen cell, *TriC* trichogen cell

train parameters were potentially responsible for unambiguous encoding changes in noxious heat.

Discussion

In carabid beetles, thermo- and hygrosensitive neurons reside in a specific type of antennal sensillum classified as DSS. The complex sensory neurons and auxiliary cells are similar in the DSS and the classical model of thermo- and hygroreceptive (coeloconic) sensilla while the cuticular part of these two morphological types of sensory organs differs fundamentally (Nurme et al. 2015). In this study, we found that several essential fine structural features of dendritic outer segments of the thermo- and hygrosensitive neurons in these two types of sensory organs also differ.

The unbranched outer dendritic segments of the two neurons in DSS of *P. oblongopunctatus* are similar in shape and extend into the cuticular peg up to its tip tightly filling the peg lumen. Their structural similarity suggests a similar sensory modality and thus, most probably, they belong to the two hygroreceptor neurons in accordance with the existing literature data (Altner and Loftus 1985; Steinbrecht 1989; Chapman 1998). Unlike all the antennal hygroreceptor neurons of other insects investigated so far, in most DSS of *P. oblongopunctatus*, at the peg tip, the dendrites of the two possible hygroreceptor neurons have numerous tiny apical branches, round in cross-section, as first demonstrated in this study. The lamellated dendritic branches of the third neuron in the DSS indicate that they belong to the possible thermoreceptor (cold) neuron (Altner and Loftus 1985; Steinbrecht 1989; Chapman 1998). In contrast to the classical thermo- and hygrosensitive peg-in-pit sensilla, however, the lamellated outer dendritic segment of the cold neuron in DSS does not necessarily terminate below the peg base; in most cases, it enters deeply into the peg lumen instead (Nurme et al. 2015). Our results also showed that another fundamental structural difference from the classical thermoreceptor model is the extensive filamentous dendritic branching of the CN in the DSS of *P. oblongopunctatus*, in addition to the lamellation. These filamentous branches, of varying diameter and shape, also enter into the peg, up to the middle of its length.

Steinbrecht (1989) hypothesised that the dendritic lamellation of the insect thermo-sensitive neurons, which increase the surface area of the receptor membrane, may support increased sensitivity to temperature. For the first

Table 1 Spike bursting response of the DN to rapid step-warmings

Measured parameter	1 °C warming		5 °C warming		Average change (%)	
	35 °C	36 °C	35 °C	40 °C	1 °C warming	5 °C warming
Firing rate (spikes s^{-1})	58.8 ± 5.64	67.36 ± 6.04*	65.91 ± 5.24	72.25 ± 7.76*	19.27 ± 6.39 a	12.76 ± 11.72 a
CV of ISIs in a spike train	0.55 ± 0.07	0.86 ± 0.11*	0.48 ± 0.05	1.43 ± 0.19*	60.31 ± 12.79 a	212.52 ± 43.1 b
Percentage of bursty spikes	51.12 ± 6.13	79.42 ± 4.16*	54.16 ± 6.10	97.44 ± 0.93*	28.31 ± 4.26 a	43.30 ± 4.26 b
Number of spikes per burst	2.22 ± 0.08	2.57 ± 0.17*	2.16 ± 0.04	3.70 ± 0.35*	14.46 ± 4.09 a	71.03 ± 16.71 b
ISIs in a burst	7.36 ± 0.45	5.26 ± 0.42*	7.98 ± 0.49	4.00 ± 0.36*	29.10 ± 3.32 a	47.5.10 ± 4.28 b
Spike burst frequency (spike bursts s^{-1})	13.52 ± 1.96	21.91 ± 2.40*	16.31 ± 2.36	23.16 ± 3.34	134.33 ± 40.49 a	93.26 ± 44.58 a

Different lowercase letters indicate statistically significant differences between the treatments at $p < 0.05$ (Mann–Whitney U test)

*Significant differences within treatments at $p < 0.05$. $N = 29$ (1 °C warming) and $N = 16$ (5 °C warming) (Wilcoxon signed rank test)

time in insect thermo-receptor neurons, we found that, in *P. oblongopunctatus*, the location and extent of dendritic lamellation in the CN may vary markedly in different DSS. In some sensilla, the major part of the dendritic outer segments is fully lamellated and it enters deeply into the peg lumen. By contrast, in other sensilla, a slight lamellation of the CN only occurs below the peg base. Intermediate levels of lamellation may also exist. Filamentous branching can also increase the receptor membrane area at the outer dendritic segments and indeed this occurs, in addition to the lamellation, in the CN of *P. oblongopunctatus*. These branches extend deeper into the peg lumen and reach higher with regard to the antennal surface compared to the lamellae and, thus, they are more exposed to the ambient air temperature than the lamellae. The presence of the filamentous dendritic branches of the antennal CN in the DSS of *P. oblongopunctatus* seems to be unique for insect thermosensitive neurons. They have never been found in the classical hygro- and thermoreceptive coeloconic sensilla (Altner and Prillinger 1980; Altner and Loftus 1985; Chapman 1998). They are also absent in other types of insect hygro- and thermoreceptors like sensilla styloconica, sensilla capitula and sensilla coelocapitula (Steinbrecht 1989; Yokohari 1981, 1983). The exact role of these two different structures, the filamentous branches and the lamellae, in thermoreception of the carabid beetles, still remains unclear. It can be speculated, however, that the unique filamentous dendritic branches of the CN in DSS of carabid beetles might be related to the unique ability of the neurons to produce temperature-dependent spike bursts at noxious heat (Must et al. 2010; Nurme et al. 2015). The total surface area of the receptor membrane at the filamentous dendritic branching, due to remarkable variations in the number and diameter of the branches, may also vary, to a large extent, in different DSS. Thus, our results suggest that the large variation in threshold temperatures for spike bursting of the CN (Must et al. 2010; Nurme et al. 2015) might be caused, partly at least, by the remarkable structural variations of their dendritic outer segment. Further comparative fine morphological studies on insect thermoreceptor neurons with the ability for temperature-dependent spike bursting are needed to shed more light on this aspect.

In the classical thermo- and hygroreceptive sensilla, unbranched dendrites of the two hygroreceptor neurons enter into the peg lumen up to its tip (Altner and Prillinger 1980; Altner and Loftus 1985; Chapman 1998), suggesting that enlargement of the surface area of the receptor membrane through dendritic apical branching observed in the hygroreceptor neurons innervating antennal DSS of *P. oblongopunctatus* is not desirable for hygroreception. An alternative interpretation on the function of this structure seems to be more reasonable. We hypothesise that these apical branches might be related to the temperature sensitivity of these, in fact, bimodal thermo-hygroreceptor neurons of *P. oblongopunctatus*. In a DSS, they are located more apically in the peg and they are more exposed to the environmental temperature than the dendritic branches of the CN. The difference in the level of exposure of the outer dendritic branches to external temperature would be a possible explanation why spike bursting in both the two hygroreceptor neurons starts at lower temperatures than in the cold neuron. However, the extent of dendritic branching in the hygroreceptor neurons largely varies in different DSS of *P. oblongopunctatus*, which might be the structural basis for their remarkable variation in threshold temperatures for spike bursting in different DSS.

For the first time in arthropods, our electrophysiological experiments on *P. oblongopunctatus* convincingly demonstrated that one of the two bimodal hygro-thermoreceptor neurons innervating antennal DSS, the dry neuron, at least, may encode noxious high temperatures in a graded manner. At preferred temperatures of the species ranging from 10 to 25 °C (Thiele 1977), both the dry and moist neurons produce regular spike trains and antagonistically respond to changes in ambient air humidity (Merivee et al. 2010). The firing rate of the dry neuron decreases and that of the moist neuron increases with an increase in air humidity and, thus, this

response parameter may precisely encode changes in air humidity at moderate temperatures. When air temperature rises above the preferred temperatures of the species, antennal dry neurons, one after the other, start to switch from regular spiking to spike bursting. The bursting dynamics is highly temperature-dependent. Our results showed that, in addition to the percentage of bursty dry neurons on the antenna, four out of six measured parameters of the bursty spike trains, CV of ISIs in a spike train, percentage of bursty spikes, the number of spikes in a burst and ISIs in a burst, are unambiguously dependent on temperature and thus may precisely encode both noxious high steady temperatures up to 45 °C as well as rapid step-changes in it. The dry neuron never generates spike bursts at moderate temperatures (23 °C) over a wide range of ambient air humidity levels ranging from RH 5 to 95 % (Merivee et al. 2010). This feature does not necessarily mean, however, that air humidity could not modify high temperature-induced spike bursts of the dry neuron to some degree but this has not so far been proven.

Because of the complexity of the background spiking, detecting bursts is a long-standing challenge in investigating the dynamics of burst activity. None of the five temperature-dependent bursty spike train parameters characteristic of the antennal DN of *P. oblongopunctatus* is applicable separately to automatically identify a burst. Four of these parameters (the number of spikes in a burst, the mean ISI in a burst, the percentage of bursty spikes in a spike train and the percentage of bursty neurons on the antenna) suppose previous extraction of spike bursts from a spike train by other methods, for example, by the ISI histogram method (Must et al. 2010; Nurme et al. 2015). Although ISIs in a burst are shorter than the mean ISI of a bursty spike train, presetting its exact threshold value for a spike burst identification, due to response variability of the DNs, is not always possible, for example, at the lower end of noxious high temperatures when the intraburst ISIs only slightly differ from the background spike firing pattern. The fifth parameter, CV of ISIs of a spike train, is not suitable for automated burst identification by its nature.

Our results show that different spike burst parameters of the DN are conjoined: when high temperatures induce one parameter to change the others inevitably change, too. For example, any change in temperature is positively correlated with the CV of ISIs, the number of spikes per burst and the percentage of bursty spikes and is negatively correlated with the mean ISI in a burst. The peculiar feature of the last parameter is its nearly linear stimulus–response curve, which means that this parameter is equally sensitive to noxious heat over the complete range of tested temperatures from 25 to 45 °C. By contrast, the number of spikes per burst and CV of ISIs change slowly with temperature increase at the low end of noxious heat (25–35 °C) but their stimulus–response curves become much steeper at higher temperatures. Thus, the contribution of these two burst parameters to the noxious heat sensation of the beetles might considerably increase at the high end of noxious heat (35–45 °C).

Temperature-dependent bursty spike trains encoding noxious heat have also been found in the antennal cold neuron of the carabids *P. oblongopunctatus* and *Platynus assimilis* (Must et al. 2010) and in the antennal cold and warm receptor neurons of the mosquito, *Aedes aegypti* (Davis and Sokolove 1975). For comparison, in mammals, bursting peripheral cold neurons have been found in the cat tongue and sclera (Schäfer et al. 1988; Gallar et al. 2003) and in corneal cold neurons in mice (Parra et al. 2010; Orio et al. 2012). These cells exhibit similar, temperature-dependent, bursty spike trains to those of insects but in an opposite order since burstiness of their spike trains gradually increases with temperature decrease.

Our results showed that the antennal dry neuron and cold neuron of *P. oblongopunctatus* have different, partly overlapping, threshold temperatures for switching from regular spiking to bursting and that their bursty discharge patterns can code different but partly overlapping ranges of noxious heat. At preferred temperatures (10–25 °C), regular spike trains produced by the antennal dry and moist neurons are responsible for sensing air humidity content and change dynamics (Merivee et al. 2010). Directly above the upper limit of preferred temperatures, at the low end of noxious heat (25–30 °C), dry neurons gradually switch from regular spiking to spike bursting accompanied by a change in their function, switching from coding humidity to coding high temperatures. When air temperature rises to the high end of noxious heat (35–45 °C), the cold neurons also start to produce temperature-dependent spike bursts instead of regular spikes, allowing cold neurons to code much higher temperatures than the dry neurons. Because ISIs within the bursts of the CN decrease much more rapidly with temperature increase compared to those of the DN, the CN is much more sensitive to changes in temperature at the high end of noxious heat than the DN. The threshold temperature for spike bursting in the moist neuron is intermediate to those of these two neurons. However, probable temperature dependence of the spike burst parameters in the moist neuron needs further investigation.

At lower temperatures ranging from 20 to 35 °C, mean firing rate of the CN in P. oblongopunctatus drops down from 30.6 to 8.4 spikes s^{-1} with temperature increase (Nurme et al. 2015). An opposite occurs at the high end of noxious heat when the CN starts to produce bursty spike trains. Raising the stimulating air temperature from 35 to 45 °C results in an increase of spike production of the neuron from 15 to 34 spikes s^{-1}. Thus, due to ambiguity, the mean firing rate of the CN is probably not used for sensing ambient temperatures by the beetles.

It has been argued (Dykes 1975; Roper et al. 2000) that the central nervous system is able to discriminate between certain temporal patterns in the spike trains with a similar mean firing rate but correspond to different temperatures. This is plausible

because high-frequency bursty spikes can be transmitted across unreliable synapses more reliably than isolated, regular spikes (Lisman 1997; Krahe and Gabbiani 2004). One possible function of spike bursting in the transmission of behaviourally relevant sensory information is to detect external signals of danger or specific interest and a number of studies support this hypothesis (Crick 1984; Gabbiani et al. 1996; Sherman 2001; Swadlow and Gusev 2001; Kepecs et al. 2002; Krahe and Gabbiani 2004; Marsat and Pollack 2006; Eyherabide et al. 2008). We hypothesise that, in carabids, information on ambient heat hierarchically coded by bursty spike trains of the dry neuron and cold neuron is probably involved in behavioural thermoregulation of the beetles, allowing them to stay at favourable temperatures and effectively avoid overheating. Unfortunately, no link between thermosensory spike bursts and behaviour has so far been made.

Switching of the dry neurons at high temperatures from coding air humidity to coding noxious heat seems advantageous for the beetles because exposure to dry air is not as dangerous for them as exposure to high temperatures. Momentary and exact information about environmental temperature is extremely important for survival of ground-dwelling carabid beetles making effective behavioural thermoregulation of the beetles in their habitat with steep temperature gradients possible. On sunny days, noxious high temperatures above 40 °C are common on the soil surface (Must et al. 2010) and may be quickly lethal to these insects within some tens of seconds (Thiele 1977; Chown and Nicolson 2004). Desiccation may also be dangerous for carabid beetles but on a much longer time scale. The ability of carabids to survive in dry air fluctuates over very wide limits. In 13 species, at 20–30 % RH and 20 °C, the survival time varied from 18 to 97 h. The survival time for the eurytopic forest inhabitant *P. oblongopunctatus* kept over calcium chloride (residual water content 1.5 mg l^{-1} air) at 21 °C was 35.6 h and 18 h at 28 °C (Thiele 1977). In consequence, at high temperatures, exact coding of air humidity loses its importance for the beetles and the dry neuron switches, in addition to the cold neuron, to code temperature making the neural early warning system of noxious heat more precise and effective.

Acknowledgments The study was supported by institutional research funding IUT36-2 of the Estonian Ministry of Education and Research and Estonian State Forest Management forest protection project (2012–2015) (T12115MIMK).

References

Altner H, Loftus R (1985) Ultrastructure and function of insect thermo- and hygroreceptors. Annu Rev Entomol 30:273–295

Altner H, Prillinger L (1980) Ultrastructure of invertebrate chemo- thermo-, and hygroreceptors and its functional significance. Int Rev Cytol 67:69–139

Altner H, Tichy H, Altner I (1978) Lamellated outer dendritic segments of a sensory cell within a poreless thermo- and hygroreceptive sensillum of the insect *Carausius morosus*. Cell Tissue Res 191:287–304

Altner H, Routil C, Loftus R (1981) The structure of bimodal chemo-, thermo-, and hygroreceptive sensilla on the antenna of *Locusta migratoria*. Cell Tissue Res 215:289–308

Ameismeier F, Loftus R (1988) Response characteristics of cold cell on the antenna of *Locusta migratoria* L. J Comp Physiol A 163:507–516

Chapman RF (1998) The insects, structure and function. Cambridge University Press, Cambridge

Chown SL, Nicolson SW (2004) Insect physiological ecology. Mechanisms and patterns. Oxford University Press, Oxford

Chown SL, Terblanche JS (2007) Physiological diversity in insects: ecological and evolutionary contexts. Adv Insect Physiol 33:50–152

Cossins AR, Bowler K (1987) Temperature biology of animals. Chapman & Hall, London

Crick F (1984) Function of the thalamic reticular complex: the searchlight hypothesis. Proc Natl Acad Sci U S A 81:4586–4590

Davis EE, Sokolove PG (1975) Temperature responses of antennal receptors of the mosquito, *Aedes aegypti*. J Comp Physiol 96:223–236

Denlinger DL, Yocum GD (1998) Physiology of heat sensitivity. In: Hallman GJ, Denlinger DL (eds) Temperature sensitivity in insects and application in integrated pest management. Westview, Boulder, pp 7–57

Dhaka A, Viswanath V, Patapoutian A (2006) TRP ion channels and temperature sensation. Annu Rev Neurosci 29:135–161

Di Giulio A, Maurizi E, Rossi Stacconi MV, Romani R (2012) Functional structure of antennal sensilla in the myrmecophilous beetle *Paussus favieri* (Coleoptera, Carabidae, Paussini). Micron 43:705–719

Di Giulio A, Muzzi M, Romani R (2015) Functional anatomy of the explosive defensive system of bombardier beetles (Coleoptera, Carabidae, Brachininae). Arthropod Struct Dev 44:468–490

Dykes RW (1975) Coding of steady, transient temperatures by cutaneous "cold" fibers serving the hand of monkeys. Biophys J 98:485–500

Ehn R, Tichy H (1996) Response characteristics of a spider warm cell: temperature sensitivities and structural properties. J Comp Physiol A 178:537–542

Eyherabide HG, Rokem A, Herz AVM, Samengo I (2008) Burst firing is a neural code in an insect auditory system. Front Comput Neurosci 2:1–17

Gabbiani F, Metzner W, Wessel R, Koch C (1996) From stimulus encoding to feature extraction in weakly electric fish. Nature 384:564–567

Gallar J, Acosta MC, Belmonte C (2003) Activation of scleral cold thermoreceptors by temperature and blood flow changes. Invest Ophthalmol Vis Sci 44:697–705

Gingl E, Tichy H (2001) Infrared sensitivity of thermoreceptors. J Comp Physiol A 187:467–475

Heinrich B (1993) The hot-blooded insects: strategies and mechanisms of thermoregulation. Springer, Berlin

Hess E, Loftus R (1984) Warm and cold receptors of two sensilla on the foreleg tarsi of the tropical bont tick *Amblyomma variegatum*. J Comp Physiol A 155:187–195

Hochachka PW, Somero GN (2002) Biochemical adaptation. Mechanisms and processes in physiological evolution. Oxford University Press, New York

Keil TA, Steinbrecht RA (1984) Mechanosensitive and olfactory sensilla of insec. In: King RC, Akai H (eds) Insect ultrastructure, vol 1. Plenum, New York, pp 477–516

Kepecs A, Wang XJ, Lisman J (2002) Bursting neurons signal input slope. J Neurosci 22:9053–9062

Klose MK, Robertson RM (2004) Stress-induced thermoprotection of neuromuscular transmission. Integr Comp Biol 44:14–20

Krahe R, Gabbiani F (2004) Burst firing in sensory systems. Nat Rev Neurosci 5:13–23

Lacher V (1964) Elektrophysiologische Untersuchungen an einzelnen Rezeptoren für Geruch, Kohlendioxyd, Luftfeuchtigkeit and Temperatur auf den Antennen der Arbeitsbiene und der Drohne (*Apis mellifica* L.). Z Vgl Physiol 48:587–623

Lisman JE (1997) Bursts as a reliable unit of neural information: making unreliable synapses reliable. Trends Neurosci 20:38–43

Loftus R (1968) The response of the antennal cold receptor of *Periplaneta americana* to rapid temperature changes and steady temperature. Z Vgl Physiol 59:413–455

Loftus R (1976) Temperature-dependent dry receptor on antenna of *Periplaneta*. Tonic response. J Comp Physiol 111:153–170

Lövei GL, Sunderland KD (1996) Ecology and behavior of ground beetles (Coleoptera: Carabidae). Annu Rev Entomol 41:231–256

Marsat G, Pollack GS (2006) A behavioural role for feature detection by sensory bursts. J Neurosci 26:10542–10547

McIver SB (1985) Mechanoreception. In: Kerkut GA, Gilbert LI (eds) Comparative insect physiology, biochemistry and pharmacology, vol VI. Pergamon, Oxford, pp 71–132

Merivee E (1992) Antennal sensilla of the female and male elaterid beetle *Agriotes obscurus* L. (Coleoptera: Elateridae). Proc Estonian Acad Sci Biol 41:189–215

Merivee E, Rahi M, Luik A (1997) Distribution of olfactory and some other antennal sensilla in the male click beetle *Agriotes obscurus* L. (Coleoptera: Elateridae). Int J Insect Morphol Embryol 26:75–83

Merivee E, Rahi M, Bresciani J, Ravn HP, Luik A (1998) Antennal sensilla of the click beetle, *Limonius aeruginosus* (Oliver) (Coleoptera: Elateridae). Int J Insect Morphol Embryol 27:311–318

Merivee E, Rahi M, Luik A (1999) Antennal sensilla of the click beetle, *Melanotus villosus* (Geoffroy) (Coleoptera: Elateridae). Int J Insect Morphol Embryol 28:41–51

Merivee E, Ploomi A, Rahi M, Luik A, Sammelselg V (2000) Antennal sensilla of the ground beetle *Bembidion lampros* Hbst. (Coleoptera, Carabidae). Acta Zool 81:339–350

Merivee E, Ploomi A, Luik A, Rahi M, Sammelselg V (2001) Antennal sensilla of the ground beetle *Platynus dorsalis* (Pontoppidan, 1763) (Coleoptera, Carabidae). Microsc Res Tech 55:339–349

Merivee E, Ploomi A, Rahi M, Bresciani J, Ravn HP, Luik A, Sammelselg V (2002) Antennal sensilla of the ground beetle *Bembidion properans* Steph. (Coleoptera, Carabidae). Micron 33: 429–440

Merivee E, Vanatoa A, Luik A, Rahi M, Sammelselg V, Ploomi A (2003) Electrophysiological identification of cold receptors on the antennae of the ground beetle *Pterostichus aethiops*. Physiol Entomol 28:88–96

Merivee E, Must A, Luik A, Williams I (2010) Electrophysiological identification of hygroreceptor neurons from the antennal dome-shaped sensilla in the ground beetle *Pterostichus oblongopunctatus*. J Insect Physiol 56:1671–1678

Must A, Merivee E, Mänd M, Luik A, Heidemaa M (2006a) Electrophysiological responses of the antennal campaniform sensilla to rapid changes of temperature in the ground beetles *Pterostichus oblongopunctatus* and *Poecilus cupreus* (Tribe Pterostichini) with different ecological preferences. Physiol Entomol 31:278–285

Must A, Merivee E, Luik A, Mänd M, Heidemaa M (2006b) Responses of antennal campaniform sensilla to rapid temperature changes in ground beetles of the tribe Platynini with different habitat preferences and daily activity rhythms. J Insect Physiol 52:506–513

Must A, Merivee E, Luik A, Williams I, Ploomi A, Heidemaa M (2010) Spike bursts generated by the thermosensitive (cold) neuron from the antennal campaniform sensilla of the ground beetle *Platynus assimilis*. J Insect Physiol 56:412–421

Nakanishi A, Nishino H, Watanabe H, Yokohari F, Nishikawa M (2009) Sex-specific antennal sensory system in the ant *Camponotus japonicus*: structure and distribution of sensilla on the flagellum. Cell Tissue Res 338:79–97. doi:10.1007/s00441-009-0863-1

Neven LG (2000) Physiological responses of insects to heat. Postharvest Biol Technol 21:103–111

Nurme K, Merivee E, Must A, Sibul I, Muzzi M, Di Giulio A, Williams I, Tooming E (2015) Responses of the antennal bimodal hygroreceptor neurons to innocuous and noxious high temperatures in the carabid beetle, *Pterostichus oblongopunctatus*. J Insect Physiol 81:1–13

Orio P, Parra A, Madrid R, González O, Belmonte C, Viana F (2012) Role of I_h in the firing pattern of mammalian cold thermoreceptor endings. J Neurophysiol 108:3009–3023

Parra A, Madrid R, Echevarria D, del Olmo S, Morenilla-Palao C, Acosta MC, Gallar J, Dhaka A, Viana F, Belmonte C (2010) Ocular surface wetness is regulated by TRPM8-dependent cold thermoreceptors of the cornea. Nat Med 16:1396–1399

Piersanti S, Rebora M, Almaas TJ, Salerno G, Gaino E (2011) Electrophysiological identification of thermo-and hygro-sensitive receptor neurons on the antennae of the dragonfly *Libellula depressa*. J Insect Physiol 57:1391–1398

Rebora M, Piersanti S, Almaas TJ, Gaino E (2007) Hygroreceptors in the larva of *Libellula depressa* (Odonata: Libellulidae). J Insect Physiol 53:550–558

Roper P, Bressloff PC, Longtin A (2000) A phase model of temperature-dependent mammalian cold receptors. Neural Comput 12:1067–1093

Ruchty M, Romani R, Kuebler LS, Ruschioni S, Roces F, Isidoro N, Kleineidam CJ (2009) The thermo-sensitive sensilla coeloconica of leaf-cutting ants (*Atta vollenweideri*). Arthropod Struct Dev 38:195–205

Schäfer K, Braun A, Rempe L (1988) Classification of a calcium conductance in cold receptors. Prog Brain Res 74:29–36

Shanbhag SR, Singh K, Singh RN (1995) Fine structure and primary sensory projections of sensilla located in the sacculus of the antenna of *Drosophila melanogaster*. Cell Tissue Res 282:237–249

Sherman SM (2001) Tonic and burst firing: dual modes of thalamocortical relay. Trends Neurosci 24:122–126

Snodgrass RE (1935) Principles of insect morphology. McGraw-Hill, New York

Steinbrecht RA (1989) The fine structure of thermo-/hygrosensitive sensilla in the silkmoth *Bombyx mori*: receptor membrane substructure and sensory cell contacts. Cell Tissue Res 255:49–57

Swadlow HA, Gusev AG (2001) The impact of 'bursting' thalamic impulses at a neocortical synapse. Nat Neurosci 4:402–408

Tang X, Platt MD, Lagnese CM, Leslie JR, Hamada FN (2013) Temperature integration at the AC thermosensory neurons in *Drosophila*. J Neurosci 33:894–901

Thiele HU (1977) Carabid beetles in their environment. Zoophysiology and Ecology, vol. 10. Springer, Berlin

Tichy H (1979) Hygro- and thermoreceptive triad in antennal sensillum of the stick insect, *Carausius morosus*. J Comp Physiol 132:149–152

Tichy H (1987) Hygroreceptor identification and response characteristics in the stick insect *Carausius morosus*. J Comp Physiol 160:43–53

Tichy H (2007) Humidity-dependent cold cells on the antenna of the stick insect. J Neurophysiol 97:3851–3858

Tichy H, Kallina W (2010) Insect hygroreceptor responses to continuous changes in humidity and air pressure. J Neurophysiol 103:3274–3286

Waldow U (1970) Elektrophysiologische Untersuchungen an Feuchte-, Troken- und Kälterezeptoren auf der Antenne der Wanderheuschrecke *Locusta*. Z Vgl Physiol 69:249–283

Wang G, Qiu Y, Lu T, Kwon HW, Pitts R, van Loon J, Takken W, Zwiebel LJ (2009) *Anopheles gambiae* TRPA1 is a heat-activated channel expressed in thermosensitive sensilla of female antennae. Eur J Neurosci 30:967–974

Yokohari F (1981) The sensillum capitulum, an antennal hygroreceptive and thermoreceptive sensillum of the cockroach, *Periplaneta americana L*. Cell Tissue Res 216:525–543

Yokohari F (1983) The coelocapitular sensillum, an antennal hygroreceptive and thermoreceptive sensillum of the honeybee, *Apis mellifera*. Cell Tissue Res 233:355–365

Yokohari F (1999) Hygro- and thermoreceptors. In: Eguchi E, Tominaga Y (eds) Atlas of arthropod sensory receptors: dynamic morphology in relation to function. Springer, Berlin, pp 191–210

Yokohari F, Tominaga Y, Tateda H (1982) Antennal hygroreceptors of the honeybee, *Apis mellifera L*. Cell Tissue Res 226:63–73

Zacharuk RY (1985) Antennae and sensilla. In: Kerkut GA, Gilbert LI (eds) Comparative insect physiology, biochemistry and pharmacology, vol VI. Pergamon, Oxford, pp 1–69

III

Nurme, K., Merivee, E., Must, A., Di Giulio, A., Muzzi, M., Williams, I., Mänd, M. 2018. Bursty spike trains of antennal thermo- and bimodal hygro-thermoreceptor neurons encode noxious heat in elaterid beetles. Journal of Thermal Biology, 72, 101-117.

Journal of Thermal Biology 72 (2018) 101–117

Contents lists available at ScienceDirect

Journal of Thermal Biology

journal homepage: www.elsevier.com/locate/jtherbio

Bursty spike trains of antennal thermo- and bimodal hygro-thermoreceptor neurons encode noxious heat in elaterid beetles

Karin Nurme[a,*], Enno Merivee[a], Anne Must[a], Andrea Di Giulio[b], Maurizio Muzzi[b], Ingrid Williams[a], Marika Mänd[a]

[a] Institute of Agricultural and Environmental Sciences, Estonian University of Life Sciences, Kreutzwaldi Street 1, 51014 Tartu, Estonia
[b] Department of Science, University of Roma Tre, Viale G. Marconi 446, I-00146 Rome, Italy

ARTICLE INFO

Keywords:
Dome-shaped sensillum
Inner structure
Moist-hot neuron
Dry-hot neuron
Cold-hot neuron
Behavioural thermoregulation

ABSTRACT

The main purpose of this study was to explain the internal fine structure of potential antennal thermo- and hygroreceptive sensilla, their innervation specifics, and responses of the sensory neurons to thermal and humidity stimuli in an elaterid beetle using focused ion beam scanning electron microscopy and electrophysiology, respectively. Several essential, high temperature induced turning points in the locomotion were determined using automated video tracking. Our results showed that the sensilla under study, morphologically, are identical to the dome-shaped sensilla (DSS) of carabids. A cold-hot neuron and two bimodal hygro-thermoreceptor neurons, the moist-hot and dry-hot neuron, innervate them. Above 25–30 °C, all the three neurons, at different threshold temperatures, switch from regular spiking to temperature dependent spike bursting. The percentage of bursty DSS neurons on the antenna increases with temperature increase suggesting that this parameter of the neurons may encode noxious heat in a graded manner. Thus, we show that besides carabid beetles, elaterids are another large group of insects with this ability. The threshold temperature of the beetles for onset of elevated locomotor activity (OELA) was lower by 11.9 °C compared to that of critical thermal maximum (39.4 °C). Total paralysis occurred at 41.8 °C. The threshold temperatures for spike bursting of the sensory neurons in DSS and OELA of the beetles coincide suggesting that probably the spike bursts are responsible for encoding noxious heat when confronted. In behavioural thermoregulation, spike bursting DSS neurons serve as a fast and firm three-fold early warning system for the beetles to avoid overheating and death.

1. Introduction

Environmental temperature is of great significance for geographical distribution, habitat selection, ecological performance and survival of small poikilothermic animals such as insects. They have no way other than behavioural thermoregulation to control their body temperature. To detect circumambient temperature insects are equipped with special thermosensory sensilla on their antennae. Although cuticular parts of these sensilla are highly variable in shape, typically they are innervated by a triad of sensory neurons composed of one temperature sensitive (cold) neuron (CN) and two antagonistically responding hygroreceptor neurons, the dry (DN) and the moist air neuron (MN), respectively (Altner and Prillinger, 1980; Altner and Loftus, 1985; Chapman, 1998; Merivee et al., 2003, 2010; Piersanti et al., 2011; Must et al., 2017). Studies on ultrastructure of the classical (coeloconic) hygro- and thermoreceptive sensilla (HTSs) have explained their innervation specifics (Altner and Loftus, 1985; Steinbrecht, 1989; Chapman, 1998; Tichy and Kallina, 2010). The unbranched outer dendritic segments (ODSs) of the two hygroreceptor neurons tightly fill the peg lumen and reach the tip of the cuticular peg. The dendrite of the CN, larger in diameter than that of the MN and DN and irregular in cross-section due to branching and lamellation, terminates below the peg base. Below the cuticular peg, all the dendrites are concentrically enveloped by the dendritic sheath and three auxiliary cells, the thecogen, trichogen and tormogen cells, respectively.

The existing data suggest, however, that firing rate of the CN does

Abbreviations: AH, absolute humidity; CHN, cold-hot neuron; CN, cold neuron; CTMax, critical thermal maximum; CV of ISI, the coefficient of variance of interspike intervals; DAN, dendrite of the A-neuron; DBN, dendrite of the B-neuron; DCN, dendrite of the C-neuron; DHN, dry-hot neuron; DN, dry neuron; DSS, dome shaped sensilla; FIB/SEM, focused ion beam/scanning electron microscope; HTN, hygro- and thermoreceptor neurons; HTS, hygro- and thermoreceptive sensilla; ISI, inter-spike interval; ISIH, inter-spike interval histogram; LA, locomotor activity; MHN, moist-hot neuron; MN, moist neuron; ODS, outer dendritic segments; OELA, onset of elevated locomotor activity; PCA, principal component analysis; RH, relative humidity; SE, standard error; SFR, stationary firing rate; TP, total paralysis

* Corresponding author.
E-mail address: karin.nurme@emu.ee (K. Nurme).

https://doi.org/10.1016/j.jtherbio.2018.01.008
Received 6 October 2017; Received in revised form 17 January 2018; Accepted 21 January 2018
Available online 31 January 2018
0306-4565/

not encode ambient temperatures, especially noxious heat above 30–35 °C, correctly. The CN is extremely sensitive to rapid changes in temperature. Its firing rate phasically or phasic-tonically increases with temperature step-decrease and vice versa, the spike production of the neuron decreases or stops for a certain period of time in response to rapid warming (Loftus, 1968; Waldow, 1970; Merivee et al., 2003; Piersanti et al., 2011). These responses of the CN depend on both initial temperature and the extent of temperature increase. At the high end of physiologically relevant temperatures (30–35 °C), rapid warmings by several degrees may cause silent periods with no spikes lasting for several seconds or more (Merivee et al., 2003; Nurme et al., 2015), making detection of further warmings impossible. Due to ambiguity derived from the fact that particular rates of spike firing can be achieved by many combinations of initial temperature and the extent of change in temperature, it has been considered unlikely that firing rate of the CN can precisely encode ambient temperatures (Loftus, 1968). In many insects, such as the American cockroach *Periplaneta americana*, the dragonfly *Libellula depressa* and some carabid beetles, the stationary firing rate of the CN does not depend on temperature at all (Loftus, 1968; Must et al., 2006a, 2006b; Piersanti et al., 2011).

Encoding noxious high temperatures by insects' thermoreceptor neurons has been a mystery for a long time; however, recently it was discovered that, in carabid beetles, at temperatures above 25–30 °C, the pattern of the spike trains produced by the CN and two bimodal hygroreceptor neurons, housed in antennal dome-shaped sensilla (DSSs) changes, and the neurons switch from regular spiking to spike bursting (Must et al., 2010; Nurme et al., 2015). Several parameters of the bursty spike trains, the percentage of bursty neurons on the antenna, the coefficient of variance of interspike intervals (CVof ISIs) and the percentage of bursty spikes in a spike train, the number of spikes and the ISIs in a burst unambiguously depend on temperature and thus may precisely encode both noxious heat up to 45 °C as well as rapid step-changes in it. It has been hypothesised that thermal information encoded by the bursty spike trains may be used by the beetles in their behavioural thermoregulation (Must et al., 2010; Nurme et al., 2015).

Surprisingly, neurons capable of temperature dependent spike bursting have not been found in insect HTSs other than the DSSs of carabid beetles. Inner fine structure of cuticular parts of the DSSs differs fundamentally from all known types of insect sensilla (Nurme et al., 2015; Must et al., 2017). In the carabid *Pterostichus oblongopunctatus*, they are composed of a round cuticular dome, approximately 6.5 μm in diameter, and of a non-perforated conical peg, about 3 μm in length, tightly inserted into the sensillum socket so that the tiny tip of the peg (diameter 0.5 μm; height 0.3 μm) is directly exposed to ambient air. As in the classical coeloconic HTSs, DSSs of *P. oblongopunctatus* are innervated by the triad of hygro- and thermoreceptor neurons (HTNs) (Must et al., 2017). However, some fundamental structural differences exist in ODSs of the sensory neurons between the two types of sensilla. In contrast to the classical HTSs, in DSSs, the strongly branched and lamellated large ODS of the CN enters deeply into the peg lumen, up to a half of its length and ODSs of both hygroreceptor neurons have numerous, small apical branches. These sensilla, although small in number, are common on the antennal flagellum of carabid beetles (Merivee et al., 2000, 2001, 2002; Di Giulio et al., 2012).

In this study we hypothesise that spike bursting is a fundamental property of insect thermoreceptor neurons responsible for detecting noxious high temperatures to avoid overheating and death, and should be widely distributed among insects, in addition to carabid beetles. Elaterid beetles (Coleoptera, Elateridae) seem to be suitable insects to test this hypothesis and the species *Agriotes obscurus* seems to be a good representative of the family. First, this species prefers to live in open agricultural grasslands and crop fields (Traugott et al., 2015) exposed to direct sunlight where, on sunny days, soil surface maximum temperatures may reach lethal high values of up to 50 °C (Must et al., 2006a). In these thermal conditions, proper sensing and avoidance of noxious heat is crucial for the beetles to survive. No data is available on the upper thermotolerance limits in *A. obscurus*. In the carabids, living in open habitats together with *A. obscurus*, threshold temperatures for total heat paralysis lie in a narrow range between 47.4 and 51.7 °C (Thiele, 1977). However, first indications of partial paralysis (of the hind legs) begin at 44.4 °C (Must et al., 2010). Threshold temperatures of both partial and total paralysis are related to critical thermal maximum of a species (CTMax) (Ernst et al., 1984; Ribeiro et al., 2012) which is widely used to assess thermal limits in ectothermic animals (Lutterschmidt and Hutchison, 1997). It is defined as the temperature above which individuals of a given species respond with disturbances to normal locomotion, subjecting the animal to likely death. Second, antennal cuticular structures, externally similar to dome-shaped sensilla of carabid beetles (Nurme et al., 2015; Must et al., 2017), have been found in a number of elaterid beetles including *A. obscurus* (Merivee, 1992; Merivee et al., 1997, 1998, 1999; Zauli et al., 2016). Because of lack of data on the inner structure of elaterid beetles, different studies and authors have incorrectly and/or inconsistently classified the sensilla campaniformia (Merivee et al., 1998, 1999; Zauli et al., 2016), DSSs (Merivee et al., 1997), and DSSs proposed as a subtype of s. coeloconica (Merivee, 1992). In elaterid beetles, these sensilla are few in number varying between 20 and 40 per antenna (Merivee, 1992; Merivee et al., 1997, 1998, 1999; Zauli et al., 2016), and they are almost evenly distributed on the flagellomeres varying between 2 and 7 depending on the species, except for the terminal flagellomere where their number is higher reaching up to 15 in *Elater ferrugineus*. We also hypothesise that these sensilla on the antennae of elaterid beetles by their morphological type and innervation are identical to the DSSs of *P. oblongopunctatus* but fine morphological studies on their inner structure and electrophysiological experiments are needed to confirm this.

The aims of this study are:

- to clarify morphological type of the possible HTSs on the antennae of *A. obscurus* on the basis of their inner fine structure using a FIB/SEM combined technique;
- through electrophysiological experiments, to test responsiveness and reaction type of the sensory neurons innervating the possible HTSs to ambient air temperature and humidity;
- through electrophysiological experiments, to test the expected ability of the sensory neurons for high temperature induced spike bursting in the range of 25–45 °C;
- through behavioural experiments, to determine CTmax and threshold temperature for total paralysis (TP) for the beetles.

The results of the study are reported in this paper.

2. Material and methods

2.1. Test beetles

Reproductively-immature adults of *A. obscurus* overwintering in soil were collected in South Estonia in September and October of 2014 and 2015. The beetles were kept in plastic boxes (20 × 20 × 10 cm) filled with moistened sand and moss in a refrigerator at 2–3 °C. Four to five days prior to the experiments, they were placed singly in 50-mm Petri dishes with moistened filter paper (Whatman International, UK) and kept at 20 °C in a Versatile Environmental Test Chamber MLR-35 1H (SANYO Electric, Japan) at 16 h light and 8 h dark (16L:8D) photoperiod. Conditioning of the test insects at room temperature was imperative to achieve good electrical contact with the sensory neurons inside the antennal DSS and an acceptable signal-to-noise ratio. The beetles were not fed but were provided with clean tap water every day. Electrophysiological recordings and behavioural experiments were carried out from March to May i.e. after the cold reactivation of the beetles.

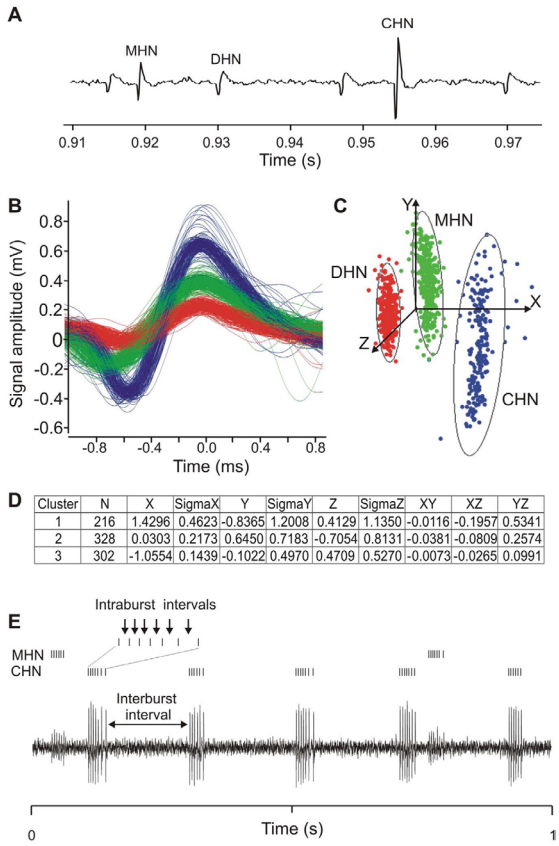

Cluster	N	X	SigmaX	Y	SigmaY	Z	SigmaZ	XY	XZ	YZ
1	216	1.4296	0.4623	-0.8365	1.2008	0.4129	1.1350	-0.0116	-0.1957	0.5341
2	328	0.0303	0.2173	0.6450	0.7183	-0.7054	0.8131	-0.0381	-0.0809	0.2574
3	302	-1.0554	0.1439	-0.1022	0.4970	0.4709	0.5270	-0.0073	-0.0265	0.0991

Fig. 1. Automated multi-unit spike sorting. (A) A 60 ms sample fragment of the 17 s original recording from an antennal dome-shaped sensillum of *A. obscurus* demonstrate characteristic spike waveforms from three different neurons. (B) The overdrawn spike shapes of firing events within 17 s period form three bundles indicating that the spikes arise from three different neurons. (C) Multi-unit spike discrimination using automated PCA clustering available in CED Spike 2 software showed 846 events in 3 classes within 17 s period of the recording (view along Z-axis). Automatically calculated cluster values are shown in (D). (B), (C) and (D) were extracted from the same recording. (E) A one second fragment of a bursty spike train. Extracted spike trains of the CHN and MHN are shown above the fragment of the original recording. The DHN was not active in this particular DSS.

2.2. Focused ion beam/scanning electron microscope (FIB/SEM) combined technique

Beetles were euthanized with CO_2 prior to dissection. Antennae were removed from the specimens, submerged in cacodylate buffer 0.1 M and the last antennomeres were cut and separated from the others, immersed in Karnovsky's fixative solution for 2 h at 4 °C, post-fixed in 1% Osmium tetroxide for 1 h at 4 °C, stained en bloc with 2% aqueous Uranyl acetate, dehydrated in a graded ethanol series and embedded in epoxy resin following the protocol of Di Giulio et al. (2015). Apical antennomeres were extracted from the resin blocks after polymerization, mounted on stubs with double sided adhesive carbon disks, gold sputtered, and analysed with a Dualbeam (FIB/SEM) Helios Nanolab (FEI, Eindhoven, The Netherlands) at L.I.M.E. (Roma Tre University, Rome, Italy). The FIB column was used to dissect the DSS sensilla by using the procedure described in Must et al. (2017) and high resolution (2048 × 1768 pixels) images were acquired by using the SEM column and backscattered electrons (Di Giulio et al., 2015). In total, 300 images from seven DSSs of different animals were made and analysed.

2.3. Electrophysiology

2.3.1. Single sensillum recordings

Our electrophysiological set-up of single sensillum recordings from antennal DSS has been described in detail in Nurme et al. (2015) and Must et al. (2017) so here we describe it in brief only. The grounded tungsten microelectrode was inserted into the lumen of the fourth or fifth antennomere. The recording tungsten microelectrode was pressed into the base of an apical DSS of the terminal flagellomere using the DC-3KS micromanipulator (Stoelting, USA) under visual control with the microscope Eclipse FN1 (Nikon, Japan) at a magnification of

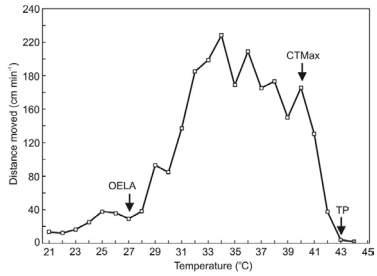

Fig. 2. Example actogram of locomotor activity of *A. obscurus* in the slow warming experiment at a constant AH (9 g m-3) condition. Programmed warming rate and warming range were pre-set at 1 °C min^{-1} and 20–45 °C, respectively. Three essential turning points in the LA/temperature curve of the beetles characterise their responses to heating: OELA, onset of elevated locomotor activity; CTmax, critical thermal maximum; TP, total paralysis.

×750–1000. The microscope was equipped with the Nikon ITS-FN1 Physiostage consisting of the X-Y Translator and stainless steel Stage mounted on the Passive Anti-Vibration Science Desk (ThorLabs, UK). All recordings were made in a 100 × 120 × 100 cm Faraday Cage FAR01 (ThorLabs, UK). The electrical signal picked up by the recording electrode via a custom-made Preamplifier Board (input impedance 10 GΩ) (Interspectrum, Estonia) was led to the input of the main amplifier ISO-DAM 8 A (World Precision Instruments, USA), filtered with a bandwidth set at 10–3000 Hz, monitored on an oscilloscope screen and relayed to a PC hard disc for data storage using the 16-bit A/D data acquisition unit Micro 1401-3 (CED, UK) at a sampling rate of 20 kHz, and Spike 2 software (CED, UK). The recordings were made from one apical DSS of each test beetle. The number of tested beetles (N) is shown in the text (see Results) together with the results of statistical analysis.

2.3.2. Stimulation and control of air humidity and temperature

In this study, we used the thermo- and hygrostimulation and control set-up as described in previous papers (Merivee et al., 2010; Nurme et al., 2015; Must et al., 2017). Here, for clarity, we explain the main principles of functioning of the set-up in brief. Thermo- and hygro-stimuli were presented to the antennal DSS by one or two air streams depending on the experiment. First, the carbon filtered air was conducted through two separate units, the 0.5 L air dryer filled with KOH pellets as desiccant and the air-moistening bubbler vessel. A wide range of relative humidity (RH) levels was achieved by mixing dried air and moistened air in an appropriate ratio. Thereafter, the air streams were warmed up to the required temperature by the heating units. Finally, the air streams at a velocity of 2 m s^{-1} through 8-mm terminal outlet tubes fixed at a distance of 10 mm from the antenna, were directed at the apical DSS. An electromagnetic air valve (Model 062 4E1; Humphrey Products, USA) EMV and a digital timer (Model 4030; Kaiser Fototechnik, Germany) were used to switch rapidly between the two air streams. Both the tested apical DSSs and the copper-constantan thermocouple junction were located at the intersection of the two air streams, with the thermocouple junction 1 mm away from the DSSs. The amplified signal from the thermocouple circuit was led to the second input channel of the data acquisition unit Micro 1401-3 (CED, UK) at a sampling rate of 1 kHz and was stored on a PC hard disc for recording temperature of the stimulating air streams. Two custom-made electronic airflow hygrometers (Interspectrum, Estonia) based on the LinPicco™ capacitive humidity analogue module A01 (response time < 5 s, accuracy < ± 3% RH) (Innovative Sensor Technology, Switzerland) were used to measure RH of the stimulating air streams before the heating units, at 20 °C. Signals from the two hygrometers were led to the third and fourth channel of the data acquisition unit Micro 1401-3 (CED, UK), respectively, and stored on the hard disc for further data management and analysis. When responses of the sensory neurons in the DSS were measured at different steady temperatures, the DSS to be adapted to the initial temperature before each next stimulation were exposed to each tested temperature for 10 min.

2.4. Behavioural experiments

For video-tracking, the beetles were placed singly into 90 × 100 ×

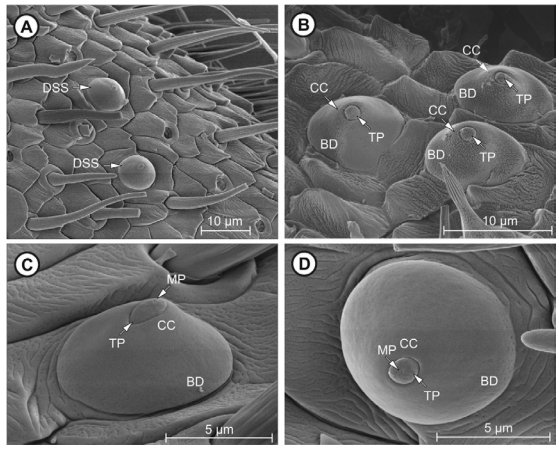

Fig. 3. External shape of the antennal DSS in A. obscurus. (A) A couple of DSS located close to each other among other types of sensilla on the dorso-posterior area of the terminal flagellomere. (B) A group of three DSS at the apex of the terminal flagellomere. Note that the peg tip (TP) is tight within the dome. (C) Side view of the DSS at a higher magnification. Note that the sensillar dome towers 4–5 µm above the antennal surface and is well exposed to ambient air. (D) Top view of the DSS shows that the cuticular dome is almost round in cross-section. Note the tiny apical moulting pore (MP) at the peg tip. BD, dome base; CC, central cap.

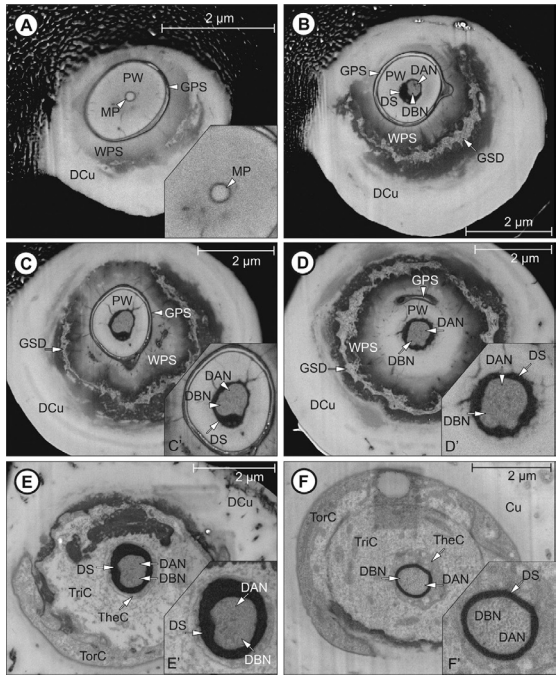

Fig. 4. Inner fine structure of the DSS. (A) Cross-section through the upper part of the dome. Note the tiny apical moulting pore (MP) with no nerve endings, and a narrow gap (GPS) between the peg wall (PW) and cuticular wall of the peg socket (WPS). (B) Cross-section through the middle part of the dome. In this particular sensillum, the dark dendritic sheath (DS) enters deep into the peg lumen. Also, note a narrow gap (GPS) between the PW and the WPS, and a gap (GSD) between the peg socket and dome cuticle (DCu). (C) Cross-section through the middle part of the dome somewhat deeper than in (B). Note that the peg socket almost entirely separates from the DCu. (D) Cross-section through the dome at the level of the peg base. Note that the walls of the peg base and peg socket are fused and the peg socket separates from the dome cuticle completely. (E) Cross-section through the dome directly below the peg base. Below the dome, inside the cuticular cavity, three auxiliary cells, the tormogen (TorC), trichogen (TriC) and thecogen (TheC) cells, respectively concentrically envelop DAN and DBN. (F) Cross-section through the antennal cuticle (Cu) below the dome, somewhat deeper than in (E). Note the two dendrites from the A-neuron, and B-neuron inside the DS and the three concentric auxiliary cells.

40 mm plastic arenas lined with polypropylene plant fleece and transferred into a Versatile Environmental Test Chamber MLR-35 1 H (SANYO Electric, Japan) pre-set at 20 °C and absolute humidity (AH) 9 g m^{-3}. Prior to recording, the beetles were allowed to rest for 5 min. Four LED lamps MR 16 (12 V, 7.5 W, 570 lm, 3000 K) illuminated the arenas. Illumination at the level of test beetles (2000 lx) was measured by a Digital Light Meter TES-1335 (TES Electrical Electronic Corp., Taipei, Taiwan). Locomotor activity (LA) of the beetles was recorded with a resolution of 1920 × 1080 pixels at 5 frames s^{-1} by a computer-centered video-tracking system using the USB Logitech HD Pro Webcam C920 (Logitech Inc., USA) fixed at a height of 40 cm above the arenas, and the computer software Debut Video Capture (NCH Software, USA). A programmed linear heating rate of 1 °C min^{-1} in the range of 20–45 °C was used during the recordings. Distance moved (start velocity > 0.1 cm/s; stop velocity < 0.1 cm/s) with the temporal resolution of 1 s was extracted offline from the recorded video files using EthoVision XT Version 9 software (Noldus Information Technology, Wageningen, The Netherlands).

2.5. Data management and statistical analysis

Recorded spike trains usually contained spikes from more than one sensory unit. Spike shapes recorded from different DSSs usually varied, and in a few cases, those produced by two different neurons overlapped to a larger or lesser extent. Spike trains in which spike shape overlapping exceeded 5% were discarded from further analysis. For extracting individual spike trains, automated spike waveform sorting in combination with automated principal component analysis (PCA), clustering and overdraw options available in CED Spike 2 software, and visual inspection were used (Fig. 1). When spikes produced by different neurons were superimposed, the Collision analysis option of CED Spike 2 and visual inspection were involved in spike sorting. Sensory modality and reaction type of the sensory units were determined by differences between their responses to rapid step-changes in stimulating air humidity and temperature (for details, see Nurme et al., 2015). Response characteristics of the neurons were measured and analysed using CED Spike 2 and MS Excel software. Mean firing rate was expressed in spikes s^{-1}. Instantaneous spike frequencies (spikes s^{-1}) were calculated as the reciprocals of inter-spike intervals. To decide if a certain response was regular or bursty the recorded spike trains were subjected to inter-spike interval histogram (ISIH) analysis and visual inspection. The threshold ISIs for spike bursting were found from ISIHs and used for classifying spikes as regular or belonging to a burst (for details, see Must et al., 2010; Bakkum et al., 2014; Nurme et al., 2015). Three turning points were determined on the LA/temperature curves of the beetles to characterise their responses to heating, threshold temperature for prolonged upsurge in LA (OELA), CTMax and threshold temperature for total paralysis, respectively (Fig. 2). CTMax was assessed as the onset of sharp decline in elevated (maximum) locomotor activity at the high end of noxious heat. Threshold temperature for total paralysis was defined as the temperature at which the beetles stopped moving and died due to thermoshock.

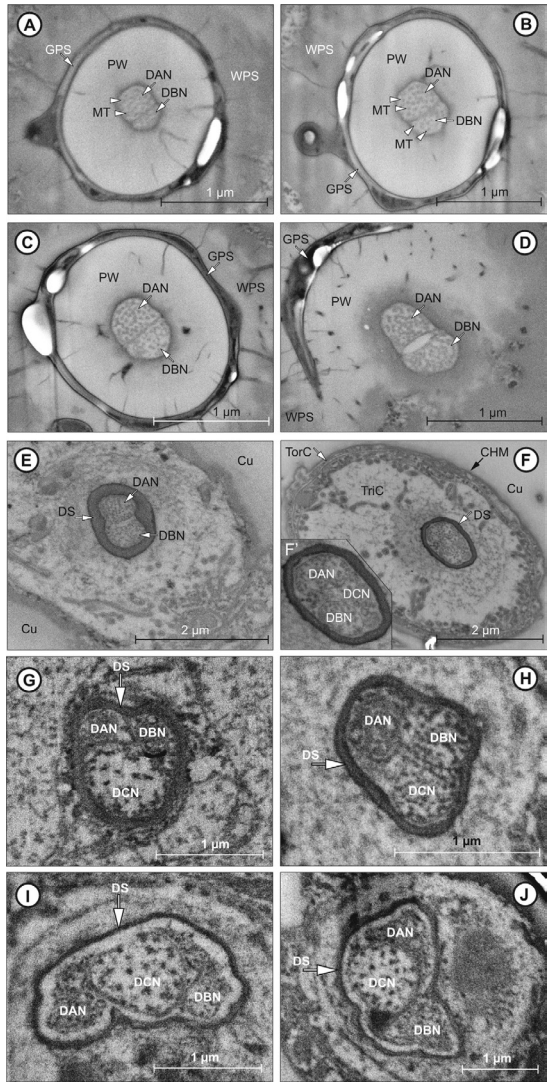

Fig. 5. Innervation of the DSS. (A) Cross-section through the apex of the DSS. Note the round, no-pore wall of the peg and two unbranched dendrites (DAN and DBN) of the A- and B-neuron. (B) Cross-section through the middle part of the peg. Tiny dark dots inside the dendritic branches represent microtubules (MT). (C) Cross-section through the middle part of the peg somewhat deeper than in (B). The unbranched DAN and DBN of equal diameter tightly fill the peg lumen. (D) Cross-section through the peg base. Note that only the dendrites of the A- and B-neuron enter into the peg lumen, DAN and DBN. (E) Cross-section through the cuticle directly below the peg base. Note that below the peg base a common dendritic sheath (DS) envelops the dendrites. (F) Cross-section through the cuticle below the peg base somewhat deeper than in (E). Note that in addition to the DAN and DBN a large third dendrite (DCN) from the C-neuron is located inside the common DS. (G–F) Cross-sections through the cuticle below the peg base of the DSSs in other four beetles demonstrating that the number of innervating neurons in DSSs is constantly three. (I) and (J) show cross-sections of the three dendrites close to their perikarya.

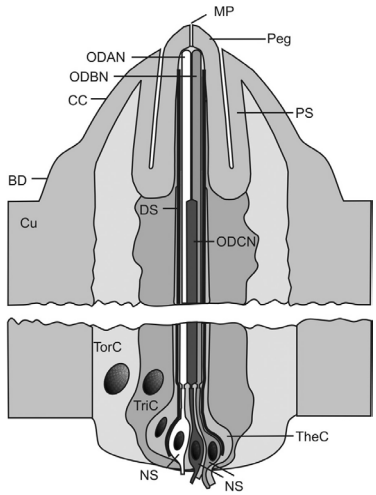

Fig. 6. Structural diagram (not to scale) of an antennal DSS in the elaterid beetle *A. obscurus*. Cu, cuticle; CC, central cap; BD dome base; DS, dendritic sheath; MP, apical moulting pore; NS, neuron somata; ODAN, ODBN and ODCN show outer dendritic segments of the A-, B- and C-neuron, respectively; Peg, cuticular peg; PS, cuticular peg socket; TheC, thecogen cell; TorC, tormogen cell; TriC, trichogen cell.

One way ANOVA and Tukey test was used to evaluate the effect of steady temperature and rapid step warming on the responses of the neurons innervated antennal DSS and to calculate the significance of different means. In the rapid step cooling and rapid change in RH experiment paired *t*-tests were used to compare responses from receptor neurons in DSS before and after stimulus onset. All mean responses were accompanied by a standard error bar (SE).

3. Results

3.1. Cuticular fine structure and innervation of antennal DSSs in A. obscurus

3.1.1. External structure

DSSs occurred in low numbers on all flagellomeres of male and female beetles except for the 1st flagellomere where they were absent. Usually, they were close to each other among other types of sensilla (Fig. 3A). Four to six of them were concentrated at the tip of the terminal flagellomere (Fig. 3B). These apical DSSs were the most easily accessible for electrophysiology. Externally, DSSs were composed of a round cuticular dome varying 5.0–9.5 μm in diameter, and a small peg positioned tightly in the peg socket and slightly, up to one μm, protruding above the dome surface (Fig. 3B,C,D). DSSs towered approximately 4–5 μm above the antennal surface and they were well exposed to ambient air. At the tip of the peg, a tiny orifice of the moulting pore was visible (Fig. 3C,D).

3.1.2. Internal fine structure

FIB/SEM analysis showed that inside the dome, the cuticular peg, for its whole length, was tightly sunken into the cuticular socket. It had a non-perforated wall, round in cross-section (Fig. 4A–C). At the level of the dome base, the cuticular walls of the peg and peg socket fused

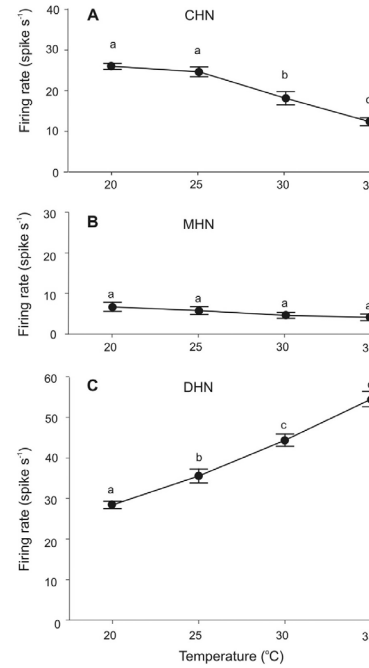

Fig. 7. Spiking activity of the neurons in antennal DSS at different levels of steady temperature. Measurements were performed at constant absolute humidity (AH) 9 g m^{-3} condition. Vertical bars show standard errors (SE) of the means. Different letters indicate significant differences between the means at $p < .05$ (Tukey test, $N = 30$).

(Fig. 4D). Thus, the length of the peg (4–5 μm) approximately equalled the height of the dome. Cross-section of the peg tip revealed a small apical moulting pore (Fig. 4A). Deeper in the dome, directly below the moulting pore, the peg lumen widened and it contained two unbranched dendrites of equal length (dendrite of the A-neuron (DAN) and dendrite of the B-neuron (DBN)) of the A-neuron and B-neuron, respectively, tightly filling the lumen (Fig. 4C–F, Fig. 5A–D). The dendritic sheath enveloping the dendrites entered distally deep into the peg lumen in some sensilla (Fig. 4B–D) but not in others (Fig. 5A–F). The dendrite of the third neuron (dendrite of the C-neuron (DCN)), larger in diameter than the DAN and DBN, ended below the peg base (Fig. 5F–J). No indications of dendritic branching and lamellation were observed. The narrow gap between the peg socket and cuticular wall of the dome was filled with the tormogen cell (Fig. 4B–D). Below the peg base, dendrites of the three sensory neurons were concentrically enveloped by three auxiliary cells, the tormogen, trichogen and thecogen cell, respectively (Figs. 4E,F; 5F). See Fig. 6 for a generalised structural diagram of the DSS.

3.2. Electrophysiological identification of the neurons innervating antennal DSSs

Three types of spike shapes produced by three sensory neurons were

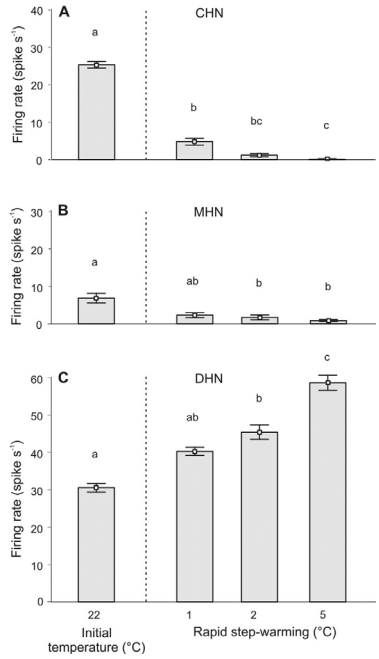

Fig. 8. Response of the three antennal DSS neurons to rapid step-increases in temperature at constant AH (9 g m^{-3}). Note that rapid step-warmings caused much larger fold-changes in firing rate of all the neurons than similar differences (e.g., by 5 °C) in steady temperature (see Fig. 7). Vertical bars show SE of the means. Different letters show significantly different means at $p < .05$ (Tukey test, N = 20).

recorded from the antennal DSS. In electrophysiological experiments, the neurons diversely responded to thermal and humidity stimuli presented. According to their response characteristics, they were classified as cold-hot neuron (CHN), bimodal moist-hot neuron (MHN) and bimodal dry-hot neuron (DHN), respectively. The CHN always produced spikes with the largest amplitude (Fig. 1).

3.2.1. Firing rate/steady temperature curves of the CHN, MHN and DHN

The stationary firing rate (SFR) of the neurons was measured at steady temperatures of 20 °C, 25 °C, 30 °C, and 35 °C. The temperature/response curves of the neurons differed considerably. The SFR of the CHN showed a general 2.1-fold decrease from 25.8 to 12.2 spikes s^{-1} with temperature increase (Fig. 7A). However, spike production of the neuron recorded at the low end of tested temperatures (20 and 25 °C) did not differ. SFR of the MHN nearly linearly decreased from 6.8 spikes s^{-1} at 20 °C to 4.2 spikes s^{-1} at 35 °C, equal to 1.6-fold change in the response but the differences were statistically not significant (Fig. 7B). By contrast to the CHN and MHN, firing rate of the DHN linearly increased from 28.4 to 54.5 spikes s^{-1} with temperature increase from 20 to 35 °C (Fig. 7C) representing to 1.9-fold change in the response. Thus, at tested steady temperatures, the fold change in SFR varied only a little among CHN, MHN and DHN ranging from 1.6- to 2.1.

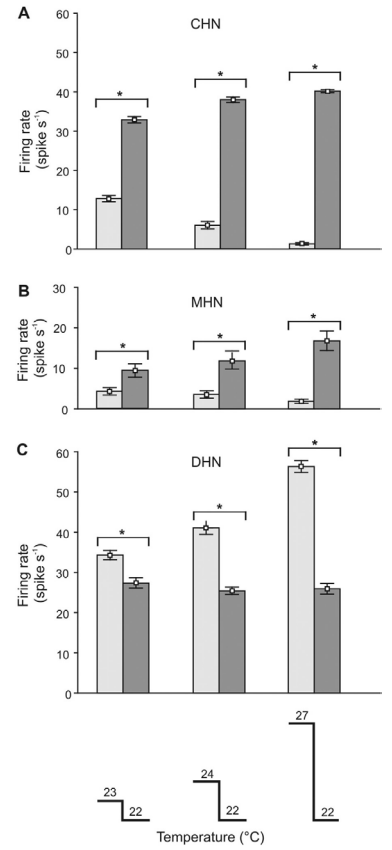

Fig. 9. Response of the DSS neurons to rapid step-coolings at a constant AH (9 g m^{-3}) condition. Note that in this experiment, the initial temperature was changed and the final temperature was held constant. Note that rapid step-cooling was a much stronger stimulus for the neurons than similar differences (e.g., by 5 °C) in steady temperature as demonstrated in Fig. 7. Vertical bars represent the SE of the means. Asterisks show significantly different means at $p < .05$ (Paired *t*-test, N = 20).

3.2.2. Responses to rapid step-warmings

We measured mean firing rate of the neurons within two seconds before and two seconds after the beginning of temperature step-increase. An initial temperature of 22 °C was used. All the three neurons were sensitive to rapid warmings with the CHN showing the strongest response. For example, rapid warming by only 1 °C caused a 5.3-fold drop from 25.4 to 4.8 spikes s^{-1} in spike production of the CHN (Fig. 8A). This response change of the CHN was approximately 2.5-fold larger than that caused by a 15 °C increase in steady temperature (Fig. 7A). Rapid step-warmings by 2 and 5 °C caused a 21.2- and 254-fold decrease in firing rate of the CHN, respectively (Fig. 8A). These

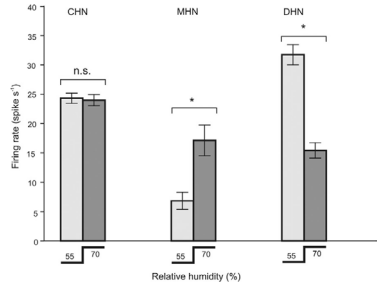

Fig. 10. Response of the DSS neurons to the 15% rapid step-increase in RH. Vertical bars indicate SE of the means. Note that the MHN and DHN antagonistically responded to the change in RH. Asterisks show significantly different means at $p < .05$. n.s., the difference was statistically not significant (Paired *t*-test, N = 30).

results showed that this neuron was much more sensitive to rapid step-warmings than to different levels of steady temperature. The MHN also responded to rapid step-warmings with a drop in its firing rate but to a much lesser extent than the CHN. A 3.0-, 4.0- and 7.6-fold fall in its spike production occurred when temperature was step-wise increased by 1, 2 and 5 °C, respectively (Fig. 8B). Contrary to the CHN and MHN, neuronal activity of the DHN increased with temperature step-increase but the fold change in its firing rate was relatively small, 1.3, 1.5 and 1.9 with the step-warmings by 1, 2 and 5 °C, respectively. Thus, our results demonstrated that firing rate of the CHN responded much more strongly responded to rapid step-warmings than that of the MHN and DHN.

3.2.3. Responses to rapid step-decreases in temperature

In rapid step-cooling experiments, initial air temperature was raised from 22 °C to 23, 24 and 27 °C for 10 s, respectively, while final (cooling) temperature was held constant at 22 °C. Mean firing rate of the neurons was measured two seconds before and two seconds after the beginning of rapid step-coolings. We observed that both CHN and MHN responded to temperature rapid step-decreases with their firing rate increase. Larger drops in temperature caused stronger responses of the neurons. Thus, step-coolings of the DSS by 1, 2 and 5 °C caused 2.6-, 6.3- and 33.4-fold increases in firing rate of the CHN, respectively (Fig. 9A). Changes in firing rate of the MHN in response to the tested step-coolings were considerably smaller compared to those of the CHN. Its calculated fold increases in spike production were 2.2, 3.1 and 8.8 with temperature drops of 1, 2 and 5 °C, respectively (Fig. 9B). By contrast, a 1.3- to 2.2-fold decrease in firing rate of the DHN was observed depending on the magnitude of temperature drop (Fig. 9C). Hence, the DHN responded to the tested drops in temperature to a much lesser extent than the CHN and MHN. Again, in a triad of the sensory neurons innervating antennal DSS, the CHN most strongly responded to the tested step-coolings.

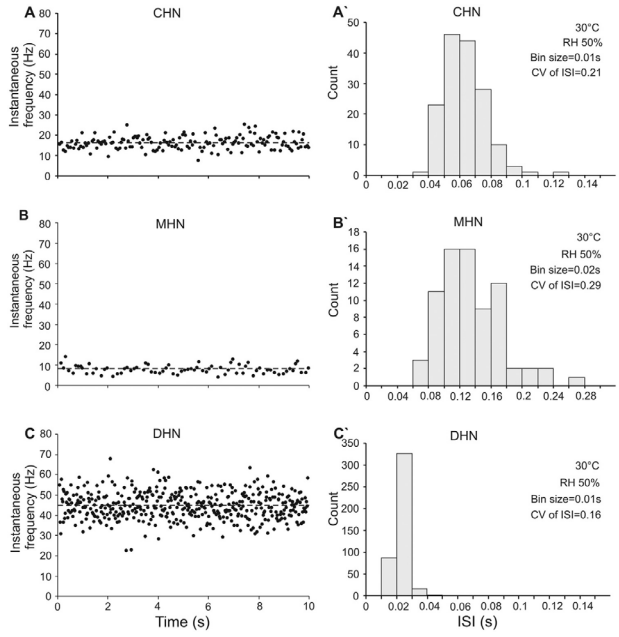

Fig. 11. Typical regular spike trains produced by the antennal DSS neurons at temperatures up to 25–30 °C. Note that instantaneous spike frequencies of the neurons almost symmetrically deviate from the mean value, and their ISIH have one maximum. Dotted lines indicate mean instantaneous spike frequencies of the respective neurons.

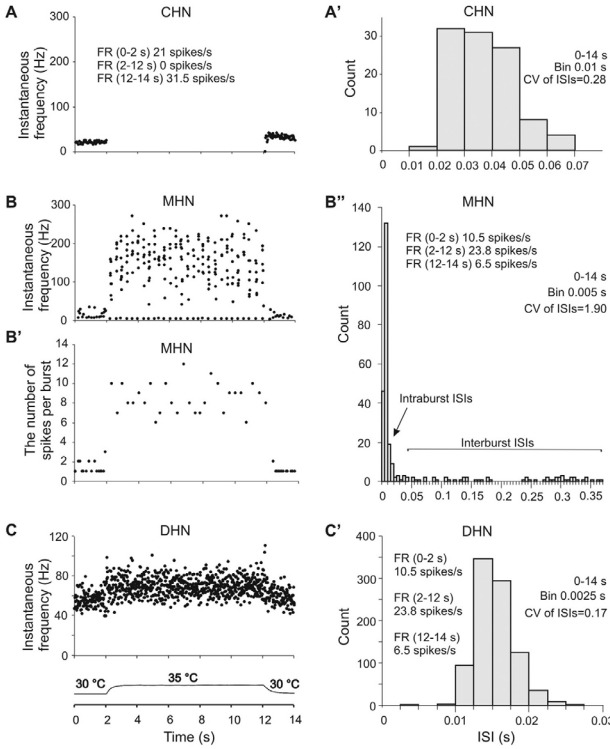

Fig. 12. Typical responses of the DSS neurons to a rapid step-warming by 5 °C at the low end of noxious heat (30–35 °C). Note that the MHN had the lowest threshold temperature for spike bursting (B, B′). The number of spikes per burst increased with temperature increase (B′). The ISIH had two clusters (B″), representing intra-burst and inter-burst intervals, respectively. The spike bursting response of the MHN was reversible, its regular spike production immediately recovered after the rapid cooling. All the three neurons originated from the same sensillum. FR, mean firing rate.

3.2.4. Responses to rapid step-changes in RH

Response of the neurons to air humidity was tested at RH 55% and 70% keeping air temperature constant at 20 °C. Their firing rates were measured within 2 s before and two seconds after the beginning of the rapid step-increase in RH. Our results showed that the CHN did not respond to this 15% change of RH (Fig. 10A). On the other hand, the MHN and DHN sensitively but antagonistically responded to this humidity change. A 2.5-fold increase from 6.8 to 17.1 spikes s^{-1} in firing rate, was observed in the MHN while the response of the DHN showed a 2.1-fold decrease from 31.7 to 15.4 spikes s^{-1} (Fig. 10 B,C).

3.2.5. Ability of the neurons for spike bursting at noxious high temperatures

At moderate temperatures of 20 °C to about 25–30 °C, the CHN, MHN and DHN usually tended to fire in a regular manner. Their instantaneous spike frequencies varied in a relatively narrow range usually deviating from the mean no more than 50–80% (Fig. 11A, B and C). ISIHs of the spike trains showed one maximum and respective CVs of ISIs remained below 0.5 (Fig. 11A′, B′ and C′).

Both at steady temperatures and rapid step-warming conditions, when stimulating temperature reached 30–40 °C, a considerable proportion of the DSS neurons on the antenna switched from regular spiking to spike bursting but the neurons of the same sensillum did not do so simultaneously (Figs. 12; 13). In most cases, the MHN had the lowest threshold temperature for spike bursting as exemplified in Figs. 12 and 14. In bursty spike trains, instantaneous spike frequencies of the three DSS neurons varied largely, due to their dividing into two categories: high spike frequencies within the bursts reaching up to 500–600 Hz, and low frequencies between the bursts (Fig. 12 B, B′, B″; 13; 15). The number of spikes in a burst varied from two up to ten and above (Fig. 12 B′; 13A‴, A⁗; 14C, D; 15; 16). Short intra-burst ISIs and long inter-burst ISIs, formed two different clusters in ISIHs and the spike trains usually had CV values of ISIs higher than 0.5 (Fig. 12B″; 13F, G; 16A‴, B‴, C‴). At the same thermal conditions (30–35 °C), especially at rapid step-warmings, solitary spike production of the CHN drastically decreased (Fig. 14) or stopped completely (Fig. 12 A). At further temperature increase (40 °C and higher), spiking activity of the silent CHN recovered, however, and continued in a bursty manner (Fig. 15A, B; 16A, A′, A″). Frequently, we observed that at high temperatures above 35–40 °C all three neurons of the same sensillum switched from regular spiking (Fig. 16A, A″, B, B″ and C, C″) to typical spike bursting lasting the whole warming period. While bursting, the sign of the firing rate response of the DSS neurons to a rapid step-warming usually changed to its opposite (Figs. 15; 16) compared to that observed at lower temperatures when the neurons produced solitary

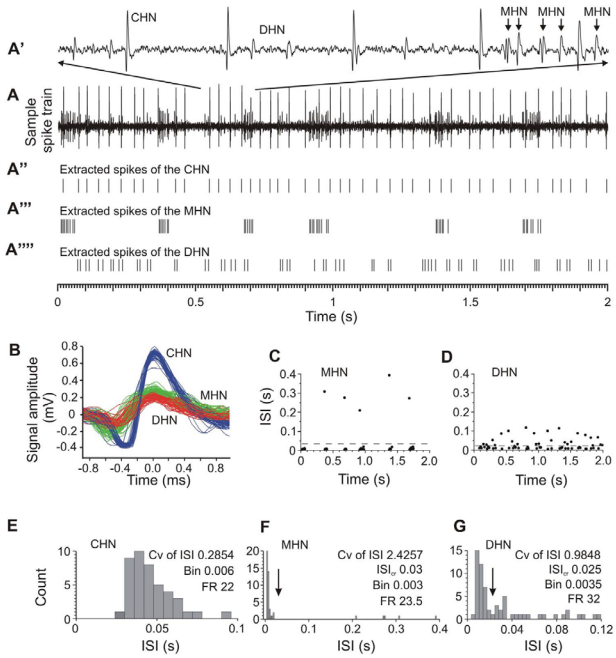

Fig. 13. Sample recording demonstrating typical response of the three DSS neurons to steady temperature of 35 °C. (A) A 2 s fragment of the 18 s original recording. (A') A group of spikes in a shorter time scale. (A''–A'''') show extracted spikes of the CHN, MHN and DHN, respectively. Horizontal lines show bursty spikes. Note that the number of spikes per burst (6 – 10) produced by the MHN is higher than that (2 – 5) of the DHN. By contrast, the CHN generates regular spikes, not grouped into bursts. (B) The overdrawn spike shapes from (A) formed three clusters demonstrating that the spikes were produced by three different neurons, the CHN, MHN and DHN, respectively. (C), and (D) ISIs of the MHN and DHN extracted from (A) and plotted against time. Dotted lines show critical ISIs for spike bursting. Note that distribution of the ISIs over time was rather stable. (E–G) ISI histograms of the spike trains extracted from (A). Arrows show critical ISIs for spike bursting. FR, mean firing rate.

spikes (Fig. 8). For example, spike activity of the bursting CHN and MHN increased (Figs. 15; 16A–A''', B–B''') and that of the DHN decreased (Fig. 16C–C''') with temperature increase. Spike bursting response of the DSS neurons to noxious heat was reversible. Regular spike production of the neurons recovered immediately after cooling (Figs. 12B, 14E, 15D). Detailed analysis of various essential parameters of the bursty spike trains at different thermal conditions, including mean firing rate, does not fit into the frames of this study, however.

3.2.6. Bursting probability of the DSS neurons at different temperatures

Spike bursting of the CHN, MHN and DHN was never observed at 20 °C even at RH extremes ranging from 5% to 95%. Further, bursting probability of the neurons was tested and analysed at temperatures 25–45 °C and at AH 9 g m^{-3}. The lowest threshold temperatures for spike bursting of the CHN, MHN and DHN remained between 25 and 30 °C. However, the bursting probability of the neurons on the antenna increased with temperature increase (Fig. 17). At 45 °C, bursting probability of the CHN, MHN and DHN was 0.695, 0.929 and 0.372, respectively. Thus, in the whole range of tested temperatures, the MHN had the highest tendency for spike bursting.

3.3. Effect of noxious high temperatures on the locomotor activity of the beetles

LA of the beetles was measured at temperatures ranging from 20 to 45 °C (AH 9 g m^{-3}). Three essential turning points were determined from the LA/temperature curves (Figs. 2, 18). Mean threshold temperature for OELA was equal to 27.5 ± 0.75 °C, coinciding with the range of temperatures (25–30 °C) at which the antennal DSS MHN and DHN started to switch from regular spiking to spike bursting (Fig. 17). A steep decline in LA maximum of the beetles (CTmax) was observed at 39.4 ± 0.37 °C. Thus, observed CTmax of the species was higher by 11.9 °C compared to its threshold temperature for OELA. At CTmax, the beetles fully recovered when rapidly cooled down to room temperature (22 °C). TP of the beetles occurred at 41.8 ± 0.37 °C, they stopped moving and died due to thermoshock. Hence the difference between the CTmax and threshold temperature for TP was rather small at 2.4 °C. From TP the beetles never recovered, even though some slight movements of their legs and antennae were observed next day.

4. Discussion

This study sheds light into the existing confused morphological classification of antennal thermo- and hygro-receptive sensilla in elaterid beetles. SEM-FIB analysis performed in *A. obscurus* showed that several characteristic morphological features, such as the presence of a cuticular dome and a small non-perforated conical peg tightly inserted into the sensillum socket so that only its tiny tip is directly exposed to ambient air, support our hypothesis that these sensilla, by their morphological type, are identical to the antennal DSS of carabid beetles (Nurme et al., 2015; Must et al., 2017). Thus, so far, DSSs have been established on the antennae in two large groups of beetles, carabids and elaterids. The cellular complex of sensory neurons and auxiliary cells in the DSS of *A. obscurus* is similar to those found in classical thermo- and

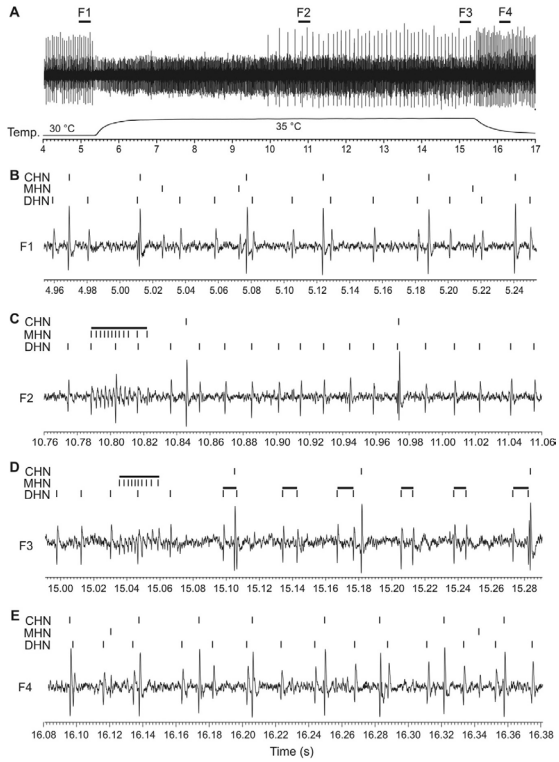

Fig. 14. Sample recording of a spike bursting response of the MHN and DHN in a rapid step-warming experiment at moderately high temperatures. (A) A 13 s fragment of the 18 s original recording. F1, F2, F3 and F4 show 0.3 s fragments of the original recording demonstrated in (B), (C), (D) and (E), respectively, in a shorter time scale. (B) At 30 °C, the CHN, MHN and DHN produce solitary spikes in a regular manner. Note the high and low spike frequencies of the DHN and MHN, respectively. (C) Five seconds after the beginning of the 35 °C warming period, the MHN generated strong spike bursts while the CHN and DHN continued solitary spike production. Horizontal line show spikes of the MHN grouped into bursts. Note that firing rate of the non-bursting CHN decreased and that of the DHN increased with temperature increase. (D) At the end of the 10 s warming period, the DHN also switched from regular spiking to spike bursting. Horizontal lines show spike bursts of the MHN and DHN. Note that the number of spikes per burst (2) of the DHN was less than that (10) of the MHN. By contrast, no indications of spike bursting was observed in the CHN. After cooling, regular spike trains of the MHN and DHN recovered demonstrating that their spike bursting response to warming was reversible (E).

hygro-receptive peg-in-pit organs (coeloconic sensilla) which are common in many other insects (Altner and Loftus, 1985; Chapman, 1998), and DSS of carabids (Nurme et al., 2015; Must et al., 2017). In *A. obscurus*, ODSs of two neurons, the A- and B-neuron, respectively, are of similar size in cross-section, tightly fill the peg lumen and unbranching extend to the tip of the peg. They are markedly smaller in cross-section than the ODS of the third neuron of the sensory triad innervating these sensilla, the C-neuron. Hansson et al. (1994) demonstrated in antennal olfactory sensilla of the male European corn borer *Ostrinia nubilalis* that a correlation exists between the diameter of the ODS and the extracellular spike amplitude. Their results imply that sensory cells with larger ODSs produce spikes with greater amplitude. Thus, it is likely that in the DSS of *A. obscurus*, the CHN which produces largest spikes of the sensory triad morphologically corresponds to the C-neuron. Consequently, the two bimodal THNs with small spikes, the MHN and DHN, respectively, are morphologically identical to the A- and B-neuron. In contrast to carabid beetles (Must et al., 2017), ODSs of the MHN and DHN in DSS of *A. obscurus* have no apical branches. Surprisingly, several important structural differences also occur between the ODSs of the CHN of *A. obscurus* and the carabid beetle *P. oblongopunctatus*. First, in *A. obscurus*, they terminate below the peg base as characteristic of the cold neuron in classical peg-in-pit organs (Altner and Loftus, 1985; Chapman, 1998) while in *P. oblongopunctatus*, they enter deep into the peg lumen (Nurme et al., 2015; Must et al., 2017). Second, the ODS of the cold neuron in classical thermo- and hygroreceptive sensilla (Altner and Loftus, 1985; Chapman, 1998) and the ODS of the CHN in DSS of *P. oblongopunctatus* (Nurme et al., 2015; Must et al., 2017) is strongly branched and/or lamellated whereas in *A. obscurus*, respective structures are absent. The functional significance of these structural differences between various insects is not known.

In this study, for the first time in the large family of Elateridae, responses of the antennal sensory neurons to thermal and humidity stimuli were electrophysiologically tested. Our results showed that the firing rate of the CHN of *A. obscurus* does not depend on changes in air RH but it is highly sensitive to different levels of steady temperature ranged from 25 to 35 °C. Our results showed, however, that firing rate of the CHN does not depend on steady temperatures in the range of 20–25 °C. In its dynamic range, firing rate of the CHN increases with temperature decrease and vice versa, spike production of the neuron decreases with temperature increase typical for the insect thermo-receptive CN (Altner and Loftus, 1985; Merivee et al., 2003; Must et al., 2010). Thus, firing rate of the CHN of *A. obscurus* can well encode

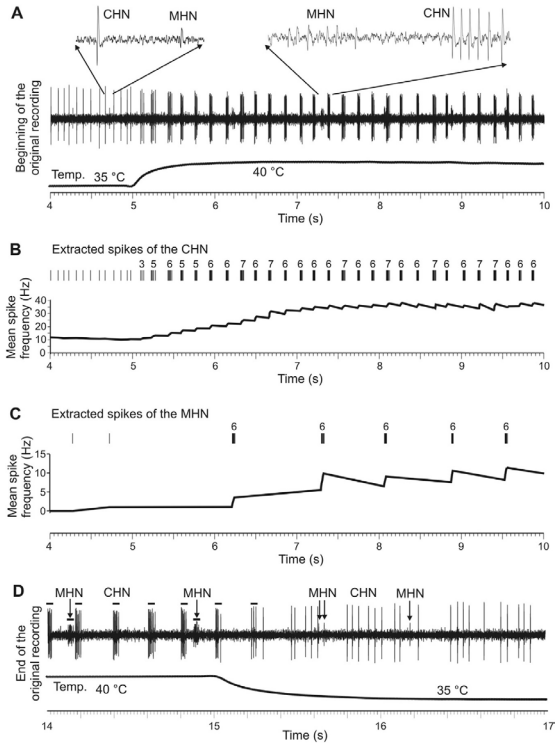

Fig. 15. Sample recording of a spike bursting response of the CHN and MHN in a rapid step-warming experiment at the high end of noxious heat. (A) A 6 s fragment of the 18 s original recording. The DHN was not active in this particular sensillum allowing better visualization of the spike trains produced by the CHN and MHN. Note that both the CHN and MHN switched from regular spiking to spike bursting in response to a rapid temperature increase. (B), and (C) Extracted spikes of the CHN and MHN from (A), respectively. The number of spikes per burst is indicated above the bursts. Note that mean spike frequency of the neurons, while bursting, increases with temperature increase. Time width 2 s (D) A 3 s fragment at the end of the original recording demonstrating reversibility of the spike bursting response in the MHN and CHN.

steady temperatures, in the range of 25–35 °C, but not below that range. Typically, the insect CN temporarily stops spike production in response to rapid step-warming as also demonstrated for the CHN of *A. obscurus* in this study. The length of the silence period depends on the initial temperature as well as on the magnitude of temperature increase and it may last up to 10 s and more at the high end of noxious heat above 35 °C. Thus, the firing rate of the CHN cannot precisely encode dangerously high temperatures close to the upper limit of its thermo-tolerance, which lies close to 44 °C in *A. obscurus*.

In contrast to the CHN, both the MHN and DHN of *A. obscurus* display high sensitivity to ambient air RH but they antagonistically respond to changes in it. At constant temperature conditions, firing rate of the MHN increases and that of the DHN decreases with RH increase indicating that these two neurons function as the moist air and dry air sensors, respectively. At constant AH conditions (9 g m^{-3}), firing rate of the DHN nearly linearly increases with temperature increase ranged from 20 to 35 °C. This increase in firing rate of the DHN is caused, predominantly at least, by inevitable RH drop by 30% accompanied with the temperature increase in that range. On the other hand, at constant AH, spike production of the MHN does not significantly depend on steady temperature. Probably, simultaneous changes in RH and temperature almost equally and in opposite directions affect firing rate of the MHN evidencing its bimodal thermo-hygroreceptive nature. By contrast, at constant AH, its firing rate remarkably decreases with rapid step-increases in temperature and vice versa, spiking activity of the MHN increases with rapid step-coolings suggesting that this neuron much more sensitively responds to rapid changes in RH caused by respective changes in temperature, than to different levels of steady RH. Bimodality is broadly distributed in insect HTNs. Because mean firing rate in bimodal hygro-thermoreceptor neurons can't unambiguously encode environmental air humidity nor temperature, its functional significance in behavioural thermoregulation remains an open question. Unequivocal information on identified peripheral sensory neurons variously involved in sensing environmental temperature and in behavioural activities is tentative and skimpy (Nation, 2002; Dhaka et al., 2006; Dillon et al., 2009; Must et al., 2010; Nurme et al., 2015).

Besides regular spike generation, spike bursting is also widely involved in neural information processing in various sensory systems of animals. Some neurons, including thermo- and bimodal HTN in antennal DSSs of carabids and the elaterid *A. obscurus*, are able to fire both in regular and bursting manner (Turner et al., 1994; Wang and Rinzel, 1995; Sherman, 2001; Gallar et al., 2003; Must et al., 2010, 2017), depending on the particular input. The spike bursting response of the antennal DSS neurons to noxious heat is reversible as we demonstrated

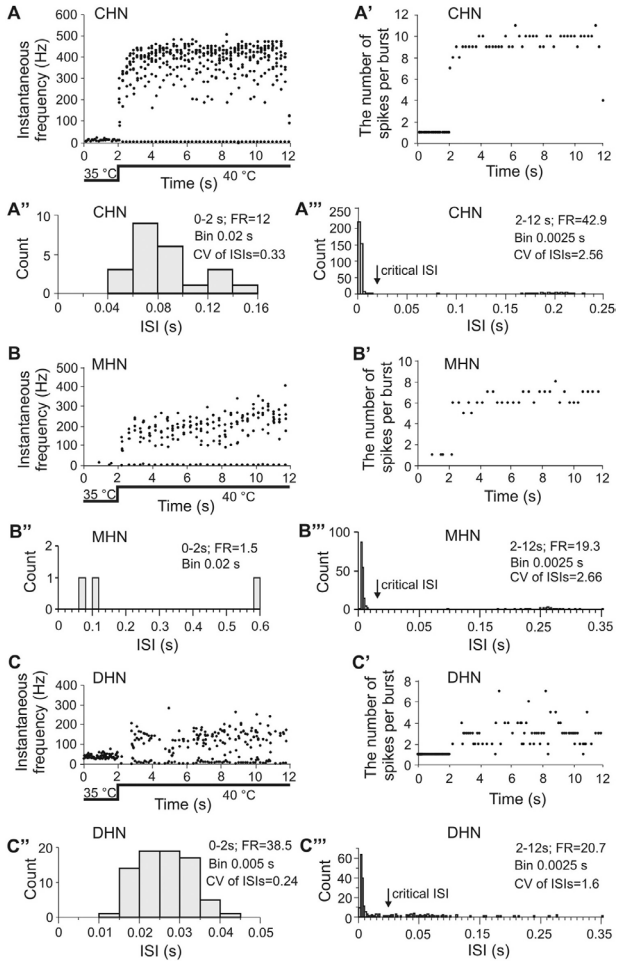

Fig. 16. Typical responses of the DSS neurons to a rapid step-warming by 5 °C at the high end of noxious heat (35–40 °C). Note that all the neurons switched from regular spiking to spike bursting. During warming, the ISIHs had two clusters, representing intra-burst and inter-burst intervals, respectively. The critical ISI was shown by the arrow. The CHN, MHN and DHN housed the same DSS.

for *A. obscurus* in this study. After cooling, regular, solitary spike production of the CHN, MHN and DHN recovers immediately. Very little is known of the exact role and advantages of bursting and regular neurons for encoding external signals, however (Chacron et al., 2004; Krahe and Gabbiani, 2004). In some cases, it has been demonstrated that both regular and bursty spike trains can encode information (Reinagel et al., 1999; Krahe and Gabbiani, 2004; Eyherabide et al., 2008; Must et al., 2010, 2017; Nurme et al., 2015). In contrast to the electrosensory system of fish (Kepecs et al., 2002; Oswald et al., 2004, 2007) and the auditory system of some insects (Boyan and Fullard, 1988; Marsat and Pollack, 2006; Eyherabide et al., 2008), no temporal information is encoded in the timing of the bursts produced by the scleral cold receptors in cats (Gallar et al., 2003), and antennal thermo- and bimodal hygro-thermoreceptor neurons of carabids (Must et al., 2010, 2017; Nurme et al., 2015) and the elaterid *A. obscurus* as demonstrated in this study. The possible functional role of high frequency spike bursting in the processing of behaviourally important sensory information is to extract specific, potentially dangerous environmental signal features, for example, noxious heat for ground-dwelling beetles and ultrasonic signals of hunting bats for flying moths and crickets (Hoy, 1992; Kepecs

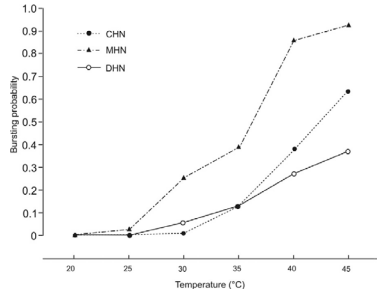

Fig. 17. Bursting probability of the DSS neurons at different temperatures ranging from 20 to 45 °C. Note that the MHN of the sensory triad was the most liable neuron for spike bursting followed by the CHN and DHN, respectively.

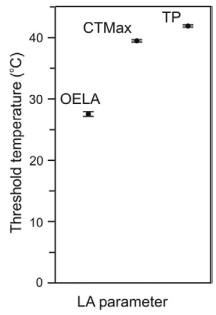

Fig. 18. Calculated means of the three main turning points extracted from the LA/temperature curves of *A. obscurus* in a slow heating experiment. Programmed heating rate was 1 °C min $^{-1}$. Note that the threshold temperature for OELA approximately coincided with the threshold temperatures at which the antennal MHNs started to switch from regular spiking to spike bursting (see Fig. 14). CTmax, critical thermal maximum; TP, total paralysis. Vertical bars show standard error of the means. N = 14–17.

et al., 2002; Krahe and Gabbiani, 2004; Marsat and Pollack, 2006; Must et al., 2010, 2017; Nurme et al., 2015). Our results showed that high temperature induced spike bursting of the HTNs triad in antennal DSS is specifically characteristic not only of carabid beetles (Must et al., 2010, 2017; Nurme et al., 2015). It seems to be a fundamental feature of the neurons in some other insect groups, too, as exemplified by CHN, MHN and DHN in antennal DSS of the elaterid *A. obscurus* in this study. Our results also showed that temperature dependent spike bursting may occur in branched and lamellated ODSs of the HTNs in carabids (Must et al., 2017) as well as in unbranched ODSs of the HTNs in elaterids. So far, no information is available on spike bursting HTNs in insect sensilla other than the antennal DSSs of carabids and elaterids. Their probable occurrence in other morphological types of insect sensilla (Yokohari, 1981, 1983; Altner and Loftus, 1985; Steinbrecht, 1989; Chapman, 1998; Ruchty et al., 2009; Tichy and Kallina, 2013) still needs to be explored.

Our results showed that threshold temperatures for spike bursting in CHN, MHN and DHN largely vary between different DSSs on the antennae of *A. obscurus*. This peculiar feature of the same sensory triad housing antennal DSSs has also been observed in carabids (Must et al., 2010, 2017; Nurme et al., 2015). Must et al. (2017) speculated that the structural basis of this variation might be remarkable variation in dendritic branching and/or lamellation of the neurons. By contrast, no dendritic branching and lamellation of the sensory neurons in DSSs of *A. obscurus* was observed suggesting that some other, unknown differences between the neurons, responsible for variation in threshold temperatures for bursting, should be involved. On the other hand, we found that in *A. obscurus*, the diameter of the DSSs varied largely from 5.0 to 9.5 µm. Therefore, variations in dome measurements influencing exposure of the DSS neurons to environmental temperature might be the structural basis for variations in threshold temperatures for switching from regular spiking to spike bursting of these neurons in this insect. In both groups of beetles, first indications for spike bursting of the neurons lie between 25 and 30 °C, and the bursting probability of the neurons quickly but with different speed, increases along with temperature increase. In *A. obscurus*, the MHN is the most liable of the sensory triad to produce bursty spike trains. At the high end of noxious heat (45 °C), bursty spike train probability of the MHNs is up to 0.93. Corresponding probabilities for the CHN and DHN are much lower, 0.70 and 0.37, respectively. In the carabid *P. oblongopunctatus*, the tendency of the neurons for spike bursting differs from that in *A. obscurus* (Must et al., 2017). In this species, the DHN has the lowest threshold temperature for spike bursting. The probability of its bursty spike trains at 40 °C is equal to 0.73 versus 0.30 of the bursty CHNs. At higher temperatures (45 °C), the probability of bursty DHNs drops to 0.42, but that of the bursty CHNs reaches 0.83. In both carabids and elaterids, threshold temperature for spike bursting is lower in bimodal HTN compared to that of the CHN, probably due to structural differences in the outer dendritic segment of the neurons. The dendrites of the both HTNs extend up to the very tip of the peg inside the DSS whereas the dendrite of the CHN terminates in the middle of the peg in the carabid *P. oblongopunctatus* (Must et al., 2017) or below the peg base in *A. obscurus*. Therefore, stimulus-receiving dendrites of the bimodal HTNs are more exposed to ambient temperature than that of the CHN. Thus, despite some essential functional differences of these CHNs and HTNs between carabids and elaterids, the probability of bursty spike trains they produce may encode noxious heat in the broad range from about 25–30 °C up to lethal high temperatures close to 45 °C in a graded manner. Moreover, in carabids, it has been demonstrated that four parameters of the bursty spike trains, the bursting probability, the CV of ISIs in a spike train, the number of spikes and the ISIs in a burst, are unambiguously dependent on ambient temperature and therefore may precisely encode noxious heat up to 45 °C crucial for survival (Must et al., 2010, 2017). Further experiments are needed to prove if these parameters also unequivocally depend on high temperatures in elaterid beetles.

It is remarkable that threshold temperatures for spike bursting of the sensory triad in antennal DSS and OELA of the beetles coincide well suggesting that specifically the spike bursts are responsible for encoding noxious heat and induce escape behaviour in these insects. Because temperature dependent spike bursting of thermo- and bimodal HTN in antennal DSS begins at considerably lower temperatures compared to CTmax this spectacular feature of the neurons might serve as fast and firm three-fold early warning system for the beetles to avoid overheating and death.

5. Conclusions

In this study, we shed light on the confused terminology of antennal sensilla in elaterid beetles. On the basis of inner fine structure, specific morphological type of thermo- and hygroreceptive organs on the antennae of elaterid beetles was conclusively determined as DSSs using FIB/SEM combined technique.

For the first time, by electrophysiological experiments, we demonstrated that the antennal DSSs of elaterid beetles are innervated by a CHN, and two bimodal, antagonistically responding HTNs, the MHN and the DHN.

For the first time, we demonstrated that all the three sensory neurons in antennal DSS of elaterid beetles may encode noxious high temperatures above 25–30 °C by bursty spike train patters in a graded manner. Thus, besides carabid beetles, elaterids are another large group of insects in which this ability has been established.

We also demonstrated that the threshold temperatures for spike bursting of the sensory neurons in DSS and OELA of the beetles coincide suggesting that most probably the spike bursts are responsible for encoding dangerously high ambient temperatures when confronted, and induce escape behaviour in these insects to avoid overheating and death.

Acknowledgements

The study was supported by the Development Fund of the Estonian University of Life Sciences 8PM170157PKTK and Institutional Research Funding IUT36-2 of the Estonian Ministry of Education and Research.

References

Altner, H., Loftus, R., 1985. Ultrastructure and function of insect thermo and hygroreceptors. Annu. Rev. Entomol. 30, 273–295.
Altner, H., Prillinger, L., 1980. Ultrastructure of invertebrate chemo- thermo-, and hygroreceptors and its functional significance. Int. Rev. Cytol. 67, 69–139.
Bakkum, D.J., Radivojevic, M., Frey, U., Franke, F., Hierlemann, A., Takahashi, H., 2014. Parameters for burst detection. Front. Comput. Neurosci. 7, 193. http://dx.doi.org/10.3389/fncom.2013.00193.
Boyan, G.S., Fullard, J.H., 1988. Information processing at a central synapse suggests a noise filter in the auditory pathway of the noctuid moth. J. Comp. Physiol. A Neuroethol. Sens. Neural Behav. Physiol. 164, 251–258.
Chacron, M.J., Longtin, A., Maler, L., 2004. To burst or not to burst? J. Comput. Neurosci. 17, 127–136.
Chapman, R.F., 1998. The Insects, Structure and Function. Cambridge University Press, Cambridge.
Dhaka, A., Viswanath, V., Patapoutian, A., 2006. TRP ion channels and temperature sensation. Annu. Rev. Neurosci. 29, 135–161.
Di Giulio, A., Maurizi, E., Rossi Stacconi, M.V., Romani, R., 2012. Functional structure of antennal sensilla in the myrmecophilous beetle *Paussus favieri* (Coleoptera, Carabidae, Paussini). Micron 43, 705–719.
Di Giulio, A., Muzzi, M., Romani, R., 2015. Functional anatomy of the explosive defensive system of bombardier beetles (Coleoptera, Carabidae, Brachininae). Arthropod Struct. Dev. 44, 468–490.
Dillon, M.E., Wang, G., Garrity, P.A., Huey, R.B., 2009. Thermal preference in *Drosophila*. J. Therm. Biol. 34, 109–119.
Ernst, M.R., Beitnger, T.L., Stewart, K.W., 1984. Critical thermal maxima of nymphs of three *Plecoptera* species from an Ozark foothill stream. Freshw. Invertebr. Biol. 3, 80–85.
Eyherabide, H.G., Rokem, A., Herz, A.V.M., Samengo, I., 2008. Burst firing is a neural code in an insect auditory system. Front. Comput. Neurosci. 2 (3), 1–17.
Gallar, J., Acosta, M.C., Belmonte, C., 2003. Activation of scleral cold thermoreceptors by temperature and blood flow changes. Invest. Ophthalmol. Vis. Sci. 44, 697–705.
Hansson, B.S., Hallberg, E., Löfstedt, C., Steinbrecht, R.A., 1994. Correlation between dendrite diameter and action potential amplitude in sex pheromone specific receptor neurons in male *Ostrinia nubilalis* (Lepidoptera: pyralidae). Tissue Cell 4, 503–512.
Hoy, R.R., 1992. The evolution of hearing in insects as an adaptation to predation from bats. In: Webster, D.B., Fay, R.R., Popper, A.N. (Eds.), The Evolutionary Biology of Hearing. Springer, New York, pp. 115–130.
Kepecs, A., Wang, X.J., Lisman, J., 2002. Bursting neurons signal input slope. J. Neurosci. 22, 9053–9062.
Krahe, R., Gabbiani, F., 2004. Burst firing in sensory systems. Nat. Rev. Neurosci. 5, 13–23.
Loftus, R., 1968. The response of the antennal cold receptor of *Periplaneta americana* to rapid temperature changes and steady temperature. Z. Vgl. Physiol. 59, 413–455.
Lutterschmidt, W.I., Hutchison, V.H., 1997. The critical thermal maximum: history and critique. Can. J. Zool. 75, 1561–1574.
Marsat, G., Pollack, G.S., 2006. A behavioural role for feature detection by sensory bursts. J. Neurosci. 26, 10542–10547.
Merivee, E., 1992. Antennal sensilla of the female and male elaterid beetle *Agriotes obscurus* L. (Coleoptera: Elateridae). Proc. Est. Acad. Sci. Biol. 41, 189–215.
Merivee, E., Must, A., Luik, A., Williams, I., 2010. Electrophysiological identification of hygroreceptor neurons from the antennal dome shaped sensilla in the ground beetle *Pterostichus oblongopunctatus*. J. Insect Physiol. 56, 1671–1678.
Merivee, E., Ploomi, A., Luik, A., Rahi, M., Sammelselg, V., 2001. Antennal sensilla of the ground beetle *Platynus dorsalis* (Pontoppidan, 1763) (Coleoptera, Carabidae). Micros. Res. Tech. 55, 339–349.
Merivee, E., Ploomi, A., Rahi, M., Bresciani, J., Ravn, H.P., Luik, A., Sammelselg, V., 2002. Antennal sensilla of the ground beetle *Bembidion properans* Steph. (Coleoptera, Carabidae). Micron 33, 429–440.
Merivee, E., Ploomi, A., Rahi, M., Luik, A., Sammelselg, V., 2000. Antennal sensilla of the ground beetle *Bembidion lampros* Hbst. (Coleoptera, Carabidae). Acta Zool. 81, 339–350.
Merivee, E., Rahi, M., Bresciani, J., Ravn, H.L., Luik, A., 1998. Antennal sensilla of the click beetle, *Limonius aeruginosus* (Oliver) (Coleoptera: Elateridae). Int. J. Insect Morphol. Embryol. 27, 311–318.
Merivee, E., Rahi, M., Luik, A., 1997. Distribution of olfactory and some other antennal sensilla in the male click beetle *Agriotes obscurus* L. (Coleoptera: Elateridae). Int. J. Insect Morphol. Embryol. 26, 75–83.
Merivee, E., Rahi, M., Luik, A., 1999. Antennal sensilla of the click beetle, *Melanotus villosus* (Geoffroy) (Coleoptera: Elateridae). Int. J. Insect Morphol. Embryol. 28, 41–51.
Merivee, E., Vanatoa, A., Luik, A., Rahi, M., Sammelselg, V., Ploomi, A., 2003. electrophysiological identification of cold receptors on the antennae of the ground beetle *Pterostichus aethiops*. Physiol. Entomol. 28, 88–96.
Must, A., Merivee, E., Nurme, K., Sibul, I., Muzzi, M., Di Giulio, A., Williams, I., Tooming, E., 2017. Encoding noxious heat by spike bursts of antennal bimodal hygroreceptor (dry) neurons in the carabid *Pterostichus oblongopunctatus*. Cell Tissue Res. 368, 29–46.
Must, A., Merivee, E., Luik, A., Williams, I., Ploomi, A., Heidemaa, M., 2010. Spike bursts generated by the thermosensitive (cold) neuron from the antennal campaniform sensilla of the ground beetle *Platynus assimilis*. J. Insect Physiol. 56, 412–421.
Must, A., Merivee, E., Luik, A., Mänd, M., Heidemaa, M., 2006a. Responses of antennal campaniform sensilla to rapid temperature changes in ground beetles of the tribe Platynini with different habitat preferences and daily activity rhythms. J. Insect Physiol. 52, 506–513.
Must, A., Merivee, E., Mänd, M., Luik, A., Heidemaa, M., 2006b. Electrophysiological responses of the antennal campaniformsensilla to rapid changes of temperature in the ground beetles *Pterostichus oblongopunctatus* and *Poecilus cupreus* (Tribe Pterostichini) with different ecological preferences. Physiol. Entomol. 31, 278–285.
Nation, J.L., 2002. Insect Physiology and Biochemistry. CRC Press, Boca Raton, London, New York, Washington, D.C.
Nurme, K., Merivee, E., Must, A., Sibul, I., Muzzi, M., Di Giulio, A., Williams, I., Tooming, E., 2015. Responses of the antennal bimodal hygroreceptor neurons to innocuous and noxious high temperatures in the carabid beetle, *Pterostichus oblongopunctatus*. J. Insect Physiol. 81, 1–13.
Oswald, A.M., Chacron, M.J., Doiron, B., Bastian, J., Maler, L., 2004. Parallel processing of sensory input by bursts and isolated spikes. J. Neurosci. 24, 4351–4362.
Oswald, A.M., Doiron, B., Maler, L., 2007. Interval coding. I. Burst interspike intervals as indicators of stimulus intensity. J. Neurophysiol. 97, 2731–2743.
Piersanti, S., Rebora, M., Almaas, T.J., Salerno, G., Gaino, E., 2011. Electrophysiological identification of thermo-and hygro-sensitive receptor neurons on the antennae of the dragonfly *Libellula depressa*. J. Insect Physiol. 57, 1391–1398.
Reinagel, P., Godwin, D., Sherman, S.M., Koch, C., 1999. Encoding of visual information by LGN bursts. J. Neurophysiol. 81, 2558–2569.
Ribeiro, P.L., Camacho, A., Navas, C.A., 2012. Considerations for assessing maximum critical temperatures in small ectothermic animals: insights from leaf-cutting ants. PLoS ONE 7 (2), e32083. http://dx.doi.org/10.1371/journal.pone.0032083.
Ruchty, M., Romani, R., Kuebler, L.S., Ruschioni, S., Roces, F., Isidoro, N., Kleineidam, C.J., 2009. The thermo-sensitive sensilla coeloconica of leaf-cutting ants (*Atta vollenweideri*). Arthropod Struct. Dev. 38, 195–205.
Sherman, S.M., 2001. Tonic and burst firing: dual modes of thalamocortical relay. Trends Neurosci. 24, 122–126.
Steinbrecht, R.A., 1989. The fine structure of thermo-/hygrosensitive sensilla in the silkmoth *Bombyx mori*: receptor membrane substructure and sensory cell contacts. Cell Tissue Res. 55, 49–57.
Thiele, H.U., 1977. Carabid beetles in their environments: a study on habitat selection by adaptations in physiology and behaviour. Zoophysiology and Ecology 10 Springer-Verlag, Berlin.
Tichy, H., Kallina, W., 2010. Insect hygroreceptor responses to continuous changes in humidity and air pressure. J. Neurophysiol. 103, 3274–3286.
Tichy, H., Kallina, W., 2013. The evaporative function of cockroach hygroreceptors. PLoS ONE 8 (1), e53998. http://dx.doi.org/10.1371/journal.pone.0053998.
Traugott, M., Benefer, C.M., Blackshaw, R.P., van Herk, W.G., Vernon, R.S., 2015. Biology, ecology, and control of elaterid beetles in agricultural land. Annu. Rev. Entomol. 60, 313–334.
Turner, R.W., Maler, L., Deerinck, T., Levinson, S.R., Ellisman, M.H., 1994. TTX-sensitive dendritic sodium channels underlie ascillatory discharge in a vertebrate sensory neuron. J. Neurosci. 14, 6453–6471.
Waldow, U., 1970. Elektrophysiologische untersuchungen an feuchte-, troken- und kälterezeptoren auf der antenne der wanderheuschrecke locusta. Z. Vgl. Physiol. 69, 249–283.
Wang, X.J., Rinzel, J., 1995. Oscillatory and bursting properties of neurons. In: Arbib, M.A. (Ed.), The Handbook of Brain Theory and Neural Networks. MIT Press, Cambridge, pp. 686–691.
Yokohari, F., 1981. The sensillum capitulum, an antennal hygroreceptive and thermoreceptive sensillum of the cockroach, *Periplaneta americana* L. Cell Tissue Res. 216, 525–543.
Yokohari, F., 1983. The coelocapitular sensillum, an antennal hygro- and thermoreceptive sensillum of the honey bee, *Apis mellifera* L. Cell Tissue Res. 233, 355–365.
Zauli, A., Maurizi, E., Carpaneto, G.M., Chiari, S., Merivee, E., Svensson, G., Di Giulio, A., 2016. Scanning electron microscopy analysis of the antennal sensilla in the rare saproxylic beetle *Elater ferrugineus* (Coleoptera: Elateridae). Ital. J. Zool. 83, 338–350.

Karin Nurme is a Ph.D. candidate at the Chair of Plant Health in the Estonian University of Life Sciences in Tartu. She is a Junior Researcher at this institution. Her research project focus is on the spike bursts in antennal sensor neurons of insects evoked by external natural stimuli and their relation with behaviour.

Enno Merivee is a Senior Researcher at the Institute of Agricultural and Environmental Sciences of the Estonian University of Life Sciences, Tartu. His Research interests focus on sensory physiology and mechanisms of searching behaviour in insects.

Anne Must is a Researcher at the Institute of Agricultural and Environmental Sciences of the Estonian University of Life Sciences, Tartu. Her research interests focus on insect behaviour and sensor physiology of insects.

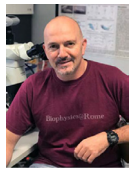

Andrea Di Giulio is an Associate Professor at the "Roma Tre" University in Italy. His research interests focus on: functional morphology of adult and immature stages of beetles; fine morphology and ultrastructure of sensilla and exocrine glands in insects; morpho-functional and behavioural adaptations in parasites of social insects; taxonomy, morphology and distribution of marine gastropods; taxonomy and morphology of ixodid ticks.

Maurizio Muzzi is a Ph.D. candidate in biology at the "Roma Tre" University in Italy. His research projects focus on the morpho-anatomical and ultrastructural characterization of exocrine glands and sensilla in beetles.

Ingrid Williams is a Senior Researcher at the Institute of Agricultural and Environmental Sciences of the Estonian University of Life Sciences, Tartu. Research interests focus on insect behaviour particularly pollination and the management of pests of oilseed rape.

Marika Mänd is the head of Chair of Plant Health at the Estonian University of Life Sciences, Tartu. Her main research interests focus on ecology and physiology of insects particularly pollination horticultural and other entomophilous crops.

CURRICULUM VITAE

First name	Karin
Last name	Nurme
Birth date	14.02.1983
E-mail	karin.nurme@emu.ee

Education

2013–2019	Estonian University of Life Sciences – PhD studies in Agriculture,
2005–2008	University of Tartu – MSc studies in Chemistry Education
2001–2005	University of Tartu – BSc studies in Science Education
1998–2000	Hugo Treffner Gymnasium

Academic degrees

Master's Degree (2008), (sup) Jaak Arold, Using Periodic Table in Learning Chemistry, University of Tartu.

Professional employment

2018–…	Doctoral School of Earth Sciences and Ecology coordinator in University of Life Sciences
2017–…	Estonian University of Life Sciences, junior researcher
2013–2013	Estonian University of Life Sciences, senior laboratory technician
2008–2012	Elementary school of Sadala, science teacher
2008–2009	Tartu Commerce Gymnasium, chemistry teacher
2006–2007	Rakvere Private Gymnasium, chemistry teacher

Professional training

2017	Universita degli Studi Roma Tre – FIB/SEM methodological training
2017	University of Tartu – About Programming
2014	Open University of Estonian University of Life Sciences – Adult training and training process management

2013	Estonian Quality Agency for Higher and Vocational Education – Training of Estonian experts in institutional accreditation
2013	Estonian University of Life Sciences – Data management and analysis with MS Excel

Participation in research projects

2015–2020	IUT36-2 " Sustainable crop protection: harnessing ecosystem services for plant production".
2017–2018	PM170157PKTK "Improvement of the Neurophysiological Research of Agricultural Insecticides at the Estonian University of Life Sciences in cooperation with the University of Rome".
2017–2018	P170264PKTE "The effect of alternative dietary foods to the development and physiological state of Colorado potato beetle".
2011–2014	ETF8685 "Reception of plant chemicals and unfavourably high temperatures in carabids and elaterids".

ELULOOKIRJELDUS

Eesnimi	Karin
Perenimi	Nurme
Sünniaeg	14.02.1983
E-mail	karin.nurme@emu.ee

Haridustee

2013–2019	Eesti Maaülikool – doktoriõpe – eriala: Põllumajandus
2005–2008	Tartu Ülikool – magistriõpe – eriala: Keemiaõpetaja
2001–2005	Tartu Ülikool – bakalaureuse õpe – eriala: Loodusteaduste õpetaja põhikoolis
1998–2000	Hugo Treffneri Gümnaasium

Teaduskraad

Magistrikraad, 2008, (juh) Jaak Arold, Perioodilisuse süsteemi kasutamine keemia õppimisel, Tartu Ülikool.

Erialane teenistuskäik

2018–…	Maateaduste ja ökoloogia doktorikooli koordinaator Eesti Maaülikoolis
2017–…	Eesti Maaülikool, nooremteadur
2013–2013	Eesti Maaülikool, vanemlaborant
2008–2012	Sadala Põhikool, loodusainete õpetaja
2008–2009	Tartu Kommertsgümnaasium, keemiaõpetaja
2006–2007	Rakvere Eragümnaasium, keemiaõpetaja

Erialane täiendkoolitus

2017	Universita degli Studi Roma Tre – FIB/SEM metoodika alane väljaõpe
2017	Tartu Ülikool – Programmeerimisest maalähedaselt
2014	Eesti Maaülikool Avatud Ülikool – Täiskasvanukoolitus ja koolitusprotsessi juhtimine

2013	Eesti Kõrg- ja Kutsehariduse Kvaliteediagentuur – Institutsionaalse akrediteerimise Eesti ekspertide koolitus
2013	Eesti Maaülikool – Andmete haldus ja analüüs MS Excelis

Osalemine teadusprojektides

2015–2020	IUT36-2 "Jätkusuutlik taimekaitse: ökosüsteemi teenuste rakendamine taimekasvatuses".
2017–2018	PM170157PKTK "Põllumajanduslikult oluliste putukate neurofüsioloogilise uurimistöö võimekuse suurendamine Eesti Maaülikoolis koostöös Rooma Tre Ülikooliga".
2017–2018	P170264PKTE "Alternatiivsete toidutaimede mõju kartulimardika arengule ja füsioloogilisele seisundile".
2011–2014	ETF8685 "Taimsete metaboliitide ja ebasoodsalt kõrgete temperatuuride retseptsioon jooksiklastel ja naksurlastel".

LIST OF PUBLICATIONS

Publications indexed by Thomson Reuters Web of Science (1.1)

Nurme, K., Merivee, E., Must, A., Di Giulio, A., Muzzi, M., Williams, I., Mänd, M. 2018. Bursty spike trains of antennal thermo- and bimodal hygro-thermoreceptor neurons encode noxious heat in elaterid beetles. Journal of Thermal Biology, 72, 101-117.

Tooming, E., Merivee, E., Must, A., Merivee, M-I., Sibul, I., **Nurme, K.**, Williams, I.H. 2017. Behavioural effects of the neonicotinoid insecticide thiamethoxam on the predatory insect Platynus assimilis. Ecotoxicology, 26 (7), 902−913.

Must, A., Merivee, E., **Nurme, K.**, Sibul, I., Muzzi, M., Di Giulio, A., Williams, I., Tooming, E. 2017. Encoding noxious heat by spike bursts of antennal bimodal hygroreceptor (dry) neurons in the carabid Pterostichus oblongopunctatus. Cell and Tissue Research, 368 (1), 29-46.

Nurme, K., Merivee, E., Must, A., Sibul, I., Muzzi, M., Di Giulio, A., Williams, I., Tooming, E. 2015. Responses of the antennal bimodal hygroreceptor neurons to innocuous and noxious high temperatures in the carabid beetle, Pterostichus oblongopunctatus. Journal of Insect Physiology, 81, 1−13.

Articles published in international journals (1.2)

Nurme, K., Must, A., Merivee, E. Accepted. Link between elevated locomotor activity and spike bursting of antennal thermosensitive neurons in the carabid beetle Pterostichus oblongopunctatus. Acta Zoologica Academiae Scientiarum Hungaricae.

VIIS VIIMAST KAITSMIST

MAREK MAASIKMETS
DETERMINATION OF EMISSION FACTORS FROM ANTHROPOGENIC PARTICLE SOURCES FOR AIR EMISSION AND HEALTH IMPACT ASSESSMENT
INIMTEKKELISTE PEENOSAKESTE ERIHEIDETE MÄÄRAMINE ÕHUEMISSIOONIDE JA TERVISEMÕJUDE HINDAMISEKS
Professor **Valdo Kuusemets**, **Erik Teinemaa** (PhD, Eesti Keskkonnauuringute Keskus OÜ), dotsent **Hans Orru** (Tartu Ülikool)
11. märts 2019

MARJU TAMM
PIGMENT-BASED CHEMOTAXONOMY – EFFICIENT TOOL TO QUANTIFY PHYTOPLANKTON GROUPS IN LAKES AND COASTAL SEA AREAS
PIGMENTIDEL PÕHINEV KEMOTAKSONOOMIA – TÕHUS VAHEND FÜTOPLANKTONI KOOSSEISU SELGITAMISEKS JÄRVEDES JA RANNIKUMERES
Professor **Tiina Nõges,** teadur **René Freiberg**
21. mai 2019

MARGOT SEPP
ORGANIC MATTER IN TEMPERATE LAKES – MONITORING AND CONNECTIONS WITH CATCHMENT
ORGAANILINE AINE PARASVÖÖTME JÄRVEDES – SEIRE NING SEOSED VALGALAGA
Professor **Tiina Nõges**
21. mai 2019

JIAYAN YE
QUANTITATIVE SCALING OF FOLIAGE PHOTOSYNTHETIC CHARACTERISTICS AND RELEASE OF CONSTITUTIVE AND INDUCED VOLATILES WITH SEVERITY OF BIOTIC STRESS
BIOOTILISE STRESSI KVANTITATIIVNE MÕJU LEHTEDE FOTOSÜNTEESILE NING KONSTITUTIIVSETE JA INDUTSEERITUD LENDUVATE ÜHENDITE EMISSIOONILE
Professor **Ülo Niinemets**
6. juuni 2019

KERSTI VENNIK
MEASUREMENTS AND SIMULATIONS OF RUT DEPTH DUE TO SINGLE AND MULTIPLE PASSES OF MILITARY VEHICLES ON TYPICAL ESTONIAN SOILS AND NATURAL RECOVERY OF RUTS
MILITAARSÕIDUKITE ÜLESÕITUDE TULEMUSENA KUJUNENUD ROOPASÜGAVUSE MÕÕTMINE JA MODELLEERIMINE EESTI MULDADEL NING ROOBASTE LOODUSLIK TAASTUMINE
Professor **Endla Reintam, Thomas Keller,** PhD (Rootsi Põllumajandusülikool), **Peeter Kukk,** PhD (Tartu Ülikool)
19. juuni 2019

ISSN 2382-7076
ISBN 978-9949-629-81-7 (trükis)
ISBN 978-9949-629-82-4 (pdf)